International Journal of Sciences

Research Article Volume 6 – December 2017 (12)

SEM-EDX Analysis of the Dental Plaque of the Knight Bayard (1473?-1524)

Permits to Study his Diet Habits and Dental Cares

Gérard Lucotte[1], Thierry Thomasset[2]

[1]Institute of Molecular Anthropology, 75005 Paris, France
[2]Service of Physico-Chemical Analyses, UTC, 50201 Compiègne, France

Abstract: We have studied by SEM-EDX analysis the dental plaque of one of Bayard's molar (1473?-1524), a famous French knight who lived at the end of the Middle Age period. Scanning electron microscopic studies permit us to establish that he ate leeks, asparagus, dried green garden peas and sorrel ; the cereal was mainly stocks of rye flour ; the meat was chicken, and the fish as herring and tench. The sugar came from chestnut tree honey. His drinking water was infested by very numerous diatoms. The established Bayard dental cares consisted of the abrasion of dental plaque, mainly, with various sorts of pumice stones.

Keywords: Bayard knight ; dental plaque ; SEM-EDX studies ; diet and drink ; dental cares

The Chevalier Bayard (1473?-1524) was the epitome of French chivalry during the late Middle Ages (**1**).
His cranium is at present kept in the Dauphiné Museum of Grenoble (France). Some observed particularities of his mandible (brachygnathy, elevated *corpus*, squared and non-protruding chin) correspond to those depicted on the true portraits of Bayard. A molar tooth was extracted from his mandible. Genomic DNA obtained from this tooth permits us to study the mitochondrial DNA (mtDNA) of Bayard (**2**) ; his mtDNA haplogroup is exactly that of a today living male related (to 32 generations) to the Bayard matrilinear ascendance. The ^{14}C evidence dating from a root of the tooth provides a date of calendar 1430-1510 interval (at 95.4% probability), consistent with a mean age of 1486, for an individual who had started eruptions of his first molars (13 years old for Bayard).

Scanning electron microscopy permits detailed examination of the dental plaque (**3**, **4**). In the present work, we use these techniques to study the molar dental plaque of Bayard's tooth in the goal to discover his alimentary habits.

MATERIAL AND METHODS

Bayard's tooth extracted is the first molar, located at the left side of the mandible (the tooth number 36, according to the Nomenclature dentaire internationale). Figure 1 shows the lingual face of this tooth ; it is the lingual dental plaque (PD) of the tooth that was examined.

Examination of the PD is realized *in situ*, at the surface of the dental plaque.
The SEM (Scanning Electron Microscopy) apparatus used is a FEI model Quanta f FEG. Both LFD (Large Field Detector) and CBS (Circular Back Scattering) procedures were used, the last one to detect heavy elements. Elemental analysis was achieved by using EDX (Energy Dispersive X-ray spectroscopy), this SEM being equipped with a probe model X-flash 6/30.

Published at: http://www.ijsciences.com/pub/issue/2017-12/
DOI: 10.18483/ijSci.1485; Online ISSN: 2305-3925; Print ISSN: 2410-4477

Gerard Lucotte (Correspondence)
lucotte@hotmail.com
+

Figure 1. Lingual view of the tooth, in optical microscopy (3x). E : enamel ; PD : dental plaque ; R1 : (broken) root 1 ; R2 (sawen) root 2.

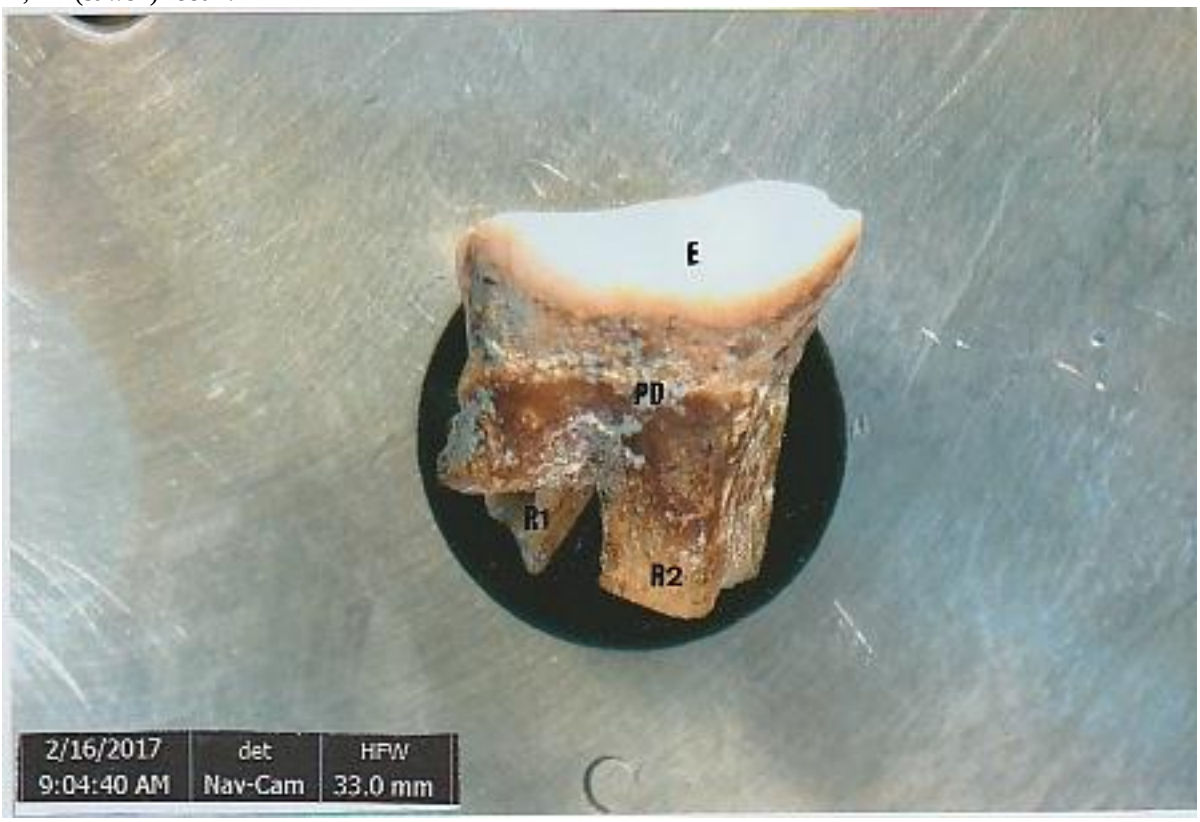

Each elemental analysis is given in the form of a spectrum, with kiloelectrons / Volts (ke/V) on the abscissa and elemental peaks heights in ordinates.

RESULTS

Figure 2 shows a SEM photograph of the PD at low magnification (30x). The lower limit of enamel (cracked vertically) and the basis of the two roots are visible. Three islands of dentine (OD1, OD2 and OD4) can be distinguished at the limit between enamel and dentine and a big island of dentine (OD3) is located in the dentine of the PD. One can see examples of holes and crevices at the PD surface, where the majority of relatively intact exogenous micro-particles are caught.

In the PD spectrum, the two major peaks are those of calcium and phosphorus ; they constitute the calcium phosphate (ortho-phosphate of calcium) of the dentine.

These two major peaks are enhanced again in OD2 (Figure 3), where one can see in the corresponding enlarged (4000x) photograph the crystals of hydroxyapatite (in the circle), implanted in the dentine matrix of calcium phosphate.

Phytoliths:

Phytoliths are fine granules (between 5 and 200 µm and above), generally of amorphous silica, produced by plants (**5**). They are deposited in the oral cavity while chewing fruits and vegetables, and then incorporated into PD during its formation. Their morphologies are specific to particular plants, so it is possible (from the recovery or observation of isolated phytoliths) to recognize taxas of higher rank (such as families, tribes or subfamilies and in some cases until species) of the plant that formed it, thus obtaining information about the diet (**6**).

Figure 2. The PD, in electron microscopy. *Above* : SEM photograph (in CBS, 30x) of the PD. E : enamel, with vertical craks (K). R1and R2 are the basis of the two roots. OD1, OD2, OD3 and OD4 (circled) are four examples of dentine islands located at the limit between enamel and the PD ; OD3 is the main dentine island in the PD. H is an example of a hole and C are examples of crevices in the PD. The black dot is the location in the PD where elemental analysis is realized. *Below* : spectrum of the PD at the black dot. C : carbon ; O : oxygen ; Fe (three peaks) : iron ; Na : sodium ; Mg : magnesium ; Si : silicium ; P : phosphorus ; S : sulphur ; K : potassium ; Ca (two peaks) : calcium.

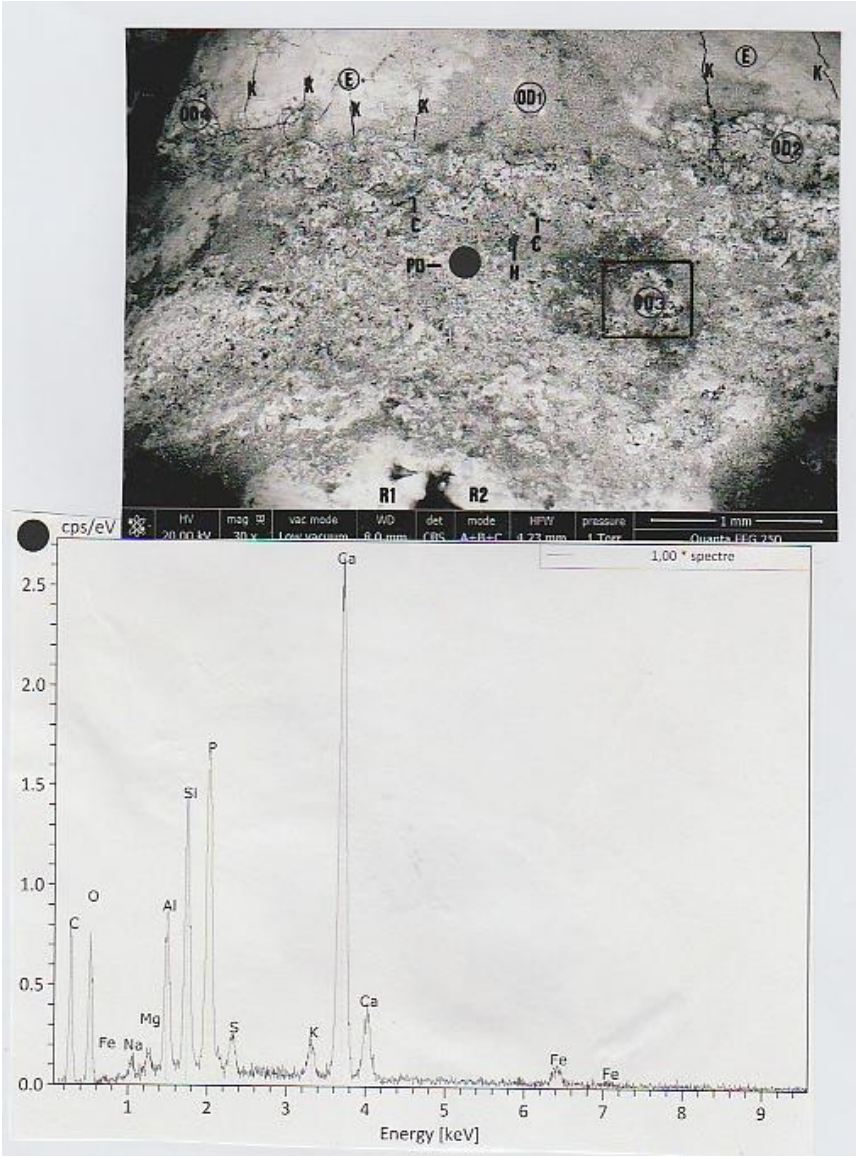

Figure 3. The OD2, in electronic microscopy. *Above* : SEM photograph (in LFD, 4000x) of some part of OD2. In the circle H : crystals of hydroxyapatite ; M : the dentine matrix. The black dot is the location in OD2 where elemental analysis is realized . *Below* : spectrum of the OD2 at the black dot.

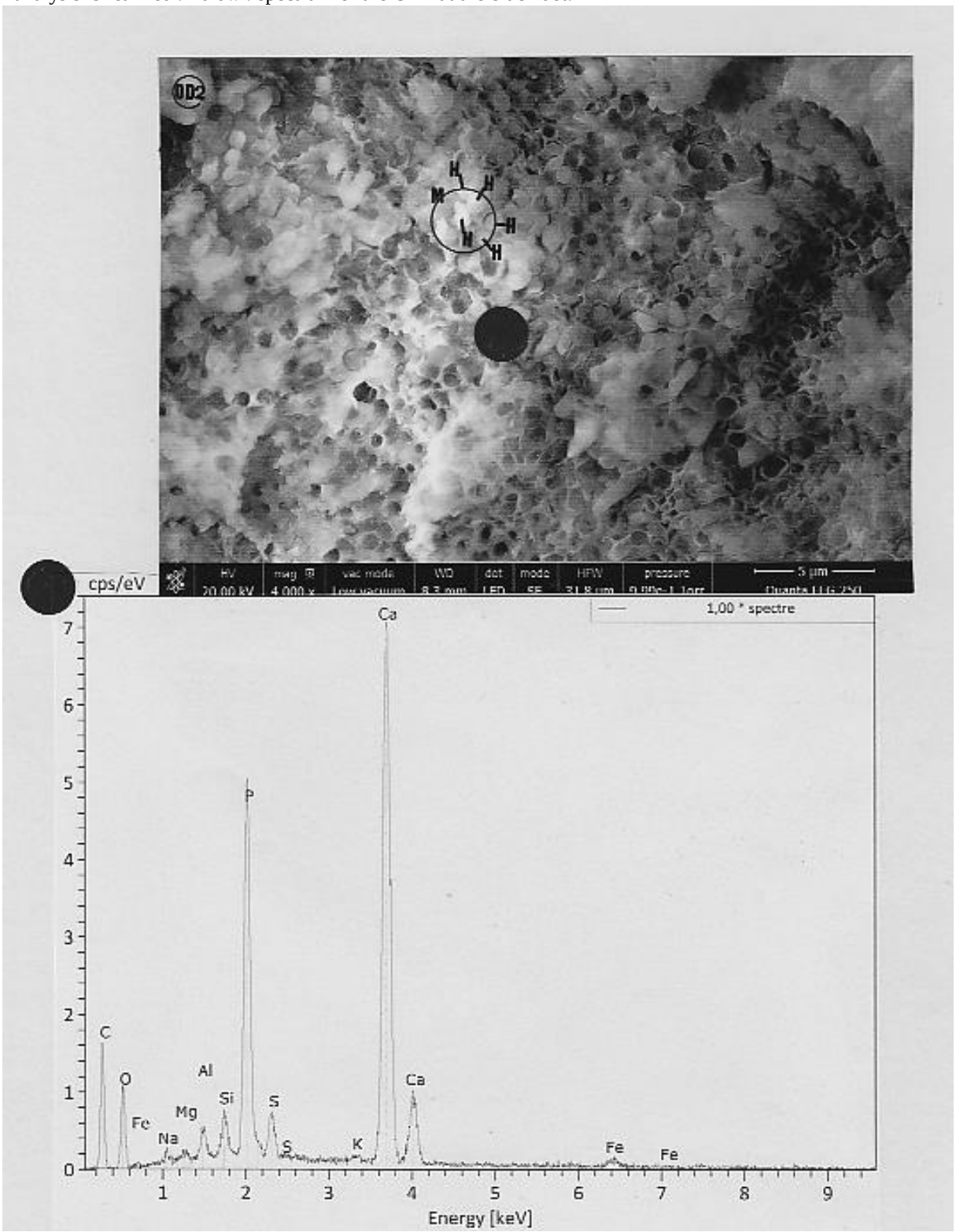

But phytoliths observed at the PD surface are very rarely of the conventional forms. Figure 4 shows, caught in a crevice, one of the rare "conventional" phytolith that we have observed : it is cylindrical, of about 3µm of width and 20 µm of length, with a twisted form ; it is mainly make up of silica. Possibly, it is a silicate fiber of some edible root (perhaps of carrot).

Most of the phytoliths observed are micro-phytoliths, of elongated forms and fine diameters. They are very numerous on the PD surface. One example of this sort of phytolith is shown in Figure 5.1. Its diameter is of 366 mm only, so it is very difficult to study its elemental composition (because it interferes with that of the PD calcium phosphate of the substratum and with those of other neighbouring micro-particles); this sort of micro-phytolith, especially for its longer forms, is mainly constituted of potassium (an element characteristic of plants) and of sulphur. Some of these micro-phytoliths (at least one hundred of samples observed) have one bulging extremity (Figure 5.2) ; they are mainly composed of silicium. We shall see later their significances.

Among the elongated micro-phytoliths, numerous are larger and with squared extremities (Figure 6). Most of them have the elemental composition of an aluminosilicate mineral, often with titanium. It is clear that they are of one mineral form ; as for those with bulging extremities and that are silicium-rich, we shall see later their significances.
Most of the biggest phytoliths are oblong (Figure 7) or triangular (Figure 8) in forms. We have observed and analysed a total of 17 oblong phytoliths, and of 28 triangular phytoliths. In most cases, they are also composed of aluminosilicate, with or without iron.

Figure 4. A cylindric phytolith. *Above* : SEM photograph (in LFD, 4000x) of the cylindric phytolith. *Below* : spectrum of this phytolith.

Figure 5. Two elongated micro-phytoliths. 1 : SEM photograph (in CBS, 15000x) of an elongated microphytolith (length in µm, width in nm) ; this sample, relatively short, is specially altered in form. 2 : SEM photograph (in CBS, 5000x) of an elongated micro-phytolith with a bulging extremity.

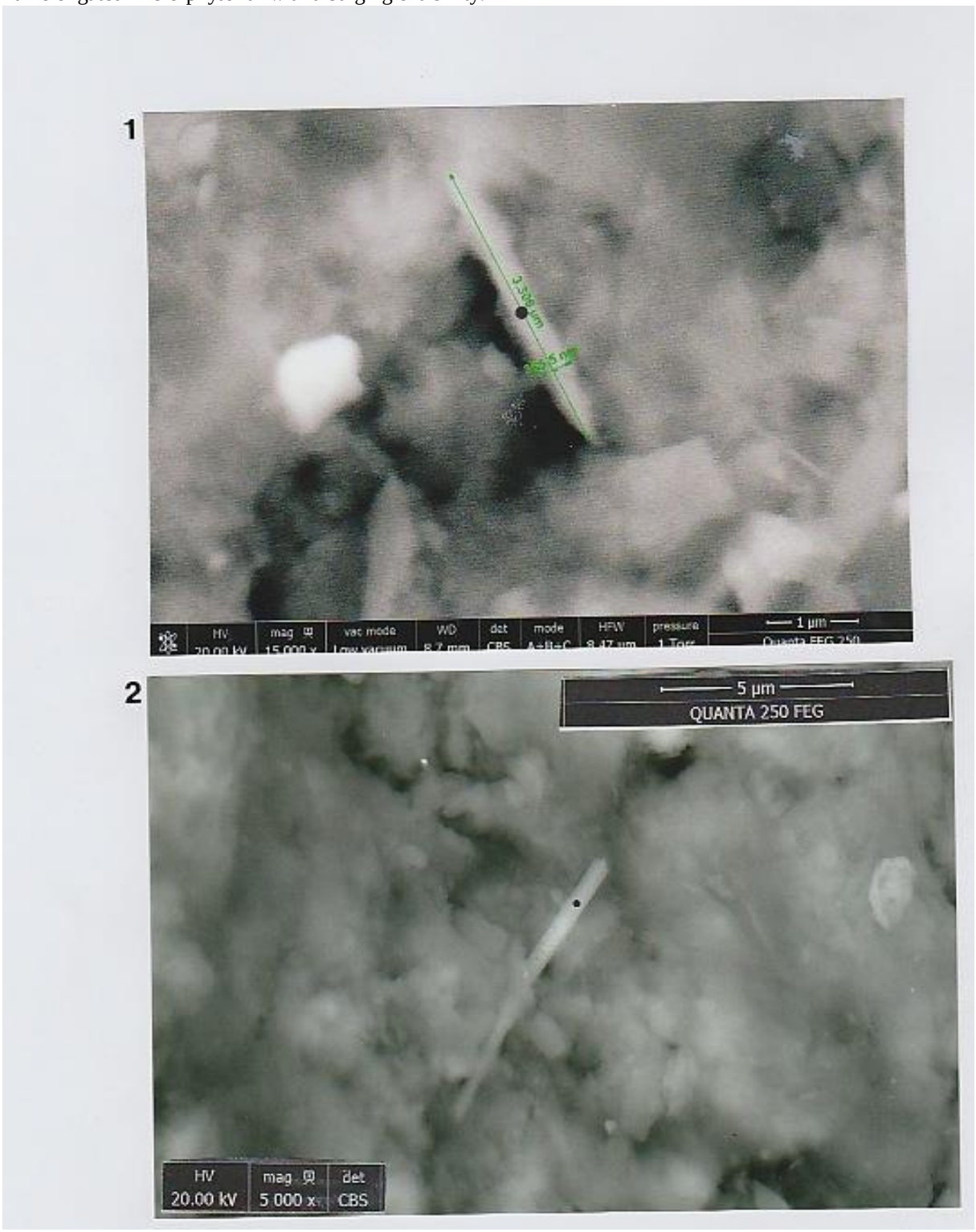

Figure 6. An elongated micro-phytolith, with two squared extremities. *Above* : sem photograph (in CBS, 10000x) of the micro-phytolith. *Below* : spectrum of this phytolith at the black dot . Ti (two peaks) : titanium.

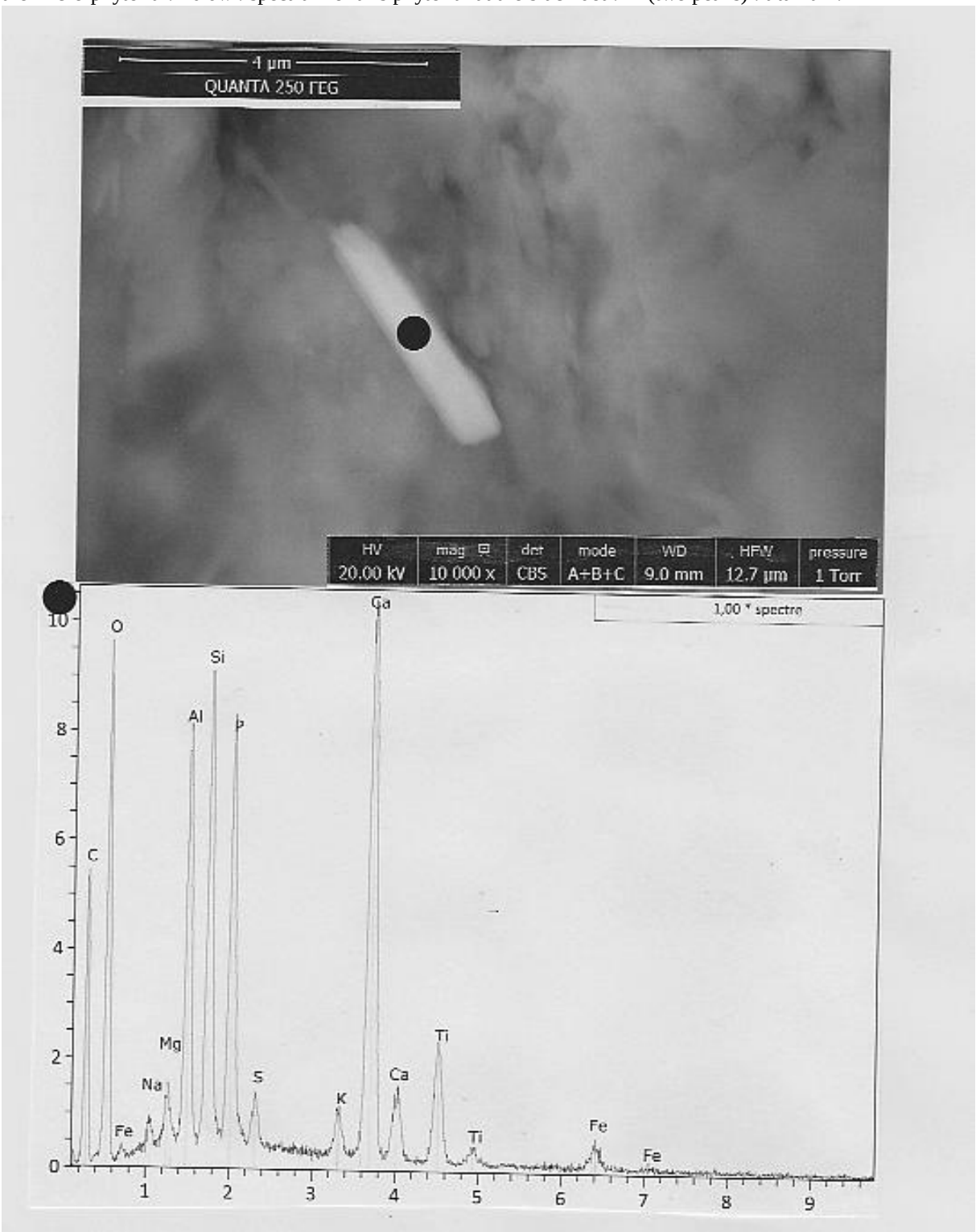

Figure 7. An oblong phytolith. *Above* : SEM photograph (in CBS, 4000x) of the elongated phytolith. 1, 2 and 3 are three calcite micro-particles ; SP : a spicule ; P : three micro-phytoliths with squared extremities ; SF : two elongated micro-phytoliths ; T : a triangular phytolith. *Below* : spectrum of the oblong phytolith at the black point.

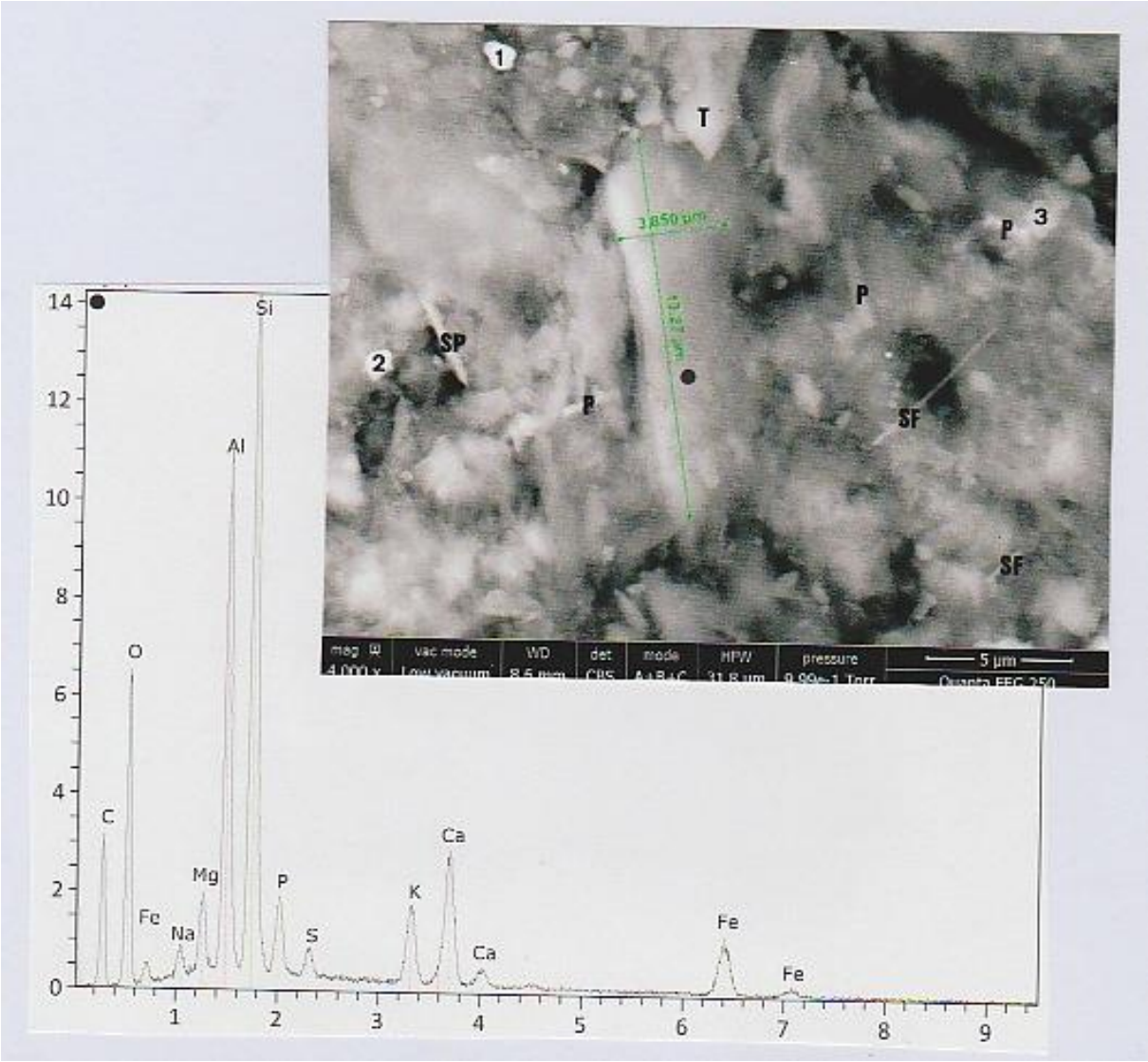

Figure 8. Examples of three triangular phytoliths. *Above* : SEM photograph (in CBS, 4000x) of the three triangular phytoliths T1, T2 and T3 (P : an elongated micro-phytolith). *Below* : spectrum of the triangular T3 phytolith at the black point.

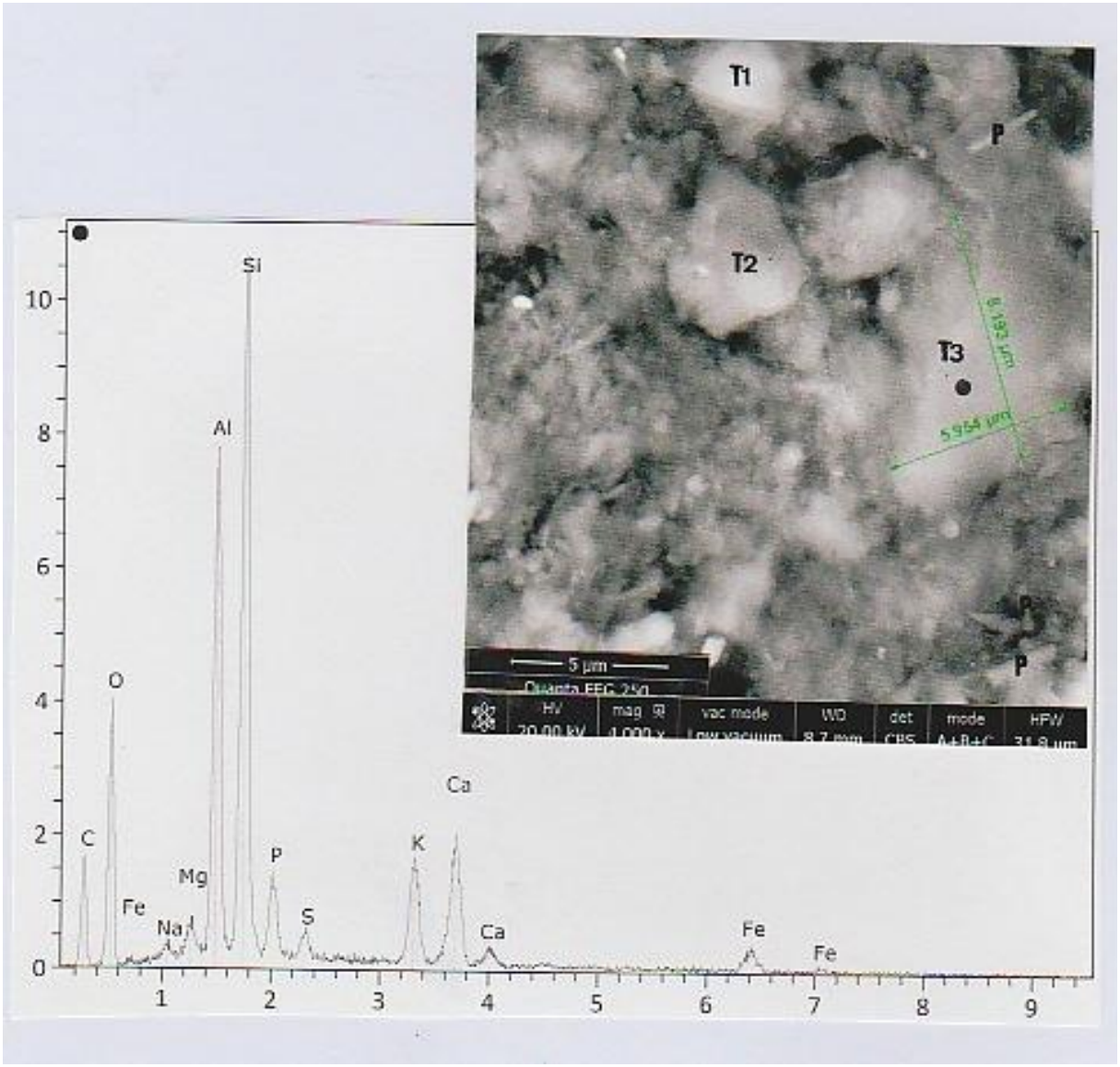

Attempts of species identifications of edible plants having these sorts of observed phytoliths:

Four species of plants, commonly eaten at the Middle-Age times, were tested ; their today representatives that are studied are as follows :

. overripe ribs (*Beta vulgaris*),

. spinach leaves (*Spinacia oleracea*),

. green leek leaves (*Allium porrum*),

. asparagus tips (*Asparagus officinalis*).

The overripe rib studied had micro-phytoliths with adequate forms (Figure 9) ; but the corresponding spectrum shows a special elemental composition (with a main peak of potassium, and a lower peak of chlorine).

There are numerous micro-phytoliths in the spinach leaves studied, but they are of little size (about 1 µm) and rounded in form (Figure 10). The corresponding spectrum shows also a special elemental composition, with a main peak of potassium and two lower peaks of calcium and magnesium (there are also some traces of iron).

Among the four edible plants studied, leek leaves are the only one that had an adequate triangular phytoliths of silica composition. Figure 11 shows today samples of leek leaves. Some part of the surface of one of them is observed in SEM at low magnification (100x), and the global corresponding spectrum shows a majority peak of calcium. Effectively (Figure 12), most of the phytoliths covering the leaf surface are rounded in forms, with a calcium carbonate composition ; but several triangular phytoliths can be observed (Figure 13), and their compositions are of silica (in the example

chosen, phytoliths numbers 6 and 7 are so thin that the calcium carbonate of the substrate appears).

Long micro-phytoliths (LMP) of asparagus tips show remarkable similarities , both in form and composition, with those already described (photograph 1 of figure 5) that are loaded on the PD surface.

Figure 14 shows some samples of coloured asparagus stems in optical microscopy, together with one of them in SEM at low magnification (50x). Relatively important pieces of matter are seen in an area of one deposit at the sample surface (Figure 15), whose elemental analysis shows two main peaks of potassium and sulphur ; the figure 15 SEM photograph shows at least five long micro-phytoliths, which have the LMP characteristics (relatively long size, uniform diameter of one to three µm, relative brightness to electrons in CBS). Elemental composition of the LMP number 2 - compared to that of the sample substratum (Figure 16) - is also characteristic, with two mean peaks for potassium and (enhanced) sulphur. The spectrum of the LMP number 3 (Figure 17) is the same than that of LMP number 2.

Macles of calcium oxalate.

At least three macles of calcium oxalate were found at the PD surface. The biggest one is shown on the SEM photograph of Figure 18. The main dimension of the macle is about 12 µm, and it is composed of two sub-parts ; one can distinguish inside little crystals of prismatic or cubic forms. Elemental analysis of these two sub-parts is summarized in the spectrum under the photograph : the calcium peak is enhanced, in comparison to its value in the calcium phosphate background ; the main mineral component is that of an aluminosilicate (relatively)-rich in iron and with titanium traces, but the oxygen peak is elevated. We deduce from the examination of this spectrum that the macle is mainly constituted of crystals of calcium oxalate.

Figure 18. Macle of calcium oxalate. *Above* : SEM photograph (in LFD, 8000x) of macles of calcium oxalate crystals (dots indicate areas in the two macle parts where elemental analyses were realized). *Below* : the corresponding spectrum.

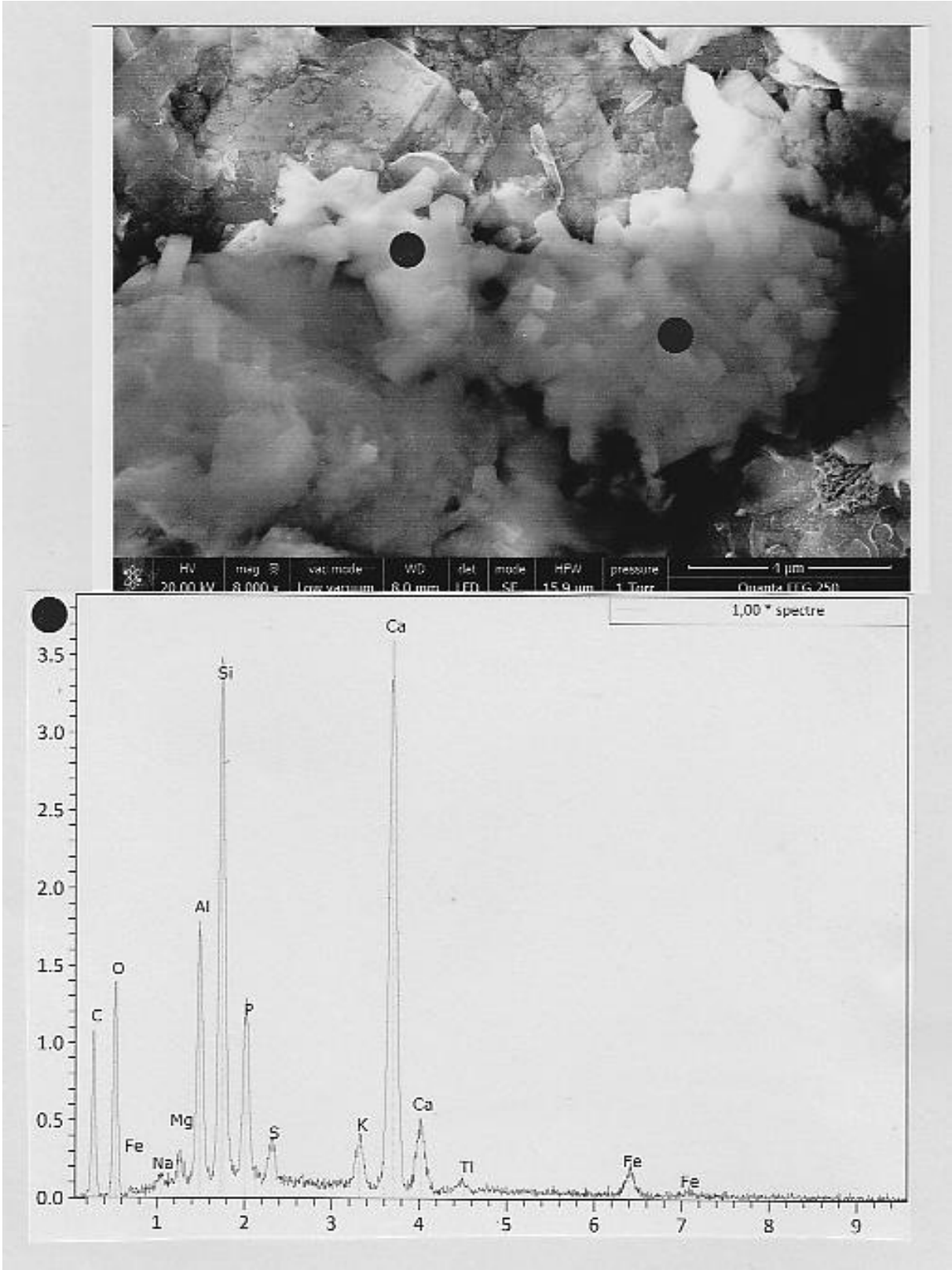

In plants, macles of calcium oxalate are found in some genus of the Polygonacae family, mainly (for edible plants) in rhubarb and in sorrel (*Rumex acetosa*).
Figure 19 shows some part of a today sorrel leaf epidermis; numerous macles are visible inside the leaf. Elemental analysis of these macles shows that they are effectively constituted of calcium oxalate (elevated peaks of calcium and oxygen on the spectrum, under a main potassium peak).

Starch grains.
Numerous (relatively big) starch grains are deposited on the PD surface. Figure 20 gives an example of such observations. Starches are round in forms, and their sizes reach and generally exceed 60µm of diameter; they can be distinguished (in CBS) from the background by their relatively clear appearances. They are kept here, despite of their fragile organic compositions, under a thin film of more resistant material (mainly of calcium); this fine coverage renders difficult the study of their own proper elemental compositions. About one thirty of them are observed in the explored area. A remarkable observation about their distributions is that they are mainly spread out, side by side, at the inferior limit of the enamel.

When trapped at the interior of a crevice (Figure 21), their elemental analyses are more easily feasible. The corresponding photograph of this figure shows at least ten big starches , contained in an elongated (of about 1mm of length) crevice; elemental analyses realized on these starches (at the interior part of the crevice) reveals substantial amounts of carbon and oxygen, despite the main calcium phosphate composition of the substrate. It is that sort of approach that was adopted in a recent study concerning starches of the dental plaque (**7**); more subtle morphological determinations of the species of the starch grains deposited on the surface of the dental plaque were made in some cases **(8)**

Figure 20. *Above* : starch grains located at the inferior limit of the enamel. The SEM photograph (in CBS, 80x) shows the enamel (E) limit (s :vertical breaks) where starches (G) are spread out ; GO-G6 surround the diatom D ; G2 and G3 surround the top of the A1 fish-bone, and G5 is located near the basis of the A2 fish-bone (all these are contained in the rectangular area indicated). *Below* : spectras of the seven pointed starches (the calcium content is more elevated than that of the calcium phosphate of the background).

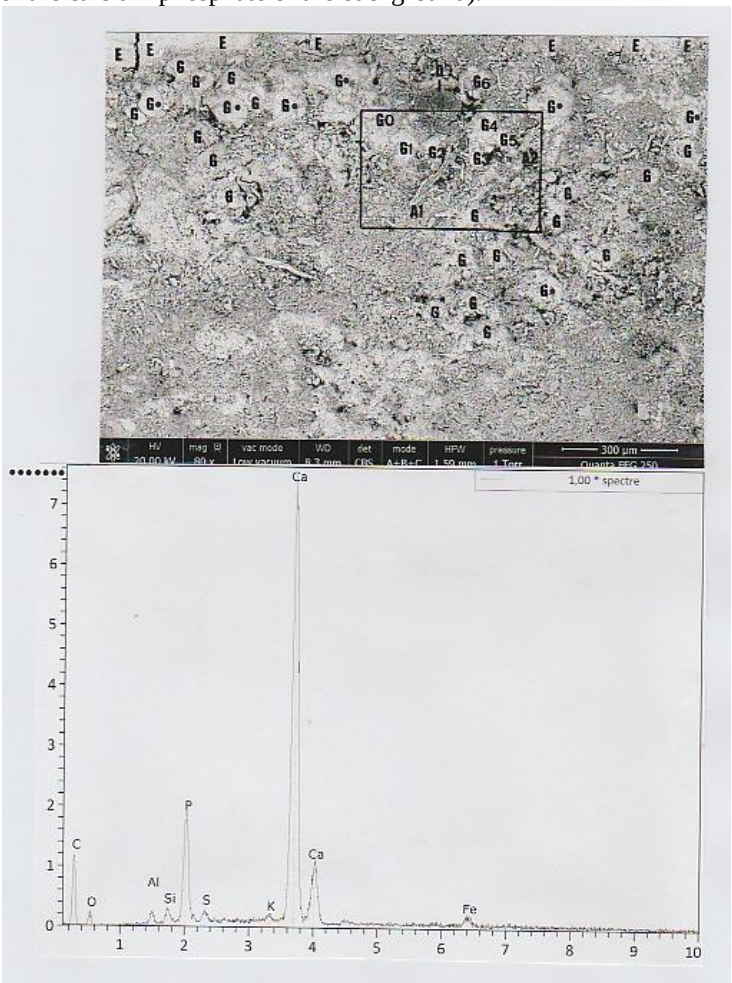

Figure 21. SEM photograph and spectrum of the starch grains trapped at the interior of a crevice. *Above* : SEM photograph (in LFD, 150x) of several starches in the crevice (dimensions are in µm) ; the black dot indicates locations in the five starches where elemental analysis are realized. *Below* : spectrum of the five starches.

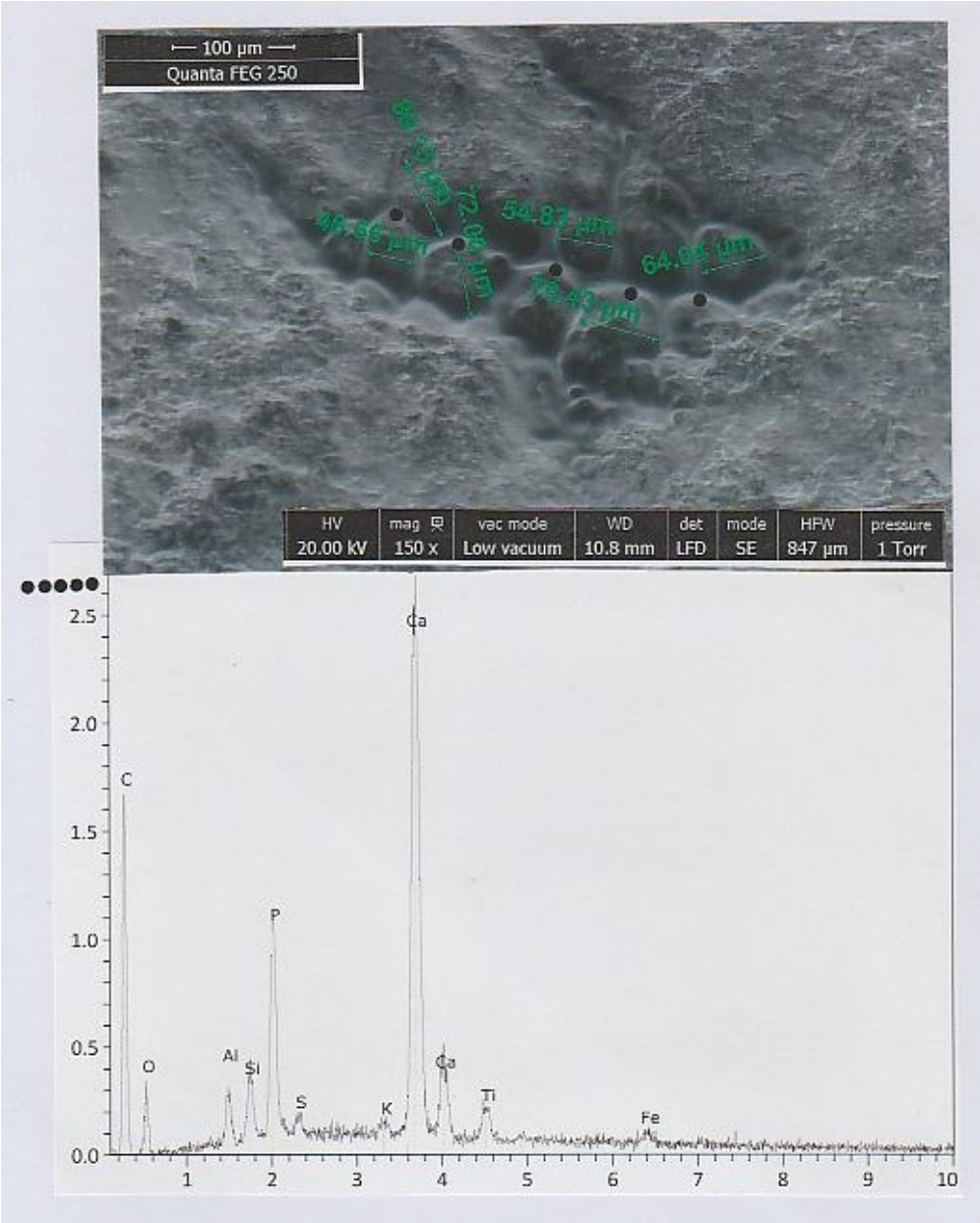

Very numerous starches of more little sizes (diameters of 1 to 7 µm) were detected on the PD surface; they can be trapped in holes or are relatively free on the PD surface. Figure 22 gives an example of one of them, trapped in a hole. By its form (round) and the absence of silicification of its wall, it can be distinguished from the three neighbouring spores of similar sizes. Its spectrum is relatively rich in organic matter (carbon and oxygen), but contaminated (because of the very little size of the micro-grain) by minerals and by the calcium phosphate substratum.

At what edible species of plant these starches belong to? Figure 23 shows the morphological appearance of starches in a today crust of bread (of wheat : *Triticum* sp.). The starches sizes are very heterogeneous in diameters, but not exceed 30µm ; most of them are deformed (elongated and winding forms), because of cooking.
Figure 24 shows the morphological appearance of starches in a today wheat flour. They are distributed in three sizes category (Brigitte Gaillard, personal communication) : type A (>10µm), type B (10-2 µm) and type C (<2 µm). None of them exceed the size of 35 µm of diameter.

Figure 25 shows the compared morphological appearance of starches in a today rye (*Secale cereale*) flour. The biggest ones (rounded or ovaloïd in forms) attain a diameter of 45 µm or more, according to [**9**]. It is the main reason why we think that the starches (at least for their bigger forms) observed on the PD surface belong to rye flours.

This diagnosis is less easy for starches of more little sizes. Possibly, most of them were trapped in PD holes by the way of some form of granulometric filtering. Drying out surely intervenes also to produce starches of reduced diameters.

Photograph of Figure 26 shows a particular group of starches, trapped in a PD hole. There are at least fourteen starch grains, each of little size (500 nm to 1 µm of diameters), in the pile. Their morphologies (when one can to discern its) is that of bipartite form, with a major *corpus* defined by angular borders.

Figure 22. An example of a micro starch grain. *Above* : SEM photograph (in CBS, 8000x) of the micro starch grain (numbered **1**). S: three spores; P: three short micro-phytoliths; T : three triangular phytoliths. *Below*: spectrum of **1**.

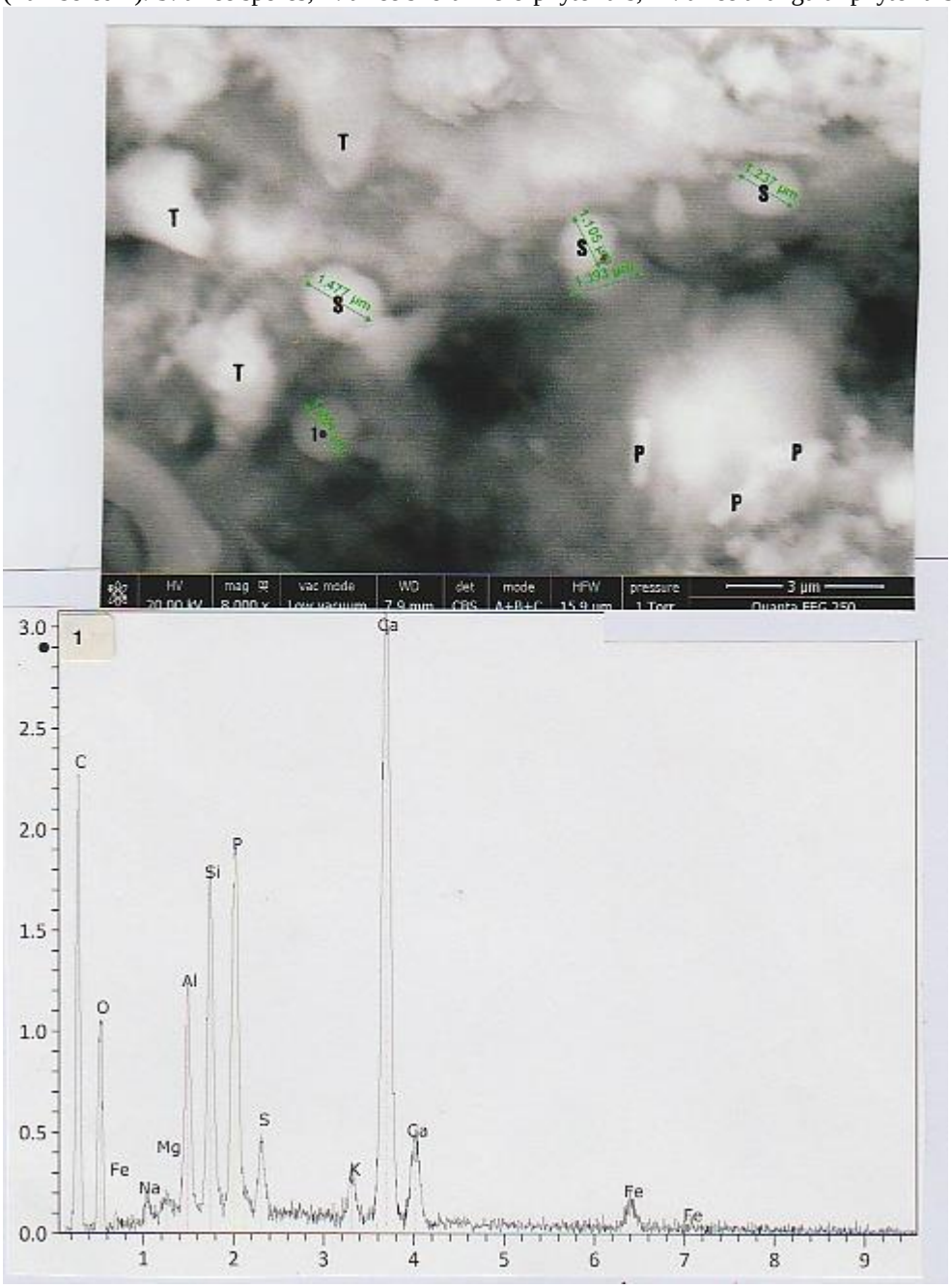

Figure 26. Garden peas starch grains. *Above* : SEM photograph (in LFD, 8000x) showing a group of garden peas starches (Si : a silica particle ; S : a spicule micro-phytolith ; P : a long micro-phytolith) ; the circle indicates the center of the group of starches where elemental analysis is realized. *Below* : spectrum in the circle.

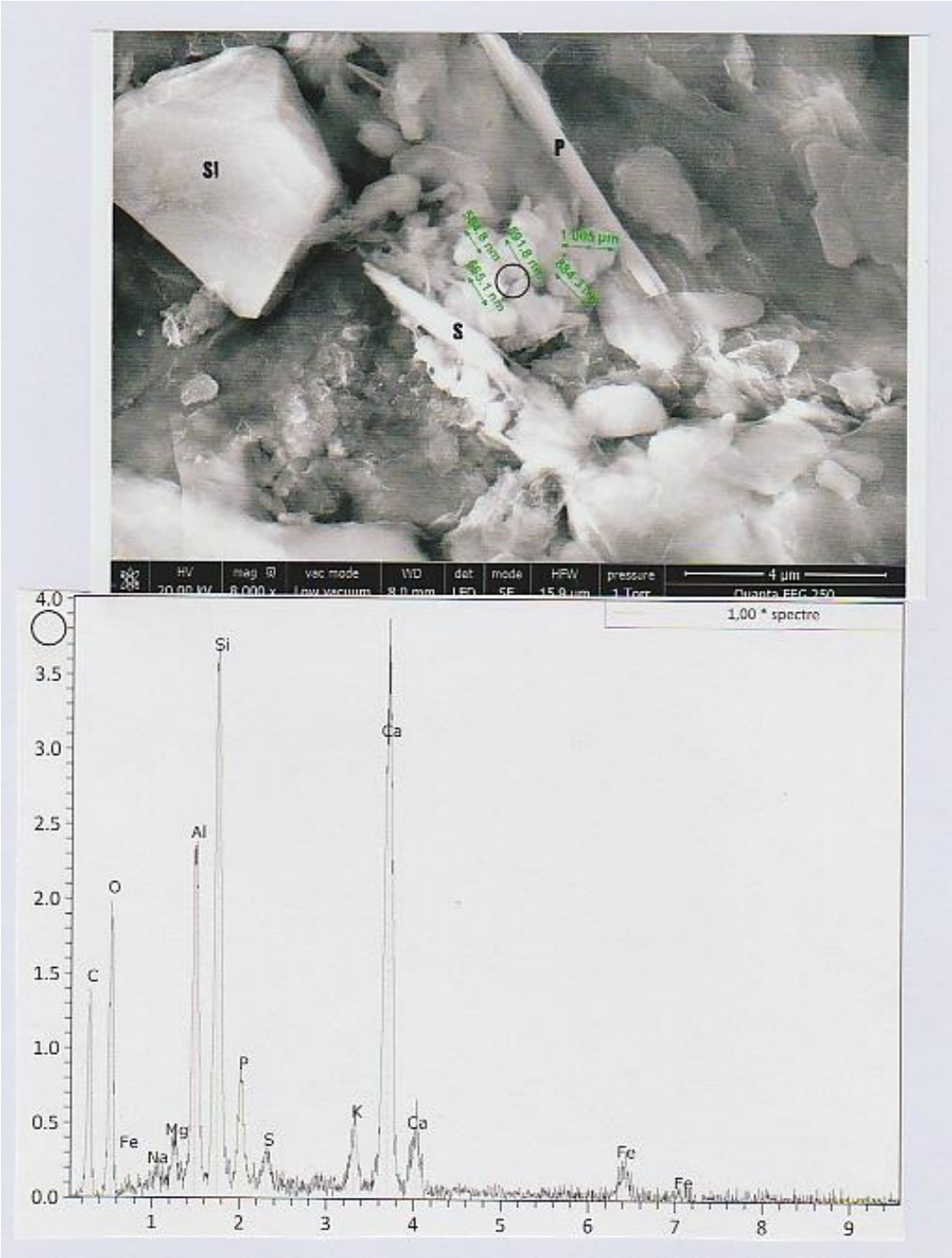

Elemental analysis of the pile shows that it is constituted by an organic matter (carbon and oxygen peaks), on a general background of aluminosilicate and calcium phosphate.

For comparisons, Figure 27 shows the starch grains morphology of today dry green garden pea (*Pisum sativum*) slice. Starches show here their characteristic bipartite form, with a bulging *corpus*.

Flat bones.

Figures 28 and 29 show an example of a bone residue (O), deposited on the PD surface. It is a little elongated (24.8 µm of length, on 6.8 µm of width) bone fragment, with a typical calcium phosphate composition.

There are evidences of two internal fractures along to its long axis. The presence of at least twenty (O1 to O20) neighbouring micro-particles, of similar aspect

and composition, attests that this bone fragment was broken open. There is one micro-pore in O (and two in O4) ; that suggests some form of bone cooking (**10**).
There is no evidence at the surface of O of any Haversian structure ; so we conclude that it does not represent some form of a compact or spongy bone.

Figure 30 shows the morphological appearance of some today macrofragments of a cooked chicken rib ; the general aspect in SEM of this flat bone is similar to that observed for O. When a more-cooked part (number 1) of this bone is compared to that of a less-cooked part (number 2), the corresponding spectras (Figure 31) show effectively a less elevated peak of oxygen for 1 than for 2, and a Ca/P proportion for 1 that is more distant than for 2 to that of the normal (non-heated) stoichiometric composition (**11**).

Fish-bones and fish-scales.
On the photograph of Figure 32 (which is an enlargement of the rectangular area indicated in figure 20) one can see two elongated fish-bone fragments (A1 and A2). They **Figure 28**. A flat osseous fragment. **1** : SEM photograph (in CBS, 1000x) of the osseous (O) fragment. **2** : an enlarged view (3000x) of O. O1 to O20 : osseous micro-fragments ; P : pore in O (P1, P2 : two pores in O4) ; K, K' : two fractures in O.

Figure 29. Dimensions and spectrum of O. *Above* : the same SEM photograph as that seen in the previous figure. *Below* : the O spectrum, at the point indicated.

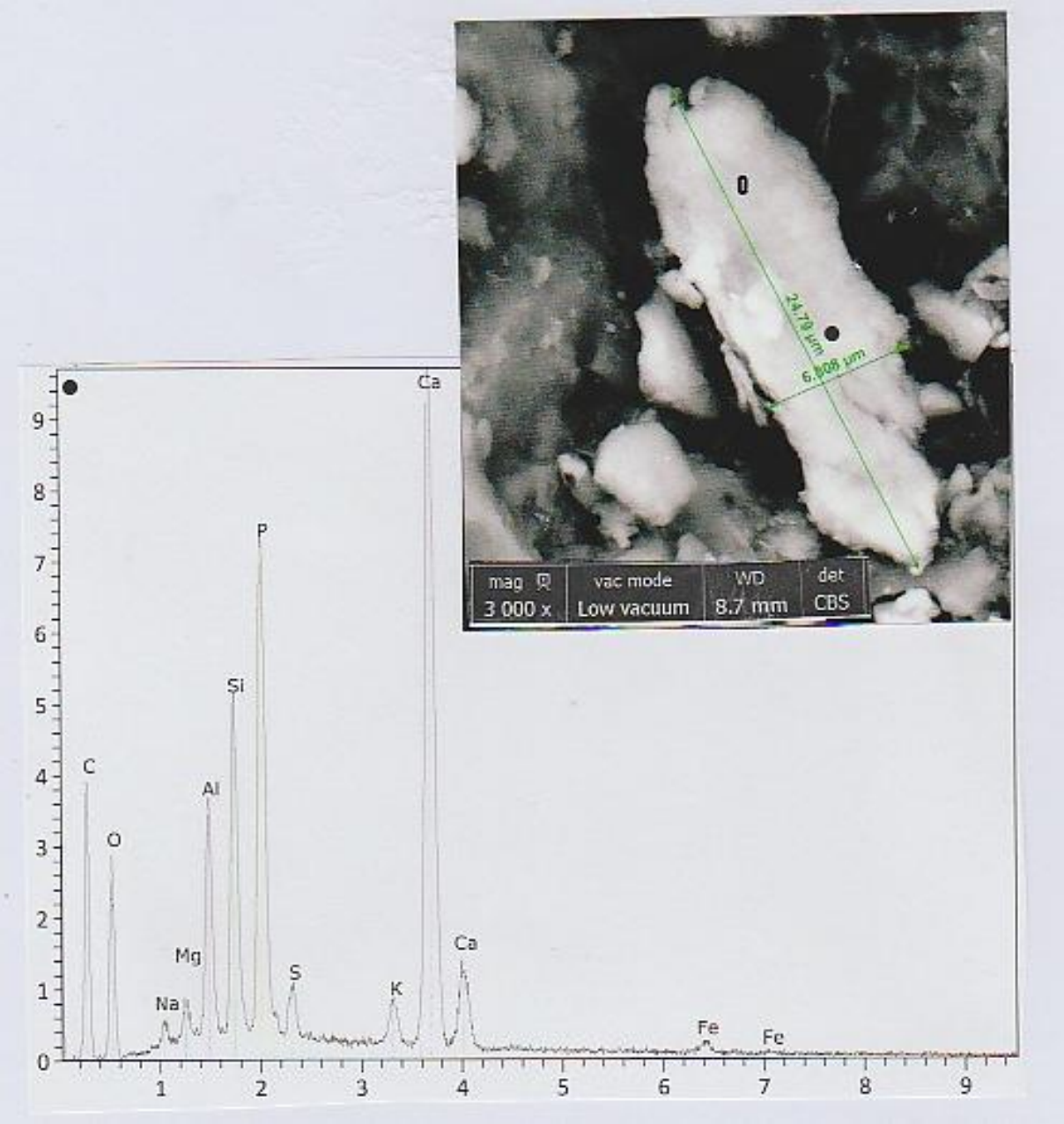

Figure 32. Enlargement of the rectangular area indicated in the photograph of figure 20. This SEM photograph (in CBS, 300x) shows the two fish-bone fragments A1 and A2. G1-G5 are five rice starch grains (as previously indicated) and G two other unomenclatured rice starches. D : three diatoms ; S : three spicules ; P : a silica phytolith.

are lengthen in forms (A1 = 170 µm and A2 = 60 µm) and their aspects are very unusual : bright to electrons in CBS, their *corpus* consists of several rows of individual particles – each of about 5 to 10 µm – regularly aligned along the separate rows.
These sorts of structures are very similar to those already described (**12**) concerning powders of micro fish-bones heated at elevated temperatures. Elemental analysis of A1 (Figure 33) confirms that this fish-bone is mainly constituted of calcium phosphate.

For comparisons, Figure 34 shows the morphological appearance of a cooked today fish-bone extremity of trout. EDX analyses show that the calcium phosphate component is greatly enhanced in the more cooked part (number 2), compared to the less-cooked part (number 1) of this fish –bone extremity ; there is also evidence of some longitudinal orientation of the calcium phosphate particles along the fish-bone axis (but the cooked temperature that was used were comparatively less lower than that for the reference material).

Figure 35 shows seven (E1 to E7) micro fish-scales , grouped in a little area of the PD [E3,E4,E5 and E6 are lumped together]. They are micro-fish scales because, oblong in forms, their maximal lengths are of about 2.5 µm (some evidence of concentric micro-stripes are visible for E7). EDX analysis of the micro-fish scale number E1 shows that it is mainly composed of calcium phosphate (with an enhanced calcium peak).

For comparisons, Figure 36 shows the morphological appearance of a cooked today fish-scale (of about 1.5 mm of diameter) of trout. This fish-scale shows the typical fish-scale morphology : it is rounded in form , and with well visible concentric stripe layers (but its upper part is completely destroyed by the heating). Elemental analysis of this fish-scale confirms that it is mainly constituted of organic matter (elevated carbon peak), with calcium phosphate (the two peaks of calcium and phosphorus are of the same height).

Figure 33. Some part of the A1 fish-bone. *Above* : SEM photograph (in CBS, 1200x) of a segment of A1 (D : a diatom ; S : a spicule). The black dot indicates the location in A1 where EDX analysis is realized. *Below* : spectrum at the black dot.

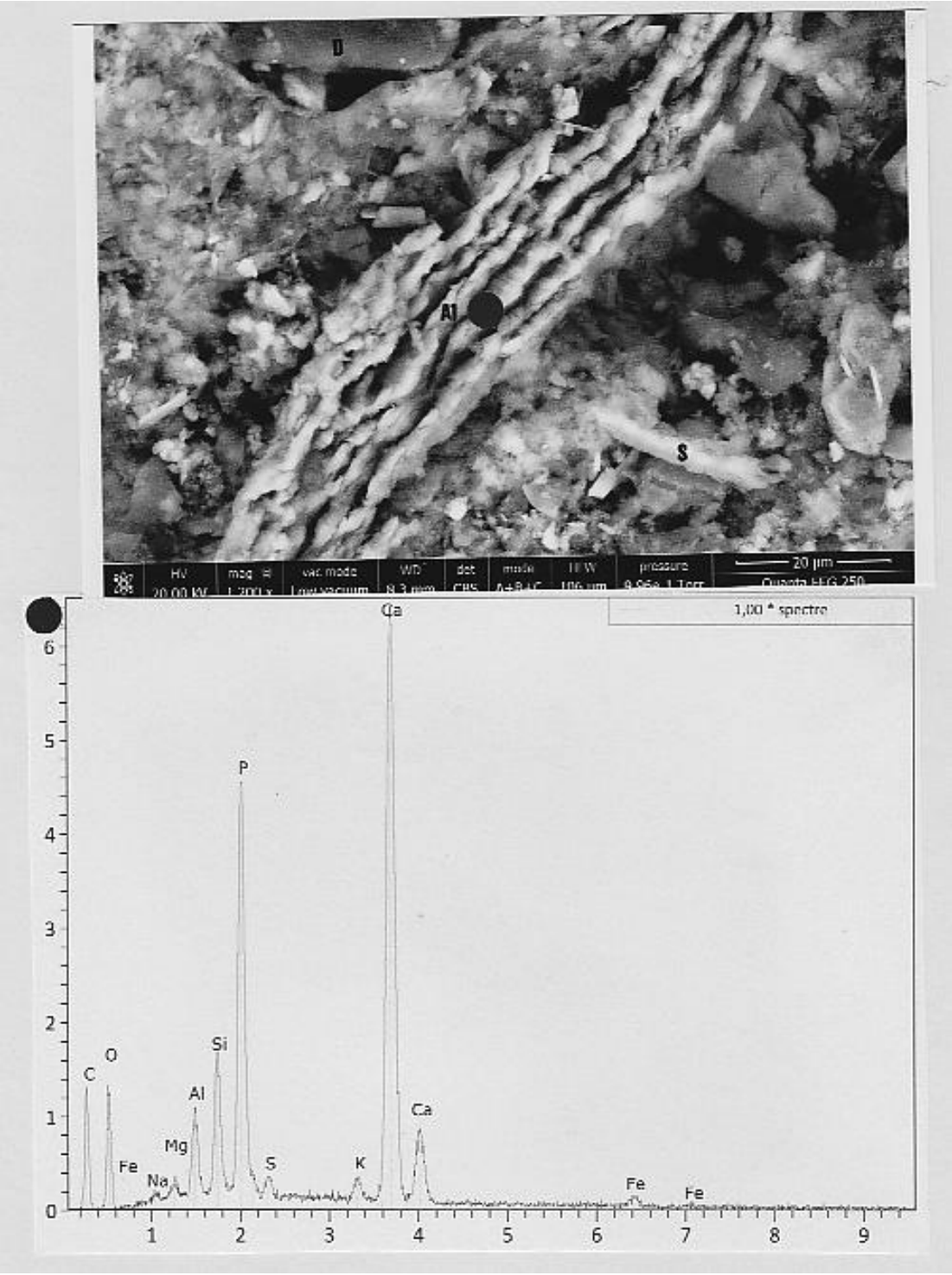

Figure 35. Seven fish-scales. *Above* : SEM photograph (in LFD, 16000x) showing seven (E1, E2, E3-6 and E7) micro fish-scales. The black dot in E1 indicates the location where EDX analysis is realized (elemental analyses of the small drops covering E1 are indicative of greases). *Below* : spectrum at the black dot.

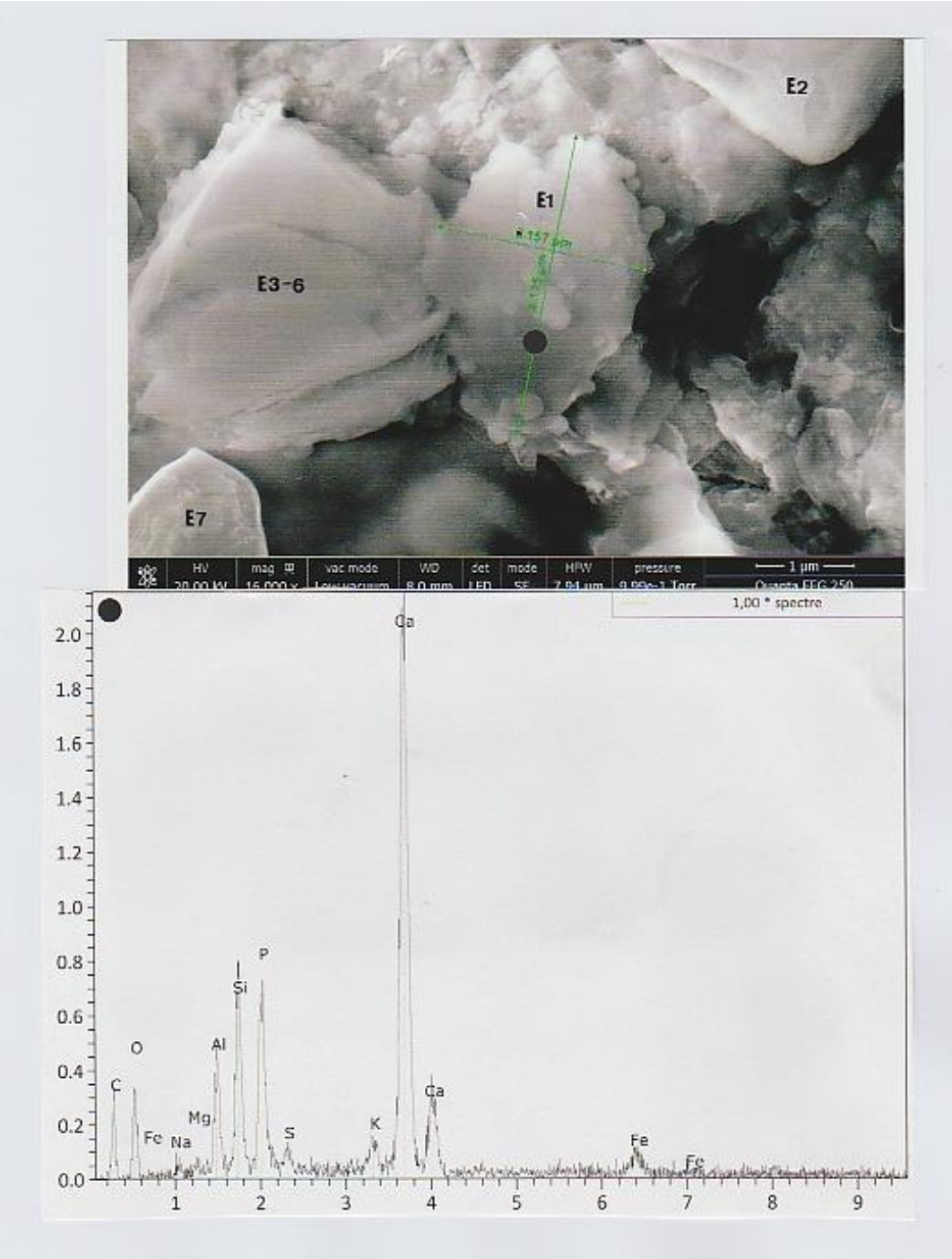

It is possible to determinate the fish-species from the fish-scale pattern (**13**). The seven fish-scales presently observed on the PD are probably micro fish-scales of tench (*Tinca tinca*).

Pollens.

We found only two pollen grains on the PD surface. By their size and morphology they can easily be distinguished from the spores (Figure 37), that are numerous on the PD surface. Most of these spores are of recent origins, especially those with echinulate ornamentation.

The first pollen grain found on the PD surface (trapped in a hole) is represented on Figure 38. It represents a typical pollen grain (**14**), of prolate form. In this quasi-equatorial view, the maximal length of this pollen grain is of about 4.2 µm and its width of 3.2 µm. Two elongated longitudinal apertures are visible on this view (and probably a third, that cannot

be seen, at the other side). The ornamentation of the wall of this pollen is greatly altered, and his spectrum shows mineral deposits.

Figure 39 shows the polar view of a pollen grain of chestnut tree (*Castanea sativa*) : its diameter (about 10 µm) is the same that a pollen of reference of these species, and one can see in that view the identifications of the three characteristic sulcis (of this trisulcate pollen form).

We have explored pollens contained in a today chestnut tree honey (Figure 40). All the pollen grains found in it are effectively pollens of *Castanea sativa* ; the photograph of this figure shows several pollen grains of that type in this honey (that are orientated in polar, equatorial or intermediate views).

Figure 37. Examples of spores found on the PD surface. **1** : SEM photograph (in LFD, 8000x) of samples of the three sorts of spores found : S1 (spherical spores : about 1 µm of diameter ; subtle wall ornamentation) ; S2 (ellipsoid spores : about 2µm of great diameter ; some fine wall ornamentation ; S3 (spherical spores : about 5µm of diameter ; echinulate ornamentation) ; the two other spores showed (S) are of type S3. **2** : SEM photograph (in LFD, 3000x) showing numerous spores (S) of type S3 ; T is a mould syncytium. **3** : spectrum of the syncytium (of organic matter, highly calcified).

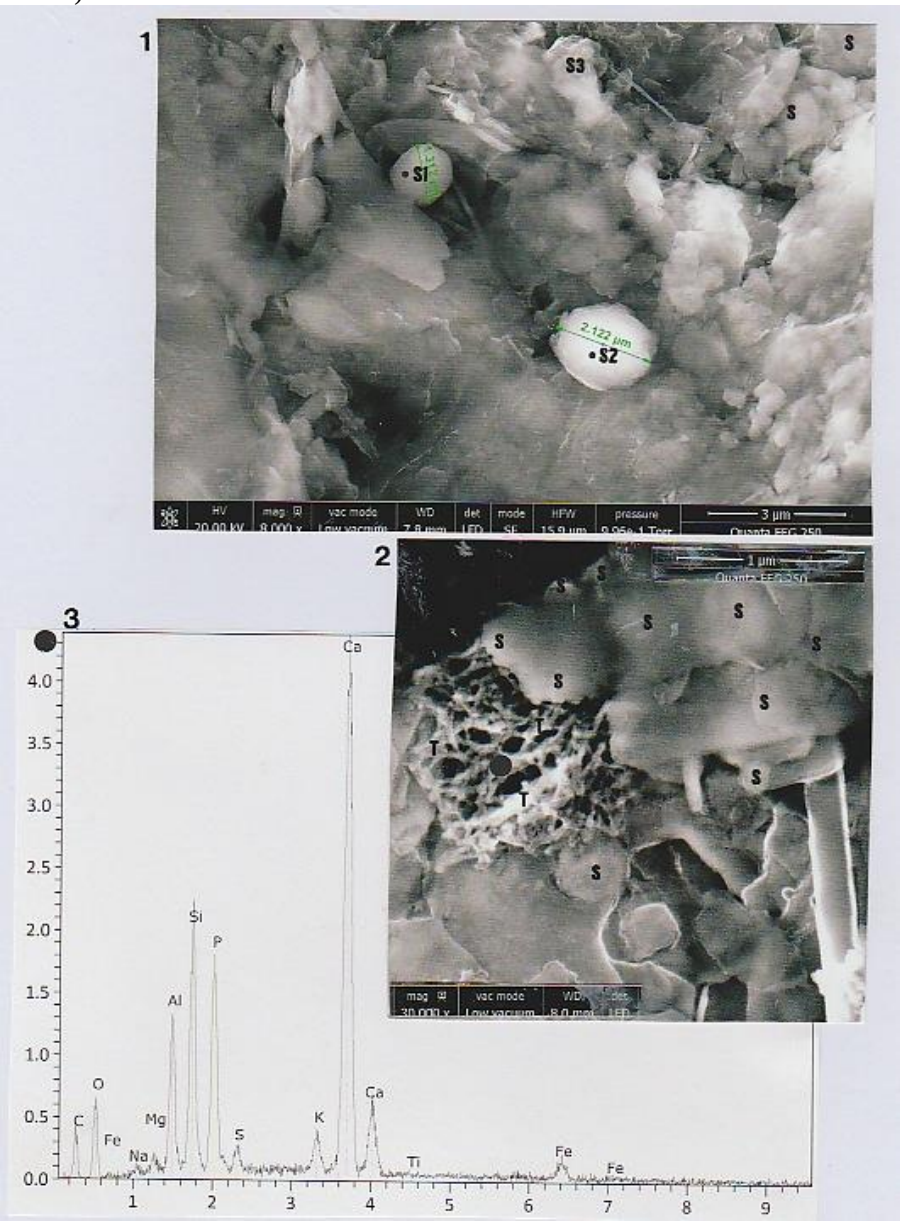

Figure 38. The first pollen grain observed. *Above* : SEM photograph (in LFD, 16000x) of this pollen grain (S : the two longitudinal grooves). *Below* : spectrum at the black point.

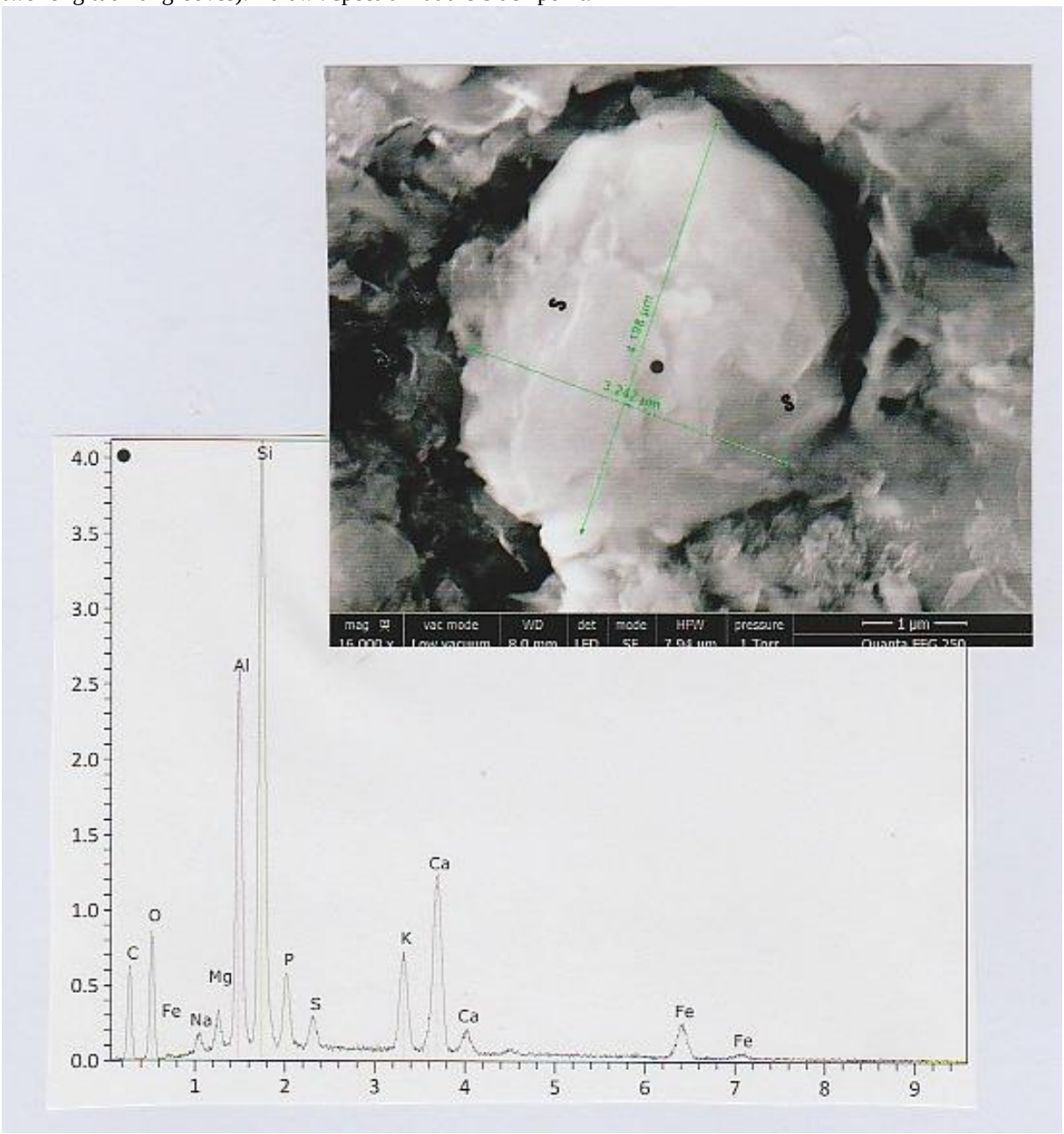

Figure 39. The second pollen grain observed. **1** : polar view (in optical microscopy) of a pollen grain of *Castanea sativa* of reference. **2** : SEM photograph (in LFD, 4000x) of the second pollen grain observed. S : the three grooves identations ; AP2 indicates a probable third pollen grain, largely covered by most superficial particles. The spectras of the two neighbouring sub-particles with angular outlines (indicated by little points) are compatible to that of carbohydrates (sugars). **3** : spectrum of this second pollen grain, taken at the black point indicated.

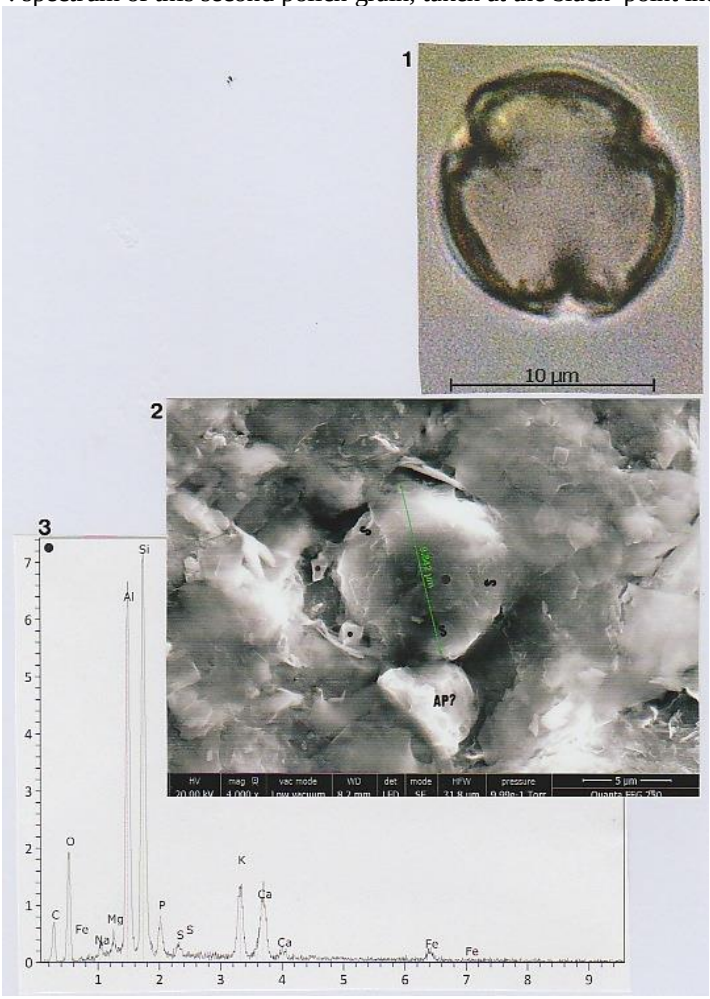

Diatoms:

There are numerous diatoms (we have analysed more than two hundred of these) on the PD surface. Figure 41 shows one of them, embedded at the PD surface. It is of ovaloïd form (about 20 µm of length on 15 µm of large) ; septas are not well visible in its *corpus*. The corresponding spectrum shows a main peak of silicium.

Figure 42 shows two (1 and 2) adjacent diatoms; septas of diatom number 1 are clearly visible. As both are covered by numerous micro-phytoliths and silica, or calcite, micro-grains, the main silicium peak of their spectras is accompanied by those of these corresponding minerals.

There are three main types of diatoms (**15**), concerning apertures of their frustule :

. type 1, said "perforate", where the frustule is perforated by pores,

. type 2, said "pennate", where the septas are relatively thin,

. type 3, said "septate", where the septas are more thick.

Figures 43, 44 and 45 show examples of diatoms of these three types, located at the PD surface.

Diatoms are often lumped in piles. Figure 46 shows one example of such a pile (comprising at least ten individuals diatoms belonging to the three types), located at the PD surface.

Presence of so many diatoms on the PD surface indicates the impurity of the drinking water. Diatoms in the dental plaque were already described (**16**), but in relationship to a marine environment.

A Chrysophycean cyst:

This observation is unique, but it permits us to establish the nature of the fresh water. Figure 47 shows this cyst : it is a rounded small (3 µm of length on 1.7 µm of large) *corpus*, linked to the algae wall by a little pedicule. Its spectrum is mainly of organic matter ; the cyst wall , strongly calcified, is covered by a fine film of mineral deposists.

Figure 41. A diatom. *Above* : SEM photograph (in CBS, 2000x) showing a fitted diatom; septas (SE) are not well visible. S: spicules; P: short elongated micro-phytoliths; SQ : groups of minerals, organized in packets or plaques. *Below* : spectrum of this diatom.

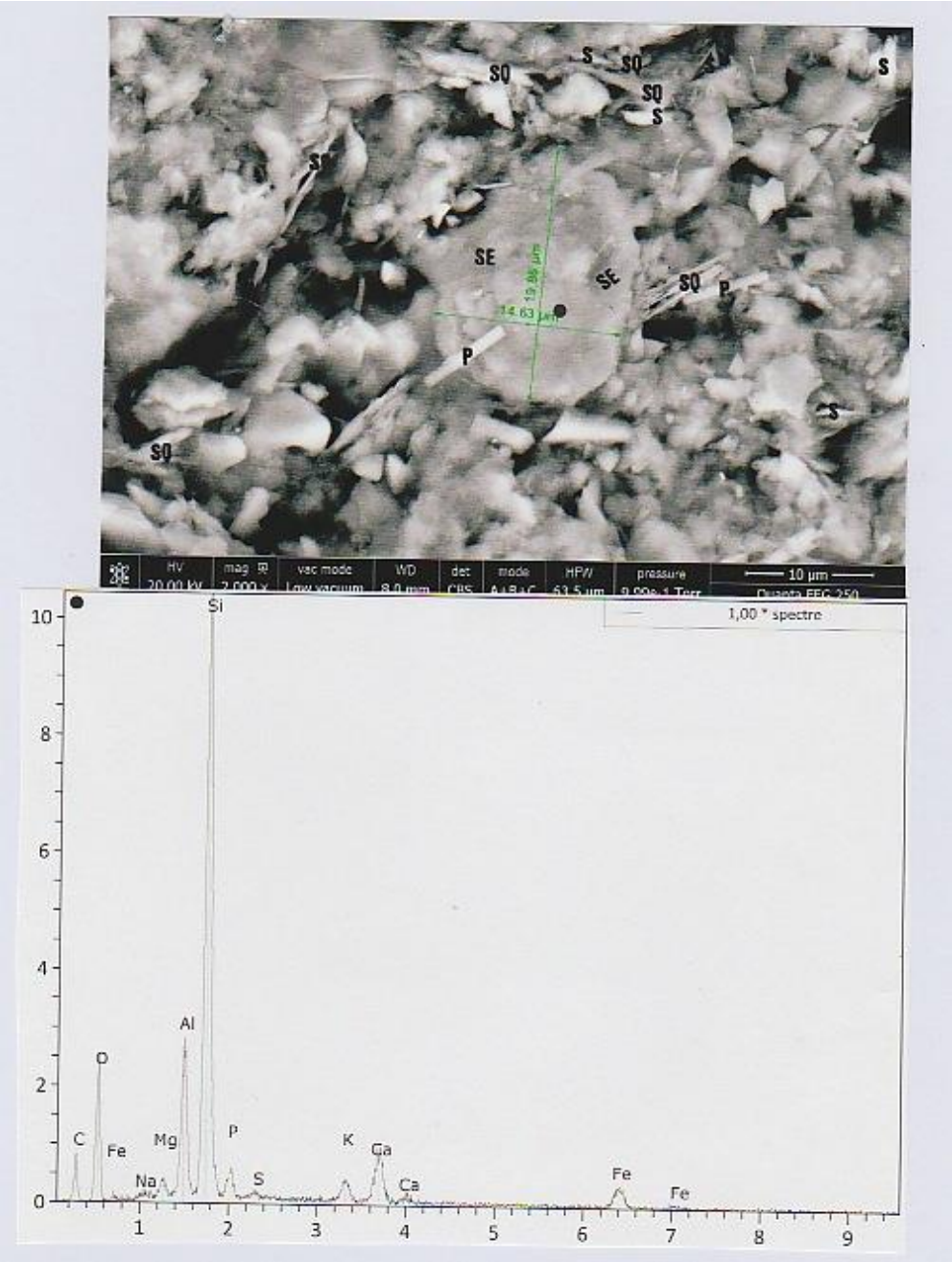

Figure 42. Examples of two diatoms (their limits are highlighted). *Above* : SEM photograph (in CBS, 2400x) of the two diatoms **1** and **2 .** Septas are visible in diatom number **1.** Micro-phytoliths (P), silica (G) and calcite (G') micro-grains cover the diatom surfaces. (the two little points in each diatom indicate the locations where EDX analyses are realized). *Below*: the two spectras of **1** and **2.**

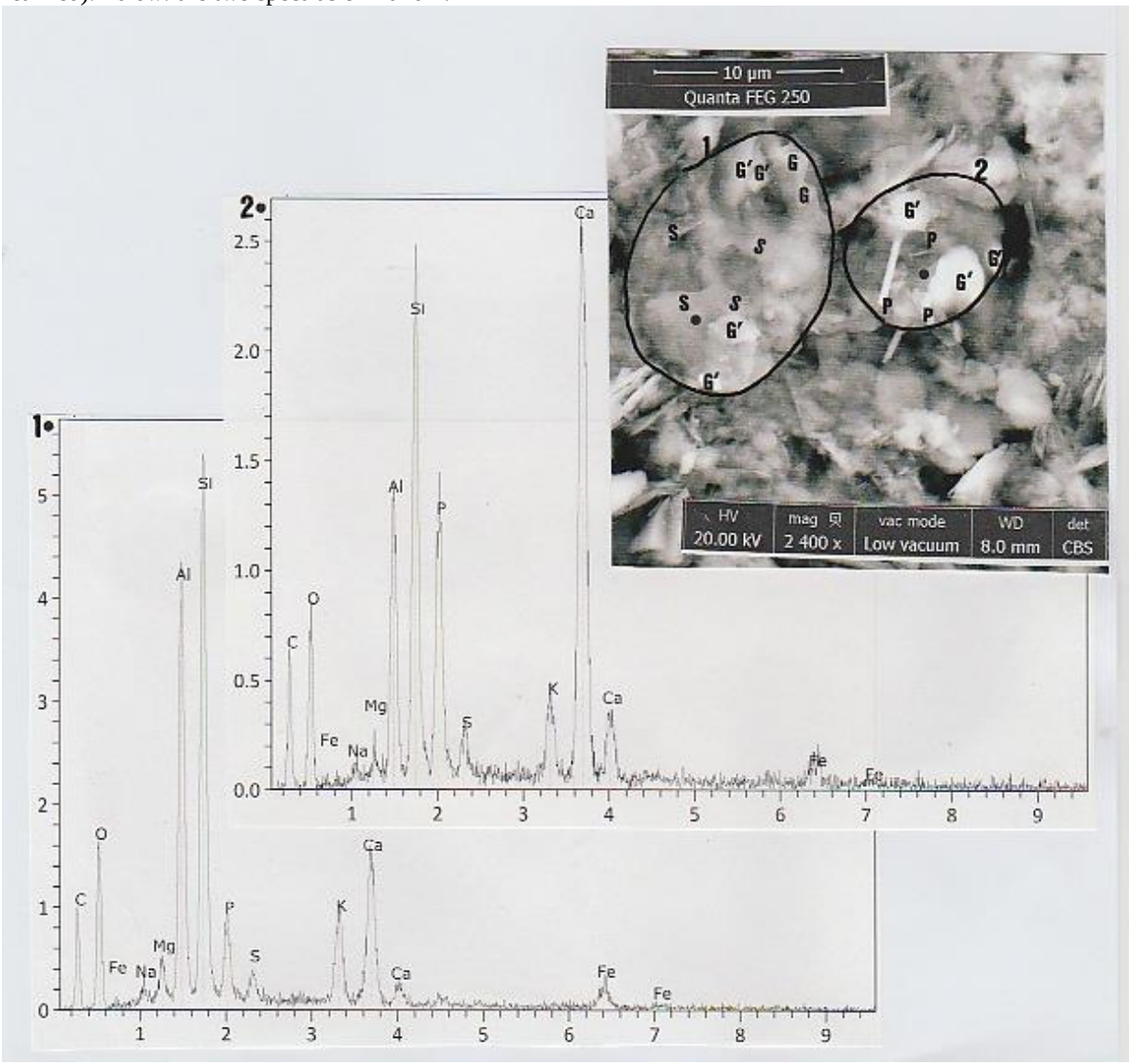

Figure 43. Example of a perforate diatom. *Above*: SEM photograph (in CBS, 5000x) of a perforate diatom (T: holes).*Below :* the corresponding spectrum. The intermediary photograph represents an artificially-coloured wall SEM view of a typical perforate diatom.

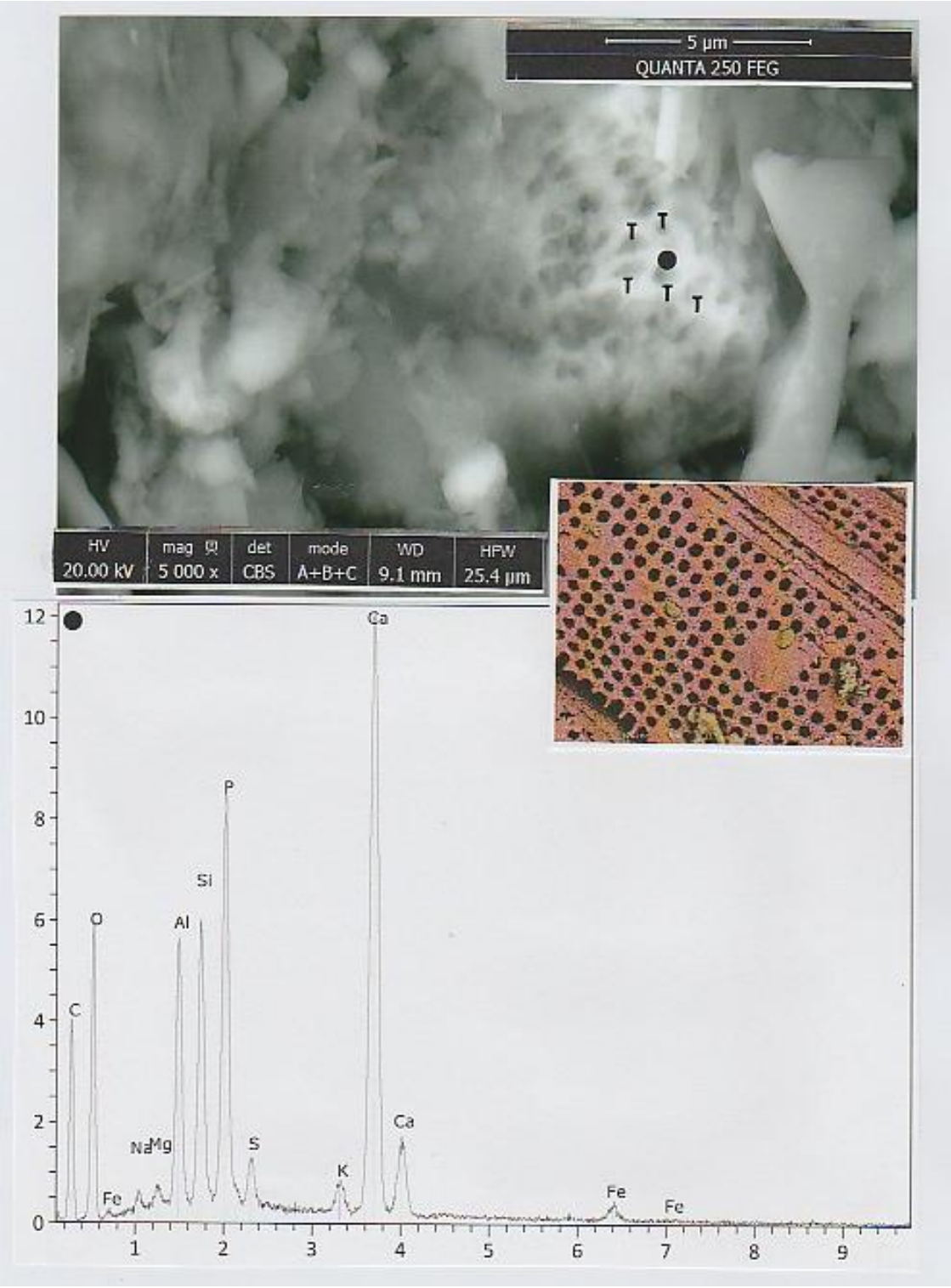

Figure 44. Examples of pennates diatoms. *Above:* SEM photograph (in CBS 400x) of a part of the PD (the rectangular area indicated is enlarged in the below SEM photograph). *Below* : SEM photograph (in CBS, 1600x) of this enlarged area; 1, 2, 3, 4 and 5 : the five diatoms (T : holes; S : septas). The lower right corner photograph is an artificially-coloured view of a typical pennate diatom.

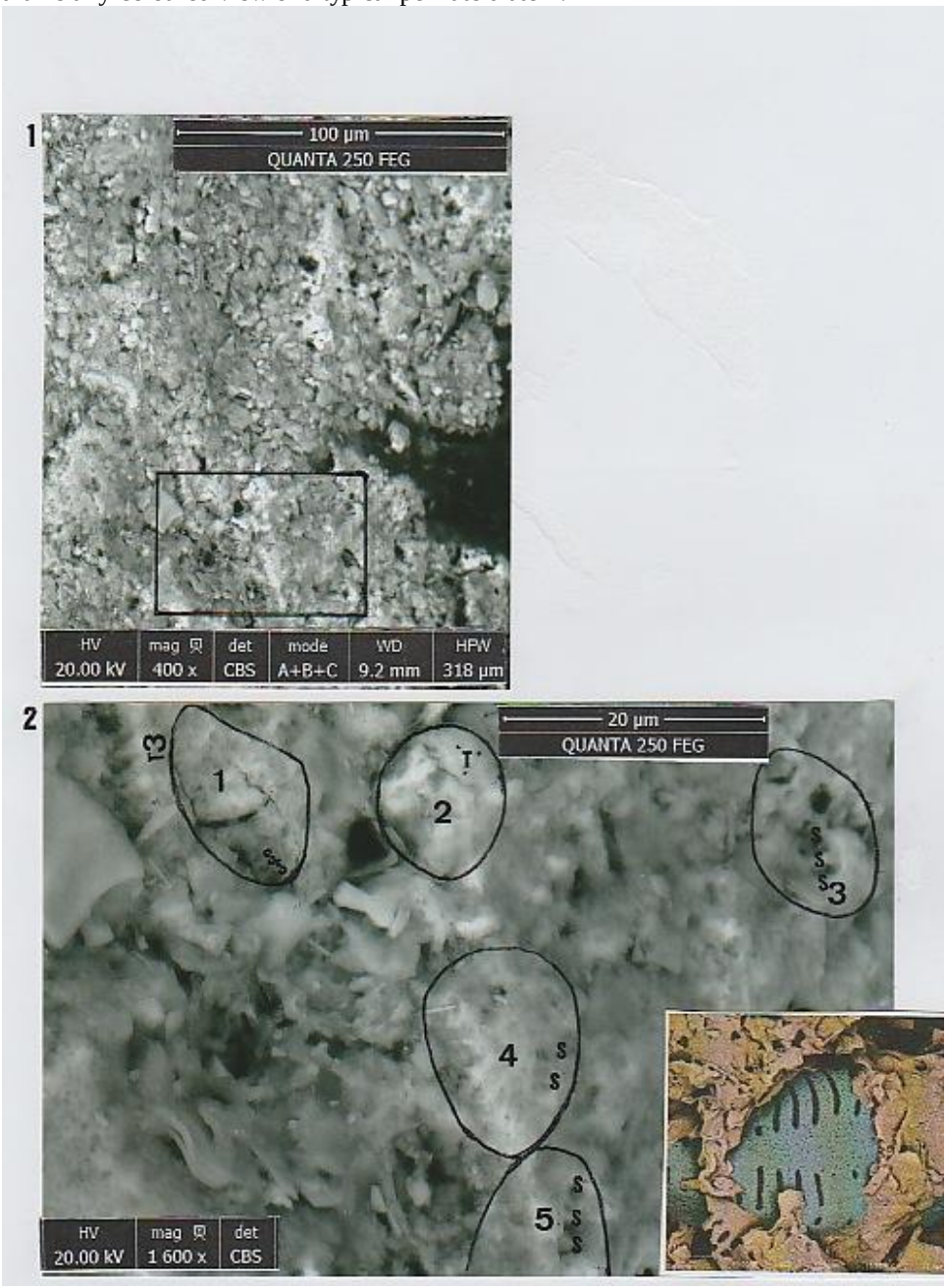

Figure 45. Example of a septate diatom. *Above***:** SEM photograph (CBS, 6000x) of a portion of the previous photograph, showing diatoms number **1** and **2** (=**1'**); S: septas in **1'**. *Below*: the corresponding 1' spectrum. The intermediary photograph is a SEM view of a typical septate diatom.

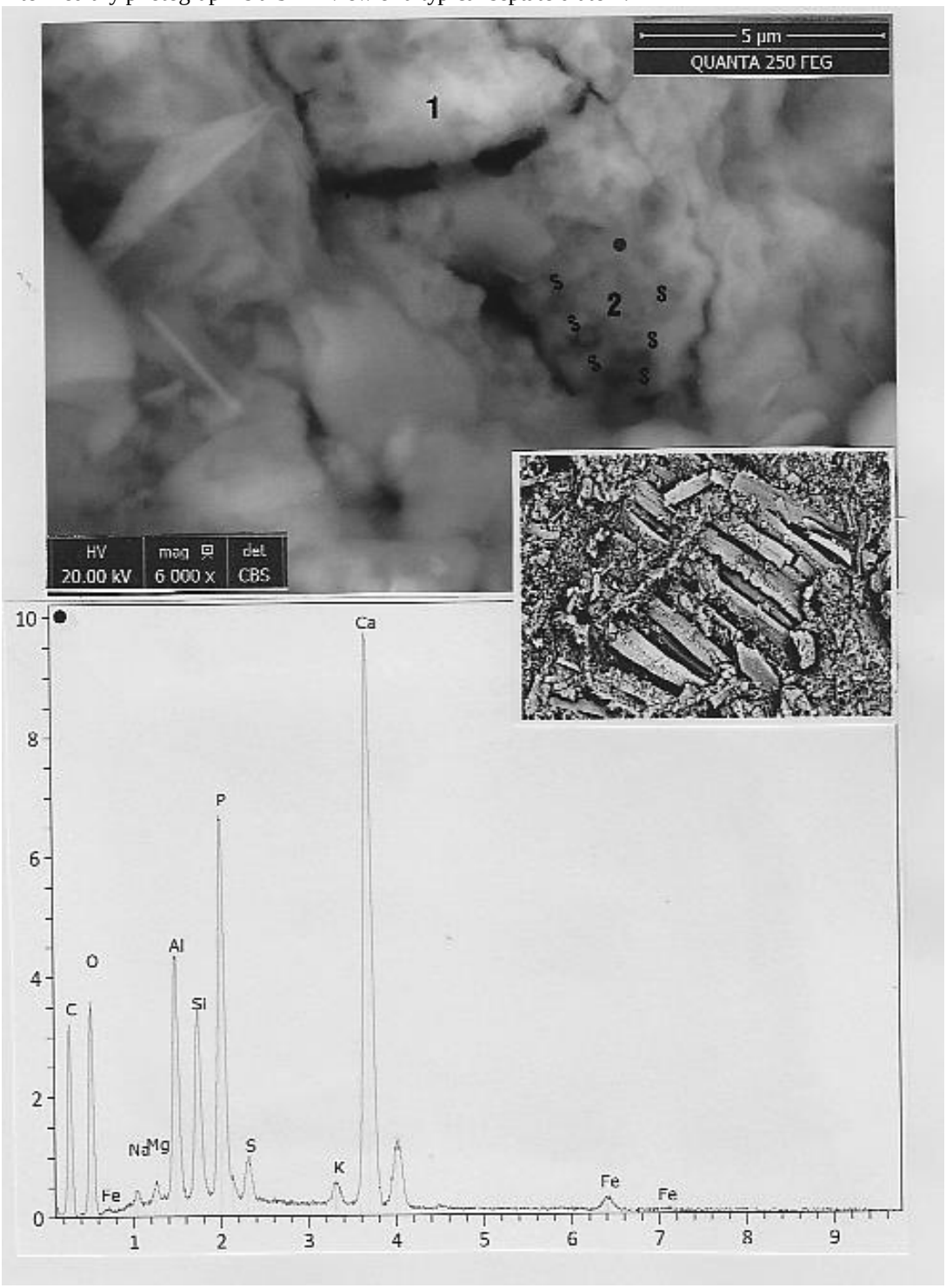

Figure 46. Example of a diatom pile. *Above*: SEM photograph (in LFD, 4000x) of this diatom pile. D1 : four diatoms of the perforate type; D2: five diatoms of the pennate type (little strokes indicate septum directions); D3: a diatom of the septate type (s: septas) *Below:* global spectrum of the pile.

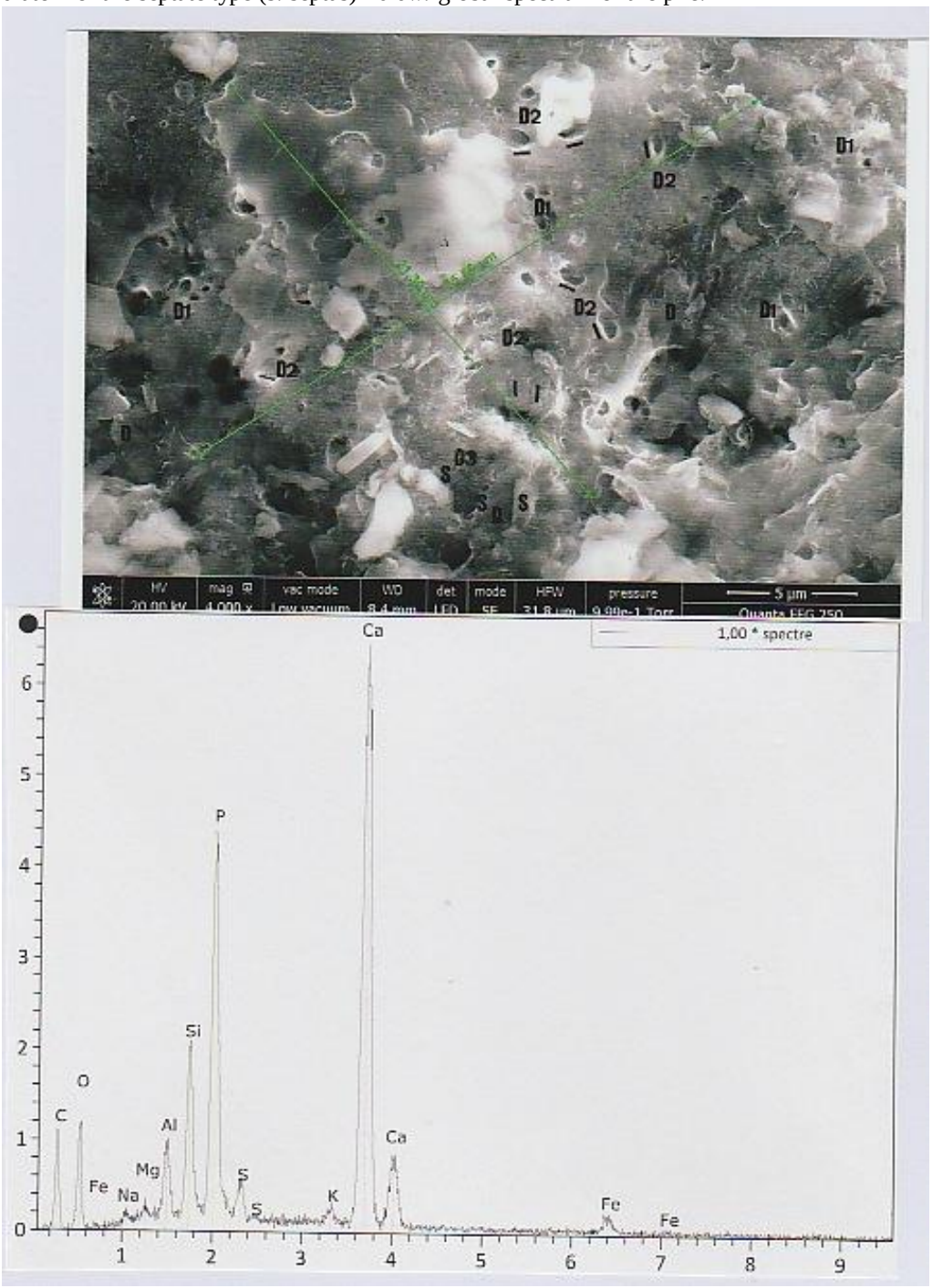

Figure 47. A cyst. *Above:* SEM photograph (in CBS, 20000x) of the cyst (P: algae wall, M: an aluminosilicate micro-grain). *Below*: spectrum of this cyst.

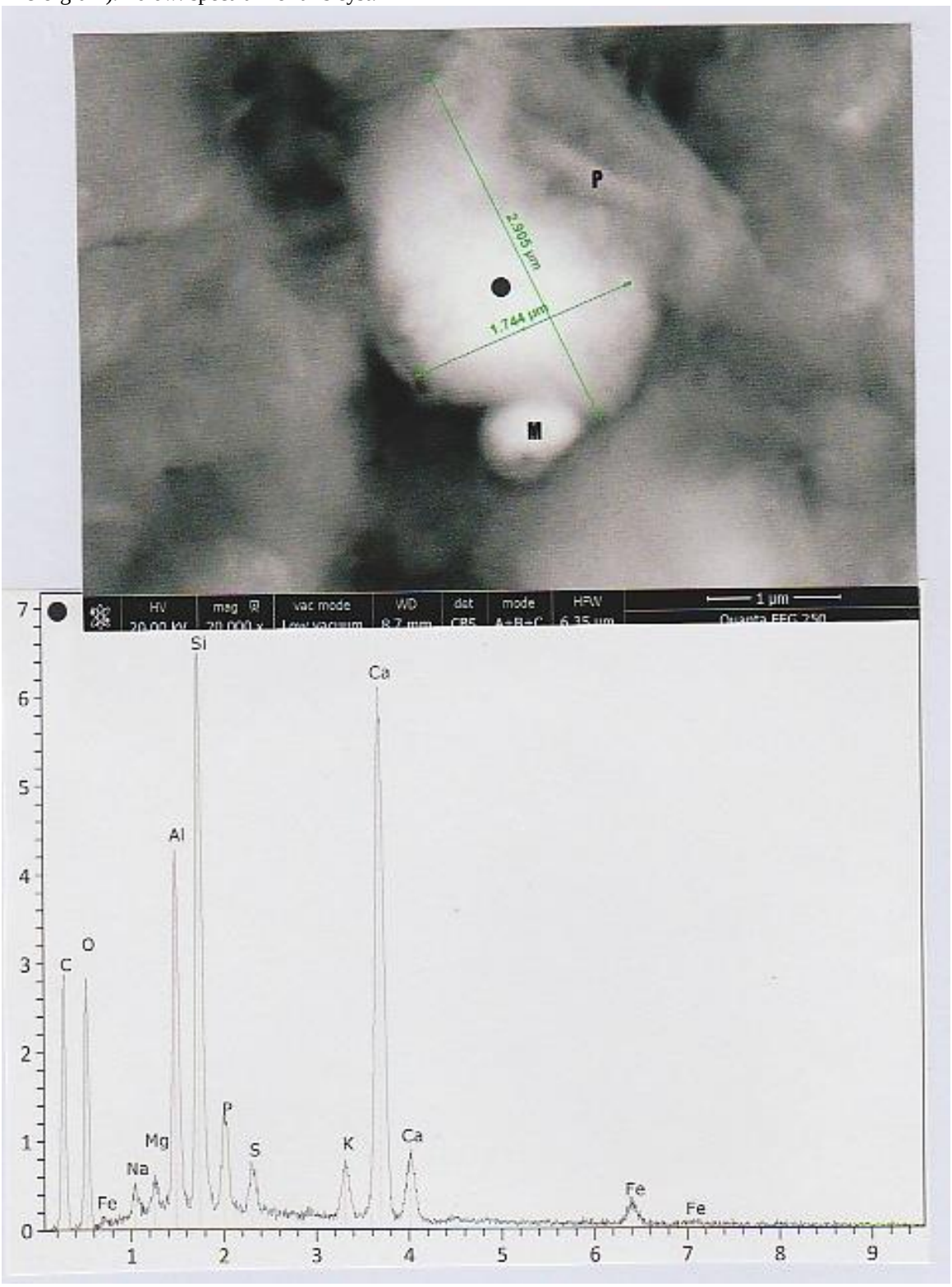

This formation is a trypical stomatocyst of Chrysophyceae. The main characteristic of this family of algae is the formation of endogeneous cysts of silica (stomatocysts) that constitute one stage of resting or resistance during the plant life (**17**). Crysophyceae species are generally of fresh water.

Chrysophycean stomatocysts were already described in some dental plaques (**7**, **18**).

Kaolinite.

Figure 48 photograph (which is an enlargement of the rectangular area indicated in the figure 2 photograph) shows the OD3 island of dentine on the PD surface.

At least ten (1 to 10) flat micro-particles (or groups of), of similar aspects, surround OD3. Their mean dimensions are of about 15 µm ; some of them (numbers 4, 9 and 10) have the appearance of hexagonal crystals.

Their spectras are characterized by two elevated (and equal) peaks for silicium and aluminium ; this is the "mineral signature" of kaolinites (**19**), that are the minerals of some sorts of clays.

We have compared this spectrum to that of a kaolinite powder of reference (Figure 49) ; the corresponding spectrum is the same (with the two elevated peaks of silicium and aluminium) than those of the kaolinites surrounding OD3 ; at least five hexagonal crystals (of the same dimensions) can be observed among the kaolinite fragments of the reference specimen. The reference spectrum shows a little peak of iron (as those of the OD3 kaolinites), that explains the red coloration of the powder examined.

Figure 48. Area of the PD surrounding OD3. *Above:* SEM photograph (in CBS 600x) of OD3.1-10: ten flat micro-particles (indicated by squares);each little dots indicate locations (inside of these micro-particles) where EDX analyses are realized. D: diatoms; **a** and **a', b** and **b'** and **c** (encircled) indicate the three locations where are white micro-particles with axial symmetry; **S**: seven spicules, with one bulging extremity. *Below*: the typical spectrum of the ten flat micro-particles.

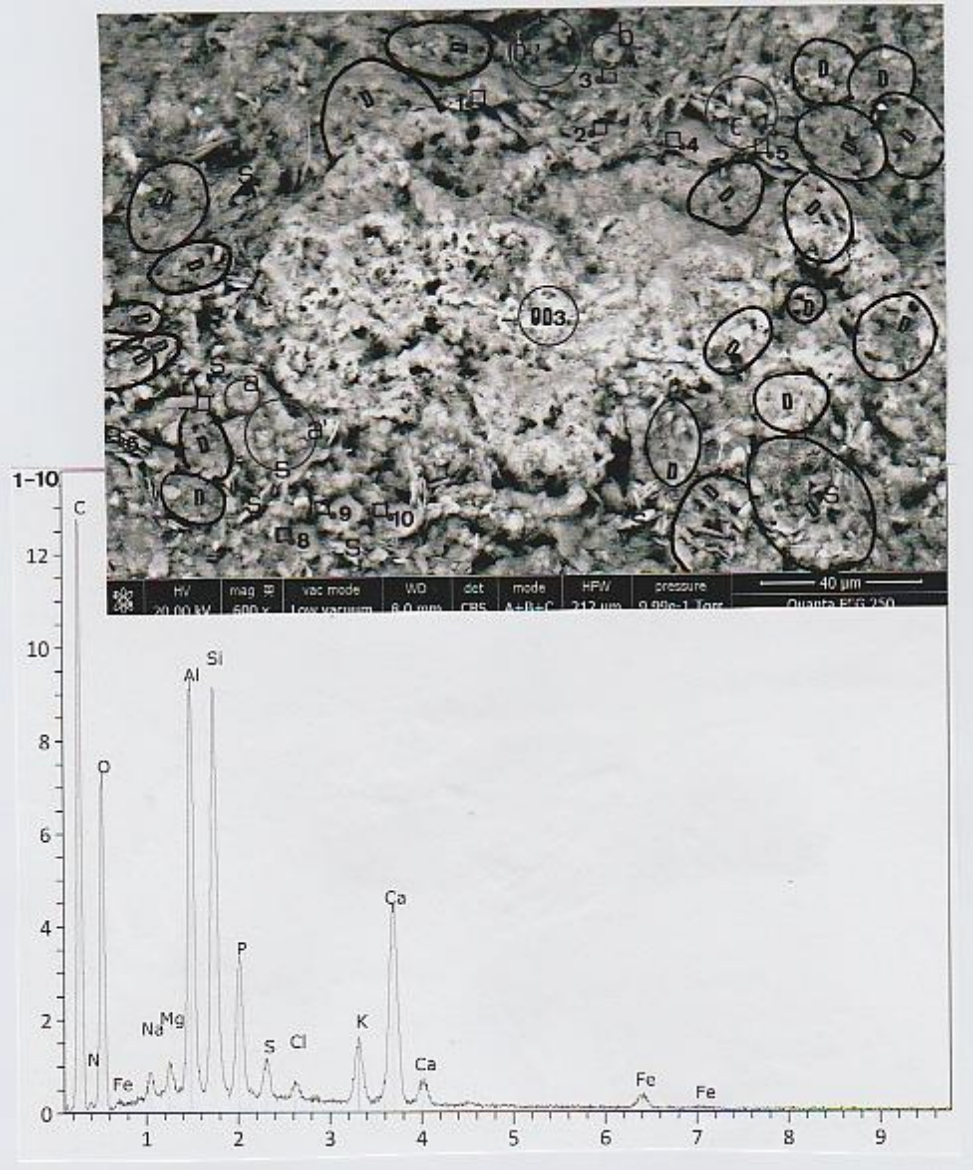

Coral.
Some other formations , also situated around OD3, can be distinguished from the previous ones (see the figure 48 photograph). They are located in three areas on the PD surface : **a** and **a'** , **b** and **b'**, and **c**. Their characterizations are as follows : there is one micro-particle of about 10 µm of diameter in **a**, and seven micro-particles of more little sizes (about 5 µm) in **a'** ; one micro-particle of 10µm in **b**, and five micro-particles of 5 µm in **b'** ; there are five micro-particles of 5 µm in **c**. All these micro-particles have an axial axis of symmetry (where one can see a cruciform mark for the greatest) and pentagonal or hexagonal outlines. Their surfaces are ornamented by small protuberances. Bright to electrons in CBS , their compositions are mainly of calcium carbonate. These various peculiarities are evocative of the coral.

To confirm that, we have studied a coral fragment of reference (a corsican coral, of red colour). Figure 50 shows the characteristics of this sample : mainly constituted of calcium carbonate, the coral surface appears are formed of very numerous jointives micro-particles loaded on the calcium carbonate matrix. Each micro-particles (of dimensions comprised between 5 and 20 µm) have tetragonal, pentagonal or hexagonal outlines ; there are small protuberances of characteristic forms at their surface.

The observations of numerous micro-particles of kaolinite and of coral around OD3 demonstrate that this dentine island had been sanded from the PD by this sort of abrasive material.
They are numerous grouped little micro-particles of this type of coral that were found at the PD surface. Figure 51 gives one example of these observed piles.

Spicules of sponge.
On the figure 48 photograph, one can see seven pointed micro-phytoliths (S) with an enlarged basis (as typologized on the photograph 2 of figure 5). They are evocative of sponge spicules.

Figure 51. An example of coral pile. *Above* : SEM photograph (in LFD, 8000x) of little micro-particles of coral grouped in a pile. *Below* : EDX analysis of the central one (indicated by a greater black dot).

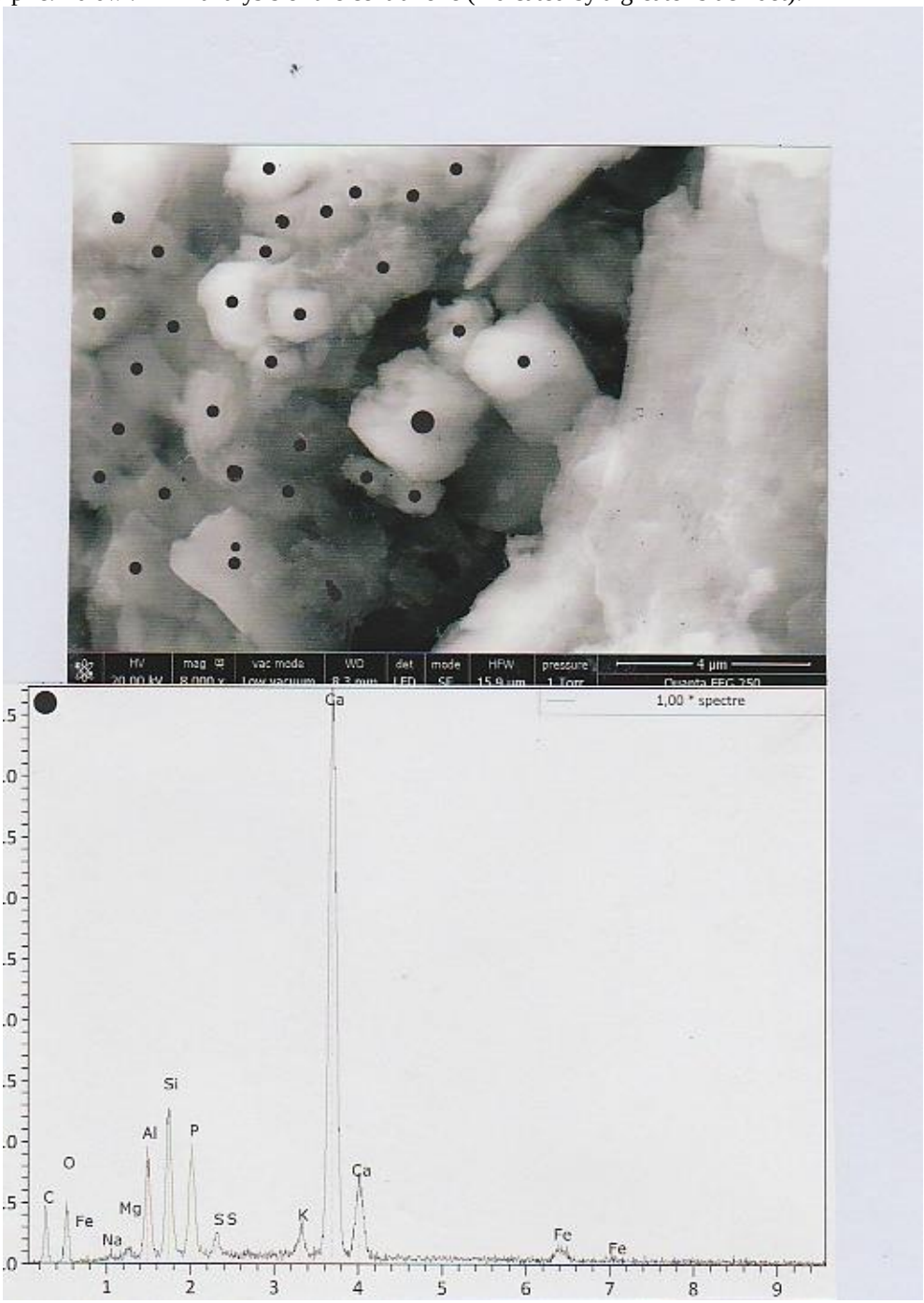

To confirm that, we have studied a today sponge fragment. Figure 52 shows a set of spicules (elongated in form, with a pointed extremity and the other extremity swelled), embedded in the organic filaments of the sponge matrix ; they are mainly composed of silicium, as shown in Figure 53.

So, at least for some forms, pointed spicules with an enlarged basis observed on the PD surface are sponge spicules.

Pumice stone.

We have observed on the PD surface many (about one hundreds of them were analysed) mineral fragments of aluminosilicate composition. Their forms vary from short micro-phytoliths (SMP) , as typologised on the figure 6 photograph, to more elongated micro-phytoliths filaments ; they have sometimes the appearance of micro-plates. Their compositions are always of aluminosilicate, relatively iron-rich (mostly with titanium).

Figure 54 shows examples of two groups of them (of the micro-plate form), trapped in a PD crevice. Whereas micro-plate number 1 shows the typic elemental composition, calcium carbonate deposits partly alter those of the micro-plates group number 2. This typical spectrum of the micro-plate is very similar to that of the short micro-phytolith illustrated on figure 6.

This typical spectrum of micro-plates and short micro-phytoliths is that of some form of lava (**20**). The elevated peak of aluminium in the spectrum indicates a volcano of the eruptive type, and the high oxygen content explains the lightness of the corresponding rock.

We hypothesized that pumice stone was used in the present case as an abrasive material. To confirm that we have studied a commercial pumice stone, in a manner similar to that conducted in (**21**).

Figure 54. Examples of two lavas micro-plate groups, located in a PD crevice (arrows indicate the two crevice extremities). *Above* : SEM photograph (in CBS, 700x) of these two (numbers 1 and 2) micro-plate groups. Above all, the crevice extremities (K-K) in CBS (600x) ; the circle indicates the crevice region examined. *Below* : spectras of micro-plates 1 and 2.

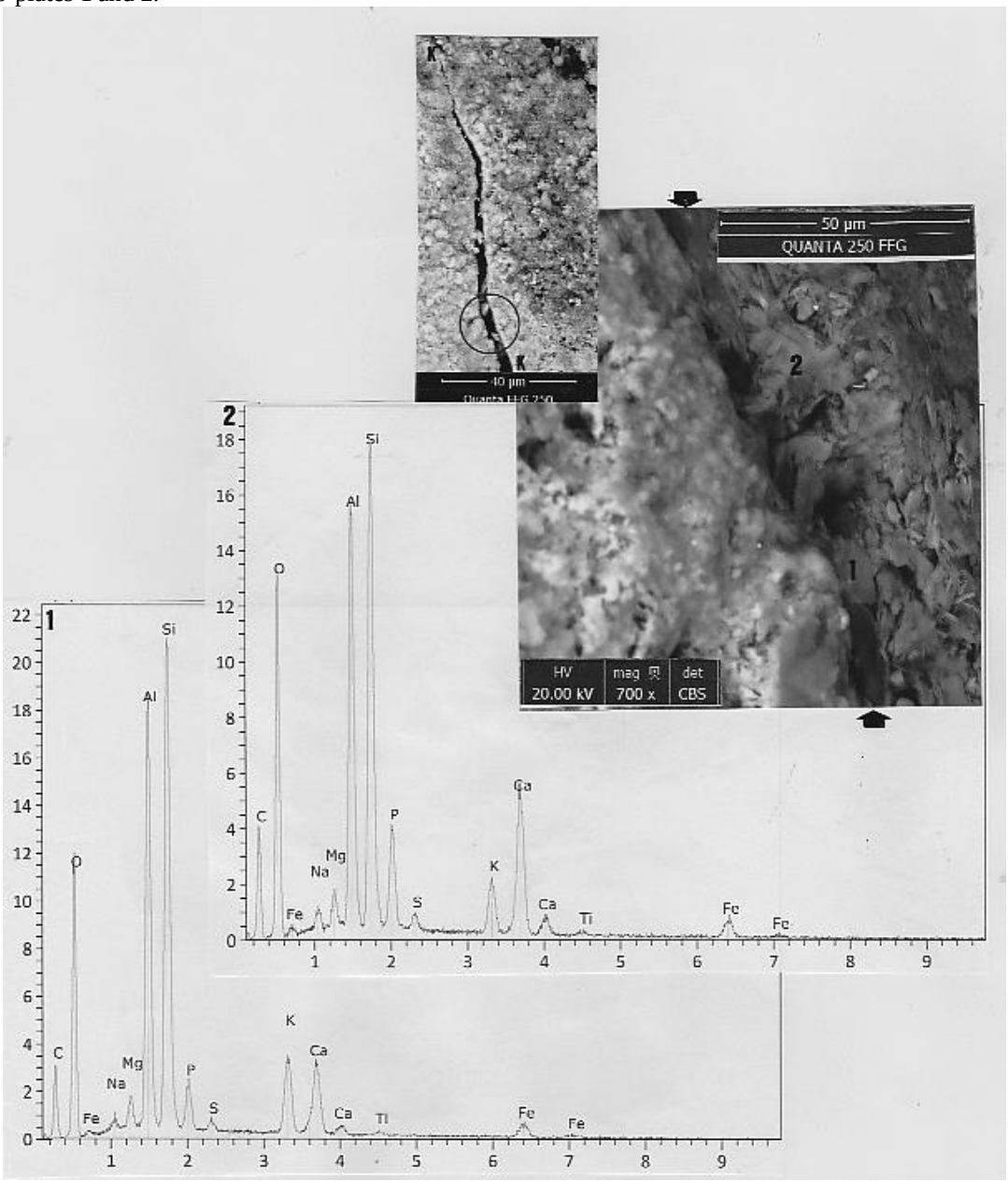

The Figure 55 photographs show the general aspect of pumice stone fragments of this sample. On the SEM photograph one can see the porous (**A**) aspect of this stone. The fragment under study consists of three sorts of morphologic appearances : a compact part (the essential component of the fragment) ; micro-fragments (as **N**), in forms of micro-plates ; and a third sort (as **S**), consisting of packaged micro-filaments.

Figure 56 shows the spectrum of a micro-plate (numbered 1). This spectrum had an elevated peak of silicium, and a more modest peak (in favour of the effusive type of the corresponding volcano) of aluminium ; there is also a peak of magnesium of equal height. The content in oxygen is substantial, and there is an important peak of iron. The calcium carbonate content explains the brightness to electrons of the micro-plate in CBS.

Figure 57 shows that the spectrum of the compact part of the fragment (numbered 2) is greatly similar to that of the previous one (but with a less important peak of iron). The spectrum of the filamentous part of the fragment (numbered 3) shows no magnesium peak and only some traces of iron.

So we found in the pumice stone studied a diversity of forms, including micro-plates and micro-filaments (as for those observed at the PD surface). Spectras of these formations are characteristics of the lava from which this pumice stone come from ; but we notice some similarities between these spectras and those of the previously studied micro-plates and short micro-phytoliths located on the PD surface.

Diversity in spectras (in the relative heights of the aluminium and the magnesium peaks, that of the potassium, or the presence or not of titanium) can be explained by the different local origins of the samples of pumice stones concerned. Some other micro-plates observed on the PD (Figure 58), where the silicium (of non-diatom origin) is the main component, have a spectrum more similar (low aluminium peak, only traces of magnesium and iron, absence of titanium) to those of some parts of the pumice stone studied. Figure 59 gives also an example of a short micro-phytolith (of the PD) without titanium.

Figure 58. Another example of micro-plates located on the PD. Above : SEM photograph (in LFD, 4000x) of a group of micro-plates. *Below* : the corresponding spectrum.

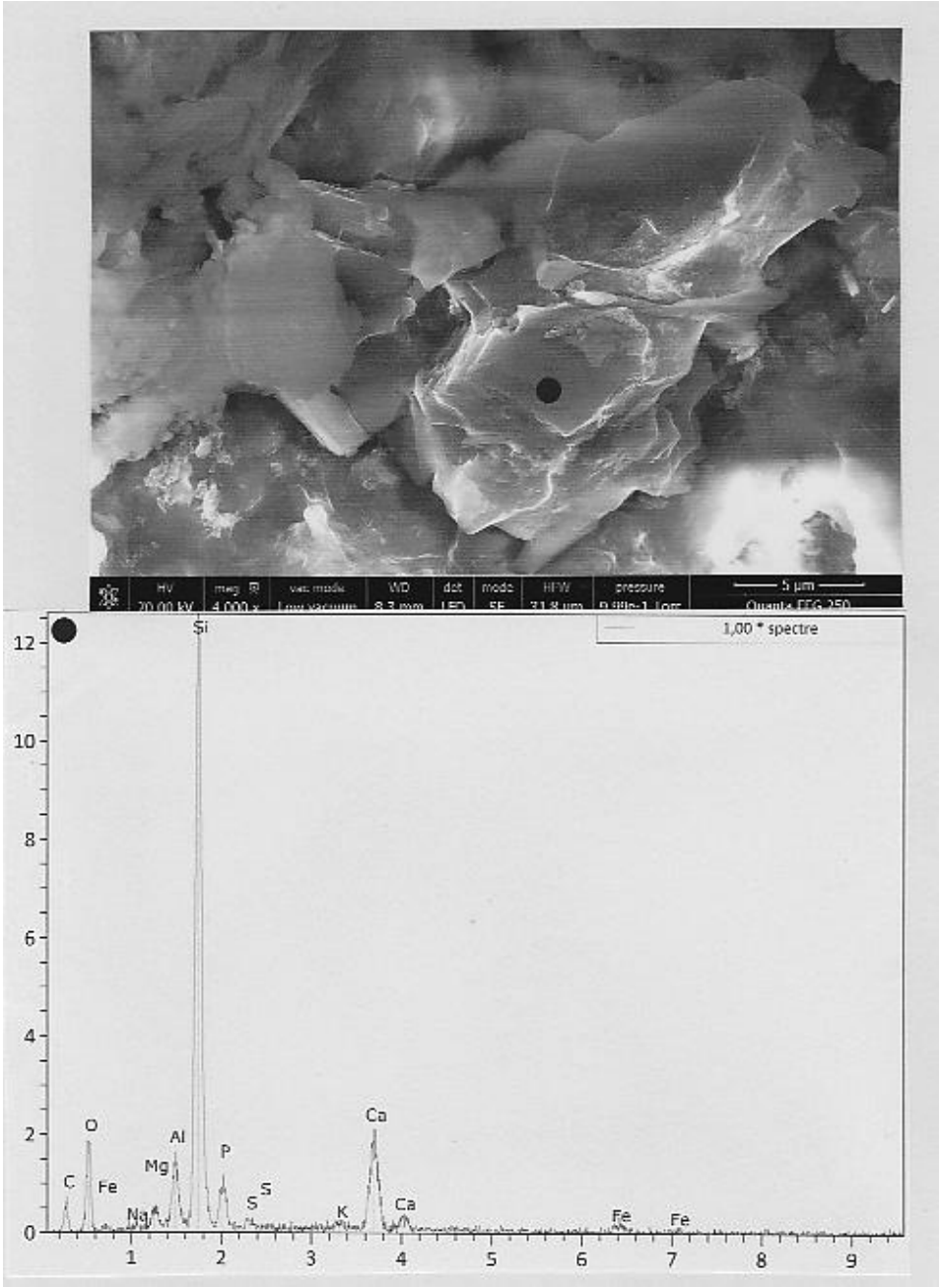

DISCUSSION AND CONCLUSIONS

In a fashion similar to that already developed in (**6**) concerning tree medieval individuals from Caravate (Italy) we have attempted strought to find, based on SEM-EDX studies of the dental plaque of one of Bayard's tooth, the main characteristics of his diet habits. Our study was evidently slanted by important bias : it is only the "resistant-to-time" particles of the diet (mainly these that silicifies) that are conserved (in holes or crevices), or embedded in the dental plaque.

The harvesting was however a little bit substantial, because we have found some rests of vegetables, of flat bones, of fish-bones fragments and fish-scales, starches and pollen grains.

To determine if these rests are compatible with those of a Middle Age alimentation we have used the very informative book of Bruno Laurioux (**22**), concerning diet habits during its late ages (of the XIVth and XVth Centuries), that correspond to the main period of Bayard's life.

Vegetables and meats.

Table 1 gives the list of the seven sorts of rests found that are characteristics of some vegetables and meats.

Table 1. The seven sorts of rests studied that are indicative of vegetables and meats.

Numbers	Rests	Corresponding figures	Samples of reference used
1	phytoliths of leek	figure 13	today leek leaf
2	phytoliths of asparagus	figure 15	today asparagus stem
3	macles of sorrel	figure 18	today sorrel leaf
4	starches of green garden pea	figure 26	today dry green garden peas cuts
5	flat bone of bird	figure 29	today cooked chicken bone
6	fish-bones	figure 33	today cooked fish-bone of trout
7	fish-scales of tench	figure 35	today cooked fish-scale of trout

Attribution of the observed (figure 4) cylindric phytolith to that of carrot is somehow speculative (and uncheckable, because present today carrots are very different to those of the corresponding roots eaten during the Middle Age period that were fibrous, white and thin).

We know that overripe ribs and spinach were regularly eaten by consumers of this period ; but phytoliths observed in today representatives of these two vegetables were not found on the dental plaque. Green and white stems of leek were also consummated at that time. Leek was eaten boiled – the most common meat being the white puree (porez blanche) - or in potages and soups (some doctors advised sub-against stought to eat leek, because it scratchs teeth). Asparagus was also consummated, when it was the season.

Figure 59. An other example of short micro-phytolith located on the PD. *Above* : SEM photograph (in CBS, 10000x) of this micro-phytolith. *Below* : the corresponding spectrum.

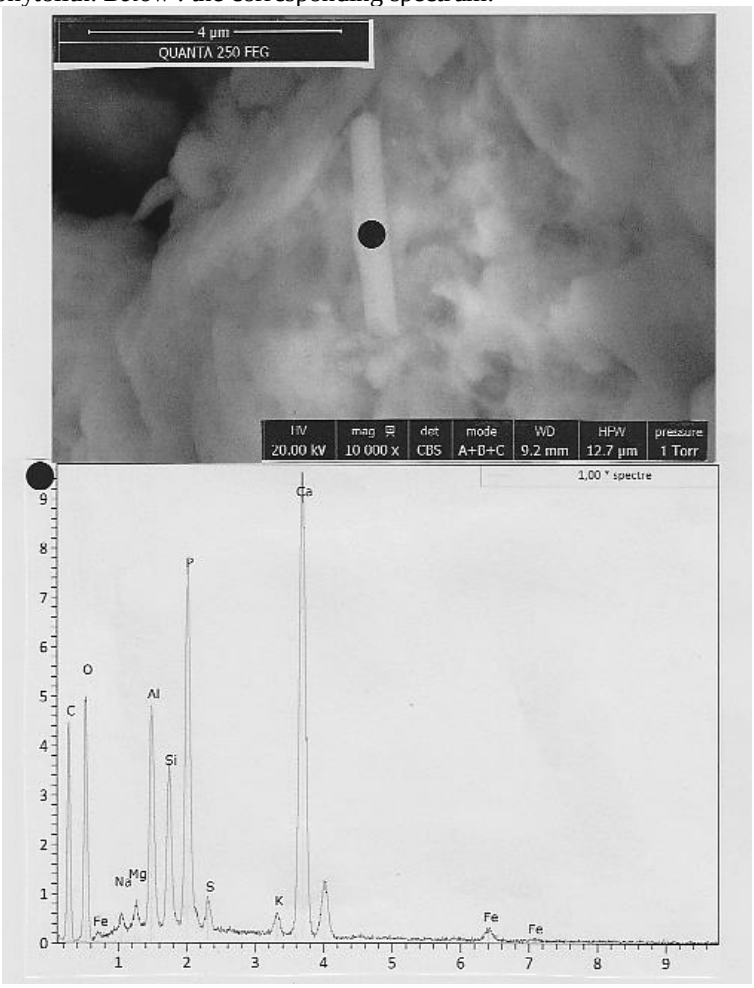

Contrary to leek- that was named as "asparagus for poors (and described, with some disdain, as "plants with bulbs" (like garlic, onions and shallots) – asparagus was very appreciated during all the Middle Age as a luxury dish, worthy of to represent at the lord tables. Some collections (**23**) pass through on, traditionally, many culinary recipes where these vegetables are involved.

Sorrel was cultivated in vegetable gardens since the beginning of the middle age (one already knew that it ameliorates digestion). Because of its acidity, it was used in some sauces. The "saulce vert" (the green sauce) had its acidity from wine, vinegar and "verjus" (verjus is a white grapes juice not ripened); in the absence of one of these products, or to reinforce it, one could use sorrel crushed leaves. A famous culinary recipe of the soup with sorrel and verjus was also very appreciated at that time.

Green (and white) garden peas, as broad beans (and eventually chick-peas, more rarely lentils) were consummated dry. Because of their seasonal productions they were often considerated as some form("the spring tiny grains") of cereals. Green garden peas were mostly eaten in "purées", composed with other vegetables.

The cooked flat bone fragment analysed here is probably that of chicken osseous (Figure 60). We cannot exclude however that it could be that of a hen or a capon or of a goose or of a heron or a pluvier (or even that of a partridge or a pheasant, that were refined dishes that ornamented some prestigious banquets at that time).

The marine fish the most consumed at this time was the herring (that was bought fresh, salted or smoked). It was more often eaten boiled, and was an essential part of the alimentary diet of rurals, but also for clergymen and even of noblemen ; since the beginning of the XIVth Century in France, herring was so much consumed that one can speak (**24**) of a true "herring" reign. The two boiled bone-fish fragments analysed here are probably those of a herring fish-bone : Figures 61 and 62 show two today herring fish bones in different states of the heating process. When boiled, fish-bone shows some traces of calcium phosphate particles oriented along the fish-bone longitudinal axis; these orientated particles are very much plentiful when the fish-bone is cooked, reproducing so a pattern similar to that seen for the fish-bone photograph of figure 33. Spectras of these formations indicate a reduction in calcium phosphate contained when the heating process increases.

Concerning now fish freshwater species, tanch was not considered (as now; it is qualified as " a pisces that eats the mud") as the best delicious fresh- fish (compared to carp, perch and pike). Tench is however often cited in alimentary recipes and menus of the Midle Age; it was caught in the numerous ponds built at this period along the rivers.

Bread

The Middle Age period is sometimes called "the Europe of pains (bread)"; the bread, together with peas and cabbage , constituted at that time the basis of the rural food (90% of the population in France). Bakers and housewives produced it in the form of great round bread miches of wreath bread, or of individual roll breads. One had calculated that the daily bread consumption was of 1-1.5 kilograms and often more (even for nobility), that is said more than twice of that of today.

In the towns the bread consummated is generally of "pure froment"(wheat); it is "the white bread". Elsewhere , it is most often " the grey bread", mostly of rye. The "famine breads" were also of rye, sometimes of oat.

We have shown (figure 24) that wheat starches are divided up in three size categories : those of more than 10 µm (macro-grains), those of 2 to 10 µm (micro-grains), and those inferior to 2µm. Those of the third category are probably phytin globoids **(25).** Rye starches(figure 25) consist of large (spherical or lenticular) macro-grains, juxtaposing aggregates of more little starch granules.

It was demonstrated that larger starches only **(26,27)** are diagnostic characteristics that permit a clear distinction between taxas. In our observations wheat starches macro-grains are in the 20 to 40µm range, but rye spherical starches frequently exceed 70µm and more. This shows that starches of the dental plaque (figure 20) are those of rye. Figure 63 shows starches from a today sample of portage oats; as described in **(28),** oat starches occur chiefly as compound structure which are aggregates of individual rounded to hexagonal granules that are in the 16 to 27µm range.

Figure 64 shows starches from today samples of a flour powder of maize and of flakes of potato. Maize starches are little (5 to 15µm) rounded to hexagonal granules. Potato starches are voluminous (80 to 200µm) rounded to ovaloid granules, where can be distinguished concentric lamellaes and hilum.

Table 2 summarizes size ranges of the starch macro-grains in the five species studied.
Table 2. Size ranges of the biggest starches in the five species.

Species	**Size ranges of the biggest starches**	**Corresponding figures**
Wheat (*Triticum sativum*)	20-40 µm	figure 24
Rye (*Secale cereale*)	50-100 µm	figure 25
Oat (*Avena sativa*)	16-27 µm	figure 63
Maize (*Zea mays*)	5-15 µm	figure 64
Potato (*solanum tuberosum*)	80-200 µm	figure 64

The fact that we do not find maize and potato starches on the PD surface constitutes a sort of negative proof in favour of the likelihood of Bayard's bread diet : we know that maize was introduced in France (in the South-West) at the beginning of the XVIIth century only (and precisely in 1612, in the Bresse region) ; concerning potato, it was also only at the beginning of the XVIIth century that this plant was cultivated (but sporadically in a first time) in France, particularly in the Savoie region. So diets coming from these two edible species were eaten in France much later after Bayard's time of life.

According to **(29)**, maize and potato starches are among the two most common sources for the contaminant starch assemblages by modern material in laboratories specialized in ancient starch analysis. But in the present work, starches – as for others rests- were studied directly by *in situ* analysis of the dental plaque surface (and not, as usually, after extraction of dental calculus from teeth). However we don't exclude that modern contamination occurred in our own samples, especially for spores of the echinulate ornamentation type(figure 37).

Did Bayard eat rye bread? We don't think that rye starches observed on the dental plaque surface (figure 20) correspond to bread: examination of the forms of wheat starch grains in a today flour powder (figure 24)shows that most of them are markedly distorted and convoluted (**30)** because of the cooking process. That does not correspond to the SEM starch appearances showed for starches on the PD (figure 20), that are of clearly rounded forms ; consequently, the observed PD starches are not bread starch grains.

Another remarkable distinctive feature of the PD rye starches is their preferential locations – side by side- in a quasi monolayer coat, at the limit between the inferior enamel part and the PD superior part (figure 20). This indicates non-cooked rye starch grains, in aggregated form, deposited here in a liquid phase : that of a "bouillie".
In the Middle Age, soups, potages and bouillies constitute the "companagium" (that accompanies bread). At that time, cereals are frequently used up in the form of bouillies (**24**) ; and rye flour bouillies constitute the most common food of the people.

According to (**31**), the medieval society (since the early of the IXth Century in France) was splitted up between three "orders", concerning the alimentary habits : that of the lords (*bellatores*, who fight), that of monks (*oratores*, who pray to) and that of the rurals (*laboratories*, who work) ; so these three corresponding alimentary models constituted true social markers of this tripartite society. As established here, Bayard's alimentation consisted greatly of leek soup, of cooked herring and of rye flour bouillie. Although he was of the lord order, he heated like as a rural ; that corresponds to that we know about the fugal alimentary habits of him (Michel Ségura , personal communication).

Sugar
Sugar (extracted from the sugar cane) was known since many times in the Muslim Civilization, but it was introduced more lately in the Christian Europe. It remained yet during the Middle Age for a long time as a product of luxury, that one export at high-costs from Oriental Countries ; at the beginning, sugar was used exclusively for medical use (it is suitable for convalescents diet).

At that time, sugar had moved up from the medicinal status (to give back vigour to convalescents) to that of an alimentary one in Italy and England. In France, initially reserved to new culinary recipes, it overflows soon those of the ancient repertoire (that is known since the XIVth Century, or previously). In this way the venerable "cameline", a famous sauce (ready-to-use, as today mayonnaise and ketchup) incorporated – since the XIVth Century in France – with ginger, long black pepper and grill-bread soaked with vinegar and verjus, "a great quantity of canella"(giving the name of cameline to this sauce) ; it is the Italian cameline that incorporated sugar in the recipe.

Since the beginning of the XVth Century, there was in fact in Occidental Mediterranean a true "sugar boom", more precocious that initially believed ; at the origin, sugar cane plantations in Sicily and in the Iberian Peninsula. At this turn of the XIVth and XVth centuries in France (probably under some Italian influence), the sugar consumption reaches Paris. Under Charles VII 's reign the "sugar taste" is from now on deeply rooted in the French customs , and at

the origin of the invention of new meals (concerning some banquets, described in *editio princeps* of the "Viandier") : as cherries with sugar, "pâtés" with funnels of sugar , pigeons with sugar and vinegar, tarts with sugar, pears with sugar and so on.

However, for most of the people during the main part of the Middle Age period, the only source of sugar was honey. We have at that time numerous descriptions (not necessarily as dessert meals) of flan tarts browned with dry fruits and honey, of lost-bread spread with almonds and honey, and of "douceurs" (equivalent to our today "petit fours") sweetened with sugar by honey.

Middle Age time is generally considered as the early beginning of beekeeping in France. Beehives were described for the first time in the "Traiyé d'Agriculture"of P. de Crescenzi, dating from the XIVth century; some of them were even equipped with sorts of "hausses", permitting to keep the swarm most on harvesting some honey part.

Initially, honey hunters of the medieval period applied their beekeeper's activities to trees. In a first time, they pinpoint trees containing swarms in some of their cavities and then climbed these trees with ladders; they closed these tree's cavities with small doors. The honey harvesting was made at the end of summer. This sort of activity was dedicated to a special corporation of workers, named the "bigres". They have the privileges to watch colonies of wild bees, to harvest honey, and to produce the wax; they filled with smoke the bees colonies. Some forests (the "bigreries") were entirely dedicated to the beekeeper activity. At that time the clergy (mainly because of the wax production intended to the candle production) controlled the "honey-flies"trade.

In regions of cereal farming, the first true beehives appeared (frequently around monasteries). They were made of straw, and were of dome and then of conic forms; most often they had a detachable lid, also made of straw, relatively waterlight. It is the real beginning of the honey production, that will be fully completed during the XVIIIth century. In the Middle Age period, the lord had a "droit d'abeillage", a right to take some quantities of bees, of honey and wax, of the beehives of his subjects; the "abeillage" remained for a long time as some part of the feudal licences.

Actually in France, the chestnut tree (*Castanea sativa*) is the most third frequent forest-tree after the oak (*Quercus*) and the ash (*Fraxinus*). In Continental France the chesnut tree is omnipresent in "Ardèche" (Rhône-Alpes) and emblematic in "les Cévennes" (Languedoc Roussillon), which are its two main bassins of production. The chestnut tree habitat is that of a mountain dweller, specially on the slopes between 300 and 1200 meters of altitude (where no other forest trees can expand). The French "châtaigneraie" spreads now about 1000 hectares ; the chestnut production is actually done in two sorts of orchards ("vergers") : the first type of verger (qualified to "ancient", or "traditional") is constituted by several varieties of the European species of *C.sativa.* Trees are here often of several times centenarians, and the chesnut harvesting is mainly made by hands. The second type of verger (called "verger of production", of less than 50 years old, is constituted by artificial hybrid varieties (between *C. sativa* and Asiatic species of *C. crenata* and *C. mollissima*); they are more accessible, and more favourable to mechanization (they are mainly located in the "Sud-Ouest" : Aquitaine, Limousin and Midi-Pyrénées).

Certainly this first type of verger was established on the places of ancient cultivations of this tree, very probably go baking to the Middle Age (and even to those of the initial roman ones). At the beginning of the Middle Age, the chestnuts were only collected at the feet under the trees of these initial forests ; than, a true cultivation of the chestnut tree sets (**32**), in order to make up famines, mainly in regions of the Mediterranean hinterland. The apogee of this cultivation climbs at the XVth Century (to note that the great châtaigneraies of the Massif Central in France were planted during the XVIIIth and XIXth Centuries, to make up of famines again), as the numerous finded tenant farmers contracts (particularly in Ardèche) testify to. During the Middle Age period , chestnut is however a "food for poor persons", eaten cooked in soups (named as "bajanat"), often with milk and more rarely with sugar.
The Dauphiné region, from wich Bayard originated from, had numerous chestnut tree vergers (even now). During the summer season bees must collect nectar mainly on chestnut tree flowers, that were the dominant tree at that time and place.

The chestnut tree honey, which is a honey-specialty, is greatly appreciated by some consumers. Its colour is amber-dark ; it produces a strong odour. Its taste is full-bodied, persistent, and somehow astringent.

Drinking water.
We have shown that there are very numerous embedded diatoms on the PD surface. Their total number is difficult to estimate. Figure 48 shows at least ten diatoms on a particular PD area of about 2x1.2 mm = 2.4 mm^2 ; as the total PD surface is of about 8cm^2 , we can deduce that the total number of diatoms expected on this surface must be of about 300-400. But this total number is probably under-estimated, because these diatoms are frequently (figure 46 as an example) lumped in piles.

Taxonomically, the Diatom group is subdivided into two main classes :
. the Centrales (marine), generally of round forms and with pores,
. the Pinnales (freshwater), mainly of elongated forms and with septas.

Because of the native (non-extracted, non-prepared) diatom material we have, it was difficult to determine their precise species status as in (**33**). But it is likely that:
. the diatoms of the type septate we observed are of the species *Diatoma vulgaris*,
. the diatoms of the type perforate we observed are of the species *Diatoma mesodon* (Syn. *Diatoma hiemale var. mesodon*),
. the little diatoms of the type pennate we observed are of the species *Fragilaria martyi* (Syn. *Opephora martyi*, *Martyana martyi*).
All these three species are ubiquists fresh water diatoms.

So, there is firm evidence that the drinking water that Bayard absorbed was highly contaminated by diatoms. There is no known toxic fresh water diatoms (**15**). Middle Age people, specially in towns, were suspicious concerning their drinking water ; for sanitary reasons, of course, but mainly because they admitted that water was not a "nutritive" matter ; in the country the suspicion was slightest, because they dring the well water. Concerning drink the Middle Age period is characterized by a great consumption of wine (and, to a lesser extent, of cider, and of beer in the North). The wine, that was of lesser alcoholemic title than that of today, was drunk as greatly diluted with water. It was drunk by all, poors and richs (and even by women and adolescents). The wine, with bread and "companage" (at that time, all that accompanied bread), constituted the basic triad of all the rural alimentation ; estimations of wine daily consumption were of one and half to two litres.

Dental cares.
Dental cares were practiced since the beginning of Middle Age (**34**), and earlier. *De curis mulierum*, of Trota de Salerne, transmits the taking of two sorts of toothpastes (*ad dealbandos dentes*) of which one of them concerns the teeth whitewash and the other the strengthening of the weared out'teeth and the breath perfume. Various minerals intervene in thought in the first one ; among them : powders of covering (as those of white marble, of cuttlefish osseous and of other shellfishes) and of more reactive chemicals (like salt and ammoniac and alun salts).

In fact, the dental care practices were developed since the Antiquity (**35**). Ancient Greeks –however in some social privileged classes only- used already toothpicks (made of noble materials), and teeth and gums were rubed with fingers surrounded with one fabric piece. In accordance with texts, these practices were associated to aesthetic preoccupations. During the Roman Empire, elixirs and remedies against tartars and bad-breath were continuously improved. At that time these hygienic practices were also developed for aesthetic reasons, and not associated to health but with beauty (women were, of course, the first concerned).

But in the Middle Age, during which the body was closely linked to the interest of the soul, diseases of the teeth were (specially) more than ever associated with the sin and with the corresponding divine punishment (as well described in **36**). It was only at the beginning of the "Renaissance" period that some texts allude to buccal cares : the morning washing must include the mouth cleaning to avoid breath strench and teeth corruption ; to be efficient, such of these habits must be repeated at the ends of the breakfast and of the dinner. But such practices are limited to knights, and not to common people.

The first known real treatise of true odontology (that of *Artzney Buchlein*) was published in 1530, in Germany ; it describes well, in particular, dental tartar and some practices of early tartarectomy. The norms adopted in this treatise are of Arabic inspiration, and take their roots from Galien and from the classical medicine.

In France one consider generally that the "Traité pour les dents" (two volumes, totalizing more than 900 pages), written in 1728 by Pierre Fauchard, as the best treatise never written at that date on this matter (**37**), and this author as "the founder of modern scientific dentistry". In fact, as well as personal experience related by the author, he made-for the essential part- a compilation of the ancient roots.

Concerning "detartaring", Fauchard be inspired by the pieces of writing of the Arab surgeon Abulcasis (936-1013), who described at this date perfectly the dental plaques (that he names as "ruginations"). He wrote "Sometimes, they are some coarsed and deformed deposits on the internal or external teeth surfaces, or between the gums. Teeth are so of black, yellow, or green colours ; consequently there is an alteration of the gums, and teeth come loss. Ruginate teeth and molars that have these deposits until they disappear , he indicated ; the teeth rugination is realized with some instruments of various forms, as function as the use you destinate".

Numerous previous authors have written on detartaring. At the end of the XVIIth Century, Pierre Dionis indicates that detartaring was commonly made : "those that are concerned by their mouth practised

sometimes to detartaring ; others have to be in the habit of doing a daily cleaning of their mouth".

Croissant de Garengeot (in 1725) proposed a sophisticated sort of detartaring : "One of the tooth illness is the tuf that covers them ; this tuf increases sometimes as considerably that it appears as exostoses. When the tuf is less important, it is that one names the tartar, that come looses the teeth… its necessary then to remove it." Garengeot continues with a detailed description of his scaling technique ; he ended scaling by a polishment. Several minerals intervene in the polishment process (probably he was also inspired by more ancient information). The abrasive minerals he quoted are as follows (in order) :

. "corail" (coral),
. "porcelaine en poudre" (kaolinite),
. "pierre de ponce" (pumice stone),
. "éponge" (sponge).

Table 3 summarizes results obtained concerning the five sorts of abrasive products we found on the Bayard's PD surface. Four of them are cited in the Garengeot text ("corail", "porcelaine en poudre", "pierre ponce" and "éponge"). Concerning silica, it is a less specific category ; silica particles found on the PD surface are not of onyx (as described in some texts about abrasive minerals in powders), because they lack of manganese.

Table 3. The five sorts of abrasive products found on the PD surface.

Numbers	Abrasive products	Corresponding figures
1	pumice stone	figures 6 and 54
2	spicules of sponge	figure 5.2
3	kaolinite	figure 48
4	coral	figure 48
5	silica	figure 58

The most plentiful (more than several hundreds of these particles are observed) abrasive material found on the Bayard PD is that of the pumice stone ; it literally covers all the PD surface. Such an abundance of these particles indicates a regular use of this sort of material to abrase the dental plaque. Subtle differences (mainly of aluminium and magnesium relative contents in the corresponding aluminosilicate particles) shows a repetitive use of such materials originating from different geographic locations. All that proves that abrasions were realized several times, with pumice stones of different origins. Bayard, who was frequently in Italy during his adult life (**1**), had no difficulties to obtain such these (relatively exotic) pumice stone materials.

Overall, results obtained here show that Bayard payed a great attention to his dental cares. One can reasonably suppose that he was also careful of his general health.

List of abbreviations

PD : dental plaque ; OD : island of dentine ; SEM : Scanning Electron Microscopy ; EDX : Energy Dispersive X-rays ; LFD : Large Field Detector ; CBS : Circular Back Scattering ; LMP : Long Micro-Phytolith ; SMP : Short Micro-Phytolith.

Acknowledgements

We thank the French Association "Les Amis de Bayard" (and specially its president Dr Jacques Viret) and "Bayard Capital" for continuous financial supports.

References

1. Jacquart J. "Bayard". Fayard Ed (Paris, France), 1987.
2. Lucotte G, Bouin Wilkinson A. Y-chromosomal profile and mitochondrial DNA of the chevalier Bayard. *Open Journal of Genetics*, 2017, 7 : 50-61.
3. Gleize Y, Castex D, Duday H, Chapoulie R. Analyse préliminaire et discussion sur la nature d'un depot dentaire très particulier. *Bulletins et Mémoires de la Société d'Anthropologie de Paris*, 2005, 17 : 5-12.
4. Charlier P, Huynh-Charlier I, Munoz O, Billard M, Brun L, Lorin de la Grandmaison G. The microscopic examination of dental calculus deposits. Potential interest in forensic anthropology of a bio-archaeological method. *Legal Medicine*, 2010, 12 : 163-171.
5. Piperno DR. "Phytoliths : a comprehensive guide for the archaeologists and paleoecologists ". Alta Mira Press (Lanham, MD, USA), 2006.
6. Lazzati AMB, Levrini L, Rampazzi L, Dossi C, Castelletti L, Licata M, Corti C. The diet of three medieval individuals from Caravate (Varese) . Combined results of ICP-MS analysis of trace elements and phytobith analysis conducted on their dental calculus. *International Journal of Osteoarchaeology*, 2016, 26 : 670-681.
7. Power RC, Salazar-Garcia DC, Wittig RM, Henry AG. Assessing use and suitability of scanning electron microscopy in the analysis of micro remains in dental calculus. *Journal of Archaeological Science*, 2014, 49 : 160-169.
8. Henry AG, Piperno DR. using plant microfossils from dental calculus to recover human diet : a case study from Tell al-Raqa'i, Syria. *Journal of Archaeological Science*, 2008, 35 : 1943-1950.
9. Heneen WK, Brismar K. Scanning electron microscopy of mature grains of rye, wheat and triticale with emphasis of grain shrivelling. *Hereditas*, 1987, 107 :147-162.
10. Solari A, Olivera D, Gordillo I, Bosch P, Fetter G, Lara VH, Novelo O. Cooked bones? Method and practice for identifying bones treated at low temperature. *International Journal of Osteoarchaeology*, 2015, 25 : 426-440.
11. Miculescu F, Ciocan LT, Miculescu M, Ernuteanu A. Effect of heating process on micro structure level of cortical bone prepared for compositional analysis. *Digest Journal of Nanomaterials and Biostructures*, 2011, 6 : 225-233.

12. Yin T, Park JW, Xiong S. Physicochemical properties of nano fish bone prepared by wet media milling. *Food Science and Technology*, 2015, 64 : 367-373.
13. Braglinière J, Le Louarn H. Caractéristiques scalimétriques des principales espèces de poissons d'eau douce de France. *Bulletin Français de Pêche et de Pisciculture*, 1987, 306 :1-39.
14. Hesse M, Halbritter H, Zetter R, Weber M, Buchner R, Frosch-Radivo A, Ulrich S. "Pollen Terminology : an illustrated handbook". Springer Ed. (Wien, New York), 2009.
15. Seckbach J, Kociolek JP. "The diatom world". Springer Ed. (London, New York), 2011.
16. Dudgeon JV, Tromp M, Diet, geography and drinking water in Polynesia : microfossil research from archaeological human dental calculus, Rapa Nui (Easter Island). *International Journal of Osteoarchaeology*, 2014, 24 : 54-63.
17. De Reviers B. "Biologie et phylogénie des algues", tome 2. Belin Ed. (Paris), 2003.
18. Power RC, Salazar-Garcia DC, Straus LG, Gonzalez Morales MR, Henry AG. Microremains from El Miron Cave human dental calculus suggest a mixed plant-animal subsistence economy during the Magdalenian in Northern Iberica. *Journal of Archaeological Science*, 2015, 60 : 39-46.
19. Sengupta P, Saikia PC, Borthakur, PC. SEM-EDX characterization of an iron-rich kaolinite clay. *Journal of Scientific and Industrial Research*, 67 : 812-818.
20. Welton JE. "SEM petrology atlas". AAPG Ed (Tulsa OK USA), 2003.
21. Dachary M, Deniel C, Plassard F, Boivin P, Devidal JL. Textural and geochemical analysis of a pumice polisher with grooves from the Magddalenian site of Duruthy (Sorde, Landes, France). *Paléo*, 2012, 23 : 315-322.
22. Laurioux B. "Manger au Moyen-Age" . Library Hachette Ed. (Paris, France), collection Pluriel, 2002.
23. Fakhoury M, Blanc L. "Les étapes gourmandes du chevalier Bayard". Le Signet du Dauphin Ed. (Lumbin, France), 2017.
24. Gauthier A. "Alimentations médiévales Ve-XVIe siècle." Ellipses Ed (Paris, France), 2009.
25. Lott JNA, Spitzer E. X-ray analysis studies of elements stored in protein body globoid crystals of *Triticum* grains. *Plant Physiology* , 1980 : 494-501.
26. Jane J, Kasemsuwan T, Leas S, Zobel H, Robyt JF. Anthology of starch granule morphology by scanning electron microscopy. *Starch / Stärke*, 1994, 46 : 121-129.
27. Yang X, Perry L. Identification of ancient starch grains from the tribe Triticeae in the North China Plain. *Journal of Archeological Science*, 2014, 40 : 3170-3177.
28. Yiu SH. Food microscopy and the nutritional quality of cereal foods. *Food Structure*, 1993, 12 : 123-133.
29. Growther A, Haslam M, Oakden N, Walde D, Mercader J. Documenting contamination in ancient starch laboratories. *Journal of Archeological Science*, 2014, 49 : 90-104.
30. Dronzek BL, Hwang P, Bushuk W. Scanning electron microscopy of starch from sprouted wheat. *American Association of Cereal Chemists*, 2012, 295 : 232-239.
31. Birlouez E. "A la table du Moyen-Âge". Ouest France Ed. (Rennes, France), 2013.
32. Pitte JR. "Terres de Castanide : hommes et paysages du châtaignier de l'Antiquité à nos jours". Fayard Ed. (Paris), 1986.
33. Ludes B, Coste M. "Diatomées et medicine légale." Lavoisier Ed. (Paris, France), 1996.
34. Moulinier-Brogi L. Hygiène et cosmétique de la bouche au Moyen Âge. In "Dents, dentistes et art dentaire". L'Harmattan Ed. (Paris), 2012.
35. Gutiérrez-Rodilla BM. Pourquoi se brosser les dents? Soins dentaires au XVIe et XVII e siècles. In "Dents, dentistes et art dentaire". L'Harmattan Ed. (Paris) , 2012.
36. Delumeau J. "La peur en Occident". Fayard Ed. (Paris), 1978.
37. Baron P. Les observations cliniques de Pierre Fauchard dans le *Traité des Dents* (1728). Quelle modernité? In "Dents, dentistes et art dentaire." L'Harmattan Ed. (Paris, France), 2012.

Figure 9. Micro-phytoliths in a today overripe rib. *Above* : SEM photograph (in LFD, 250x) of some part of the rib. *Below* : spectrum of a micro-phytolith at the black point.

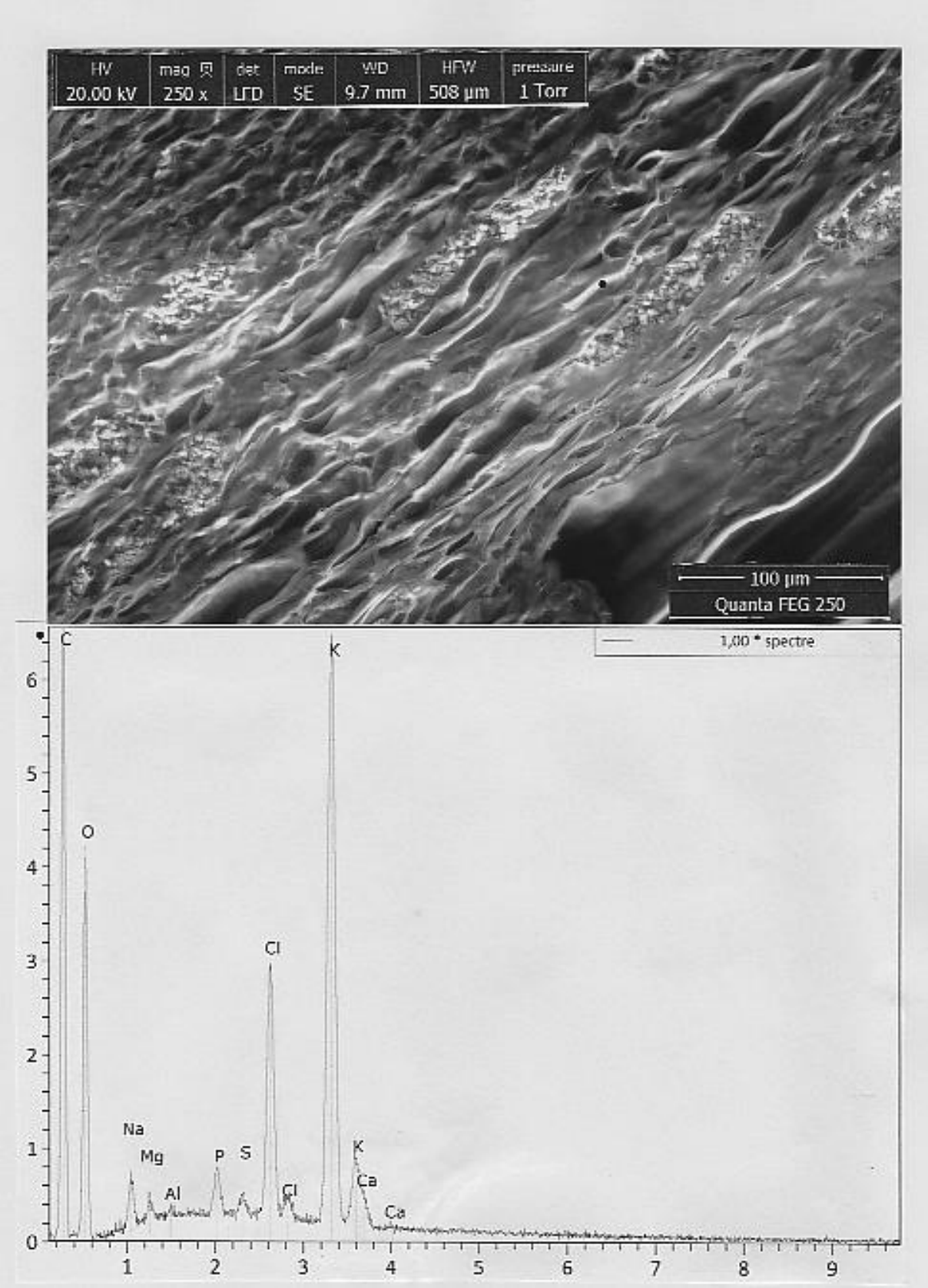

Figure 10. Micro-phytoliths of a today spinach leaf. *Above* : SEM photograph (in LFD, 1600x) of some part of the leaf. *Below* : spectrum of a micro-phytolith at the black point.

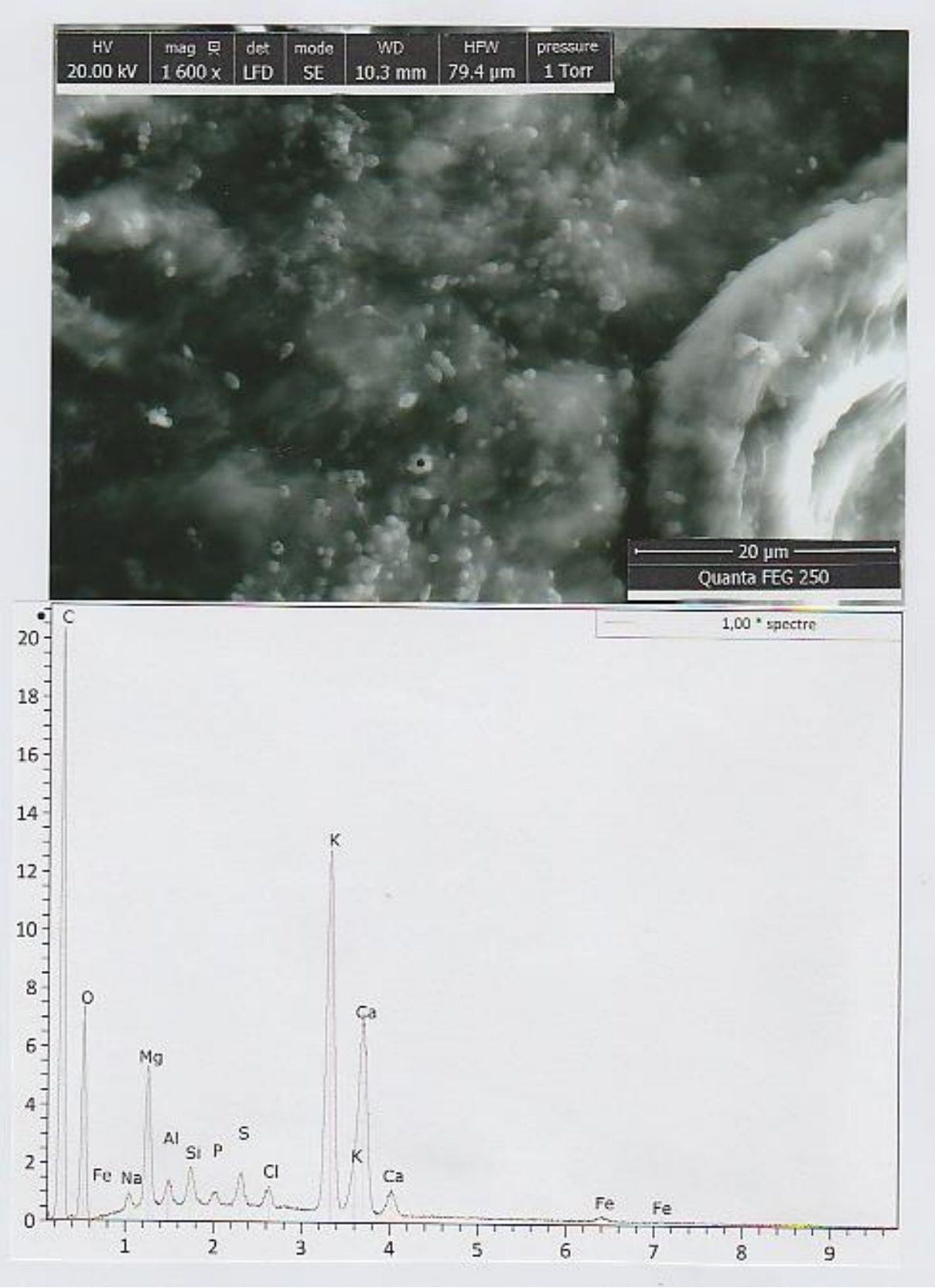

Figure 11. Samples of today leek leafs. **1** : three samples of leafs, in optical microscopy (3x) ; it is the left sample that is analysed (circle). **2** : SEM photograph (in CBS, 100x) of some part of this sample located at the interior of the circle. **3** : the global corresponding spectrum.

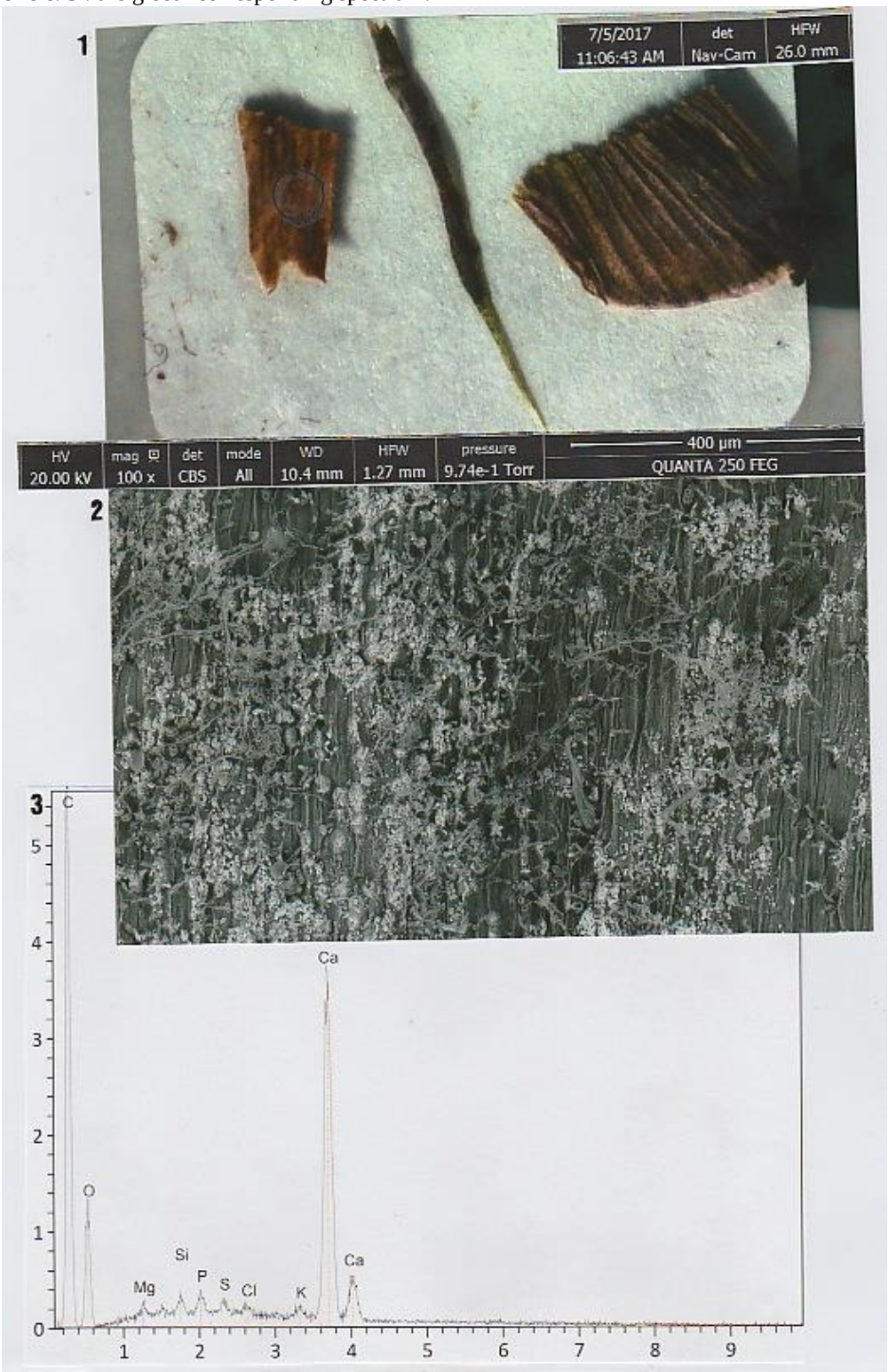

Figure 12. *Above* : SEM photograph (in CBS, 800x) of some part of the previously described area ; 1, 2 and 3 indicate the three phytoliths analysed. *Below* : Spectrum of these three phytoliths.

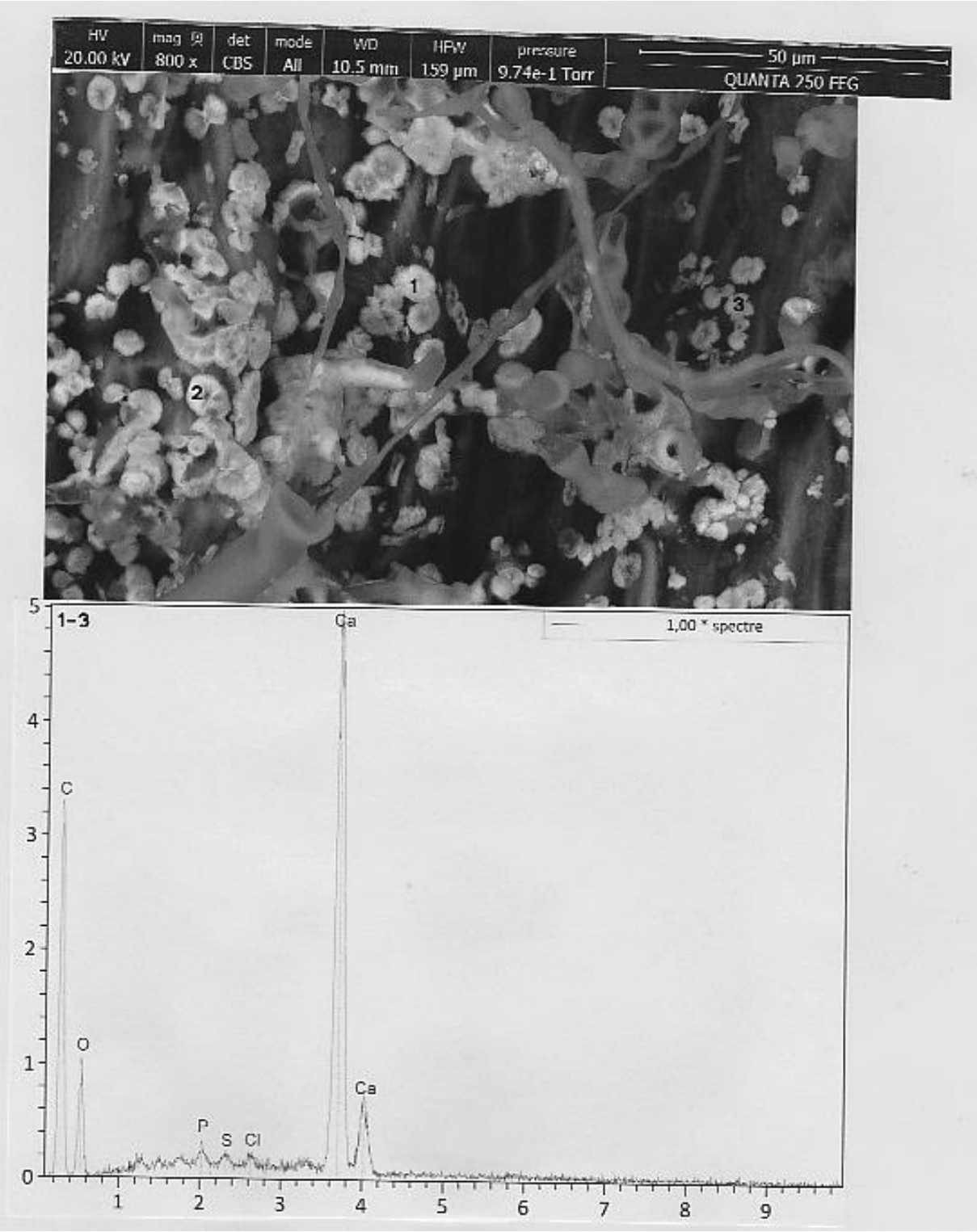

Figure 13. SEM photograph and alalyses of seven grouped triangular silicium phytoliths. *Above* : SEM photograph (in CBS, 4000x) showing seven (1-7) phytoliths. *Below* : (inferior part) spectrum of phytoliths 1-5 ; (superior part) spectrum of phytoliths 7 and 8.

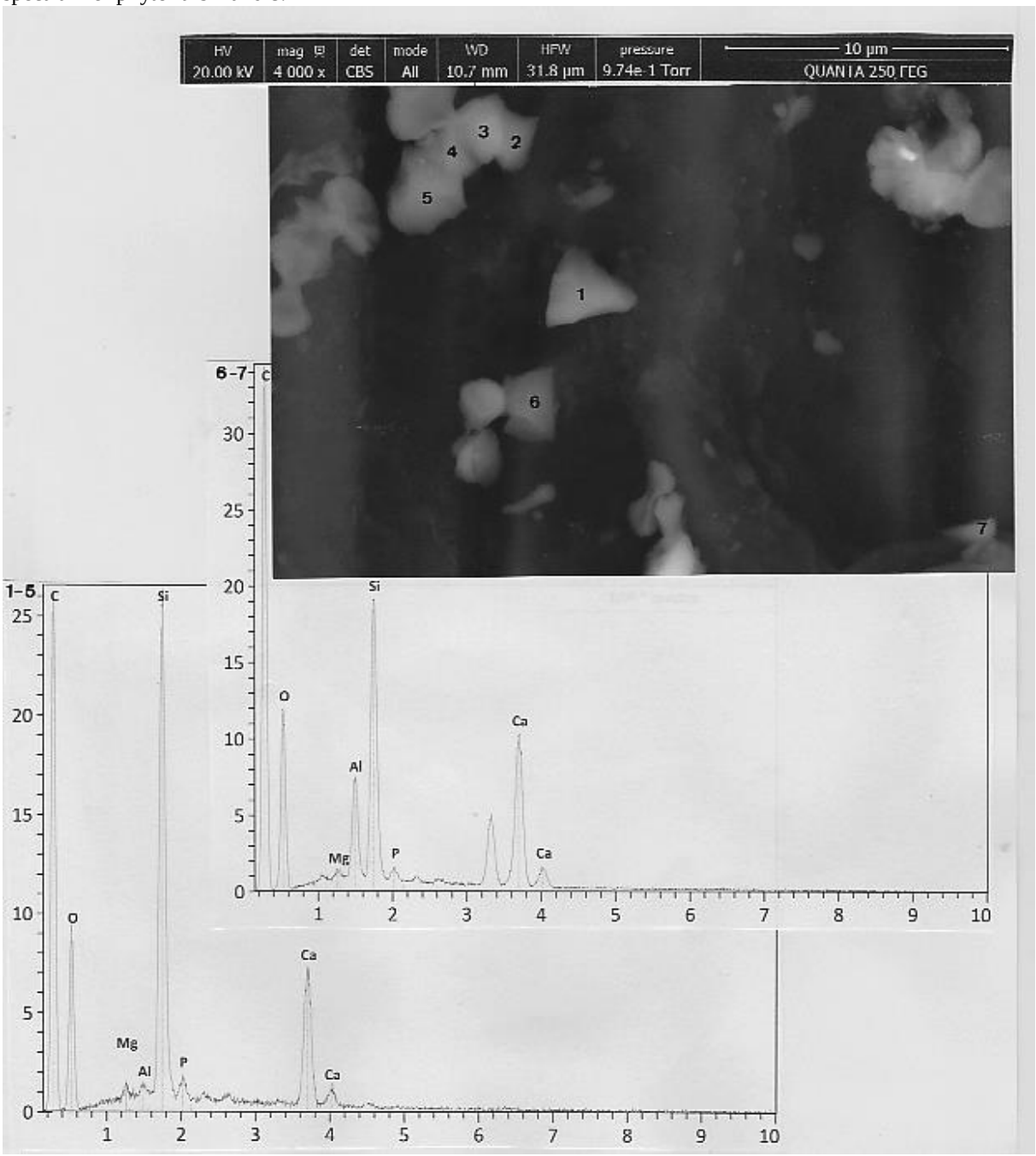

Figure 14. Samples of today asparagus stems. **1** : five samples of stems, in optical microscopy (3x) ; it is the central sample (circle) that is analysed. **2** : SEM photograph (in CBS, 50x) of some part of this stem ; particles located in the circle are analyzed.

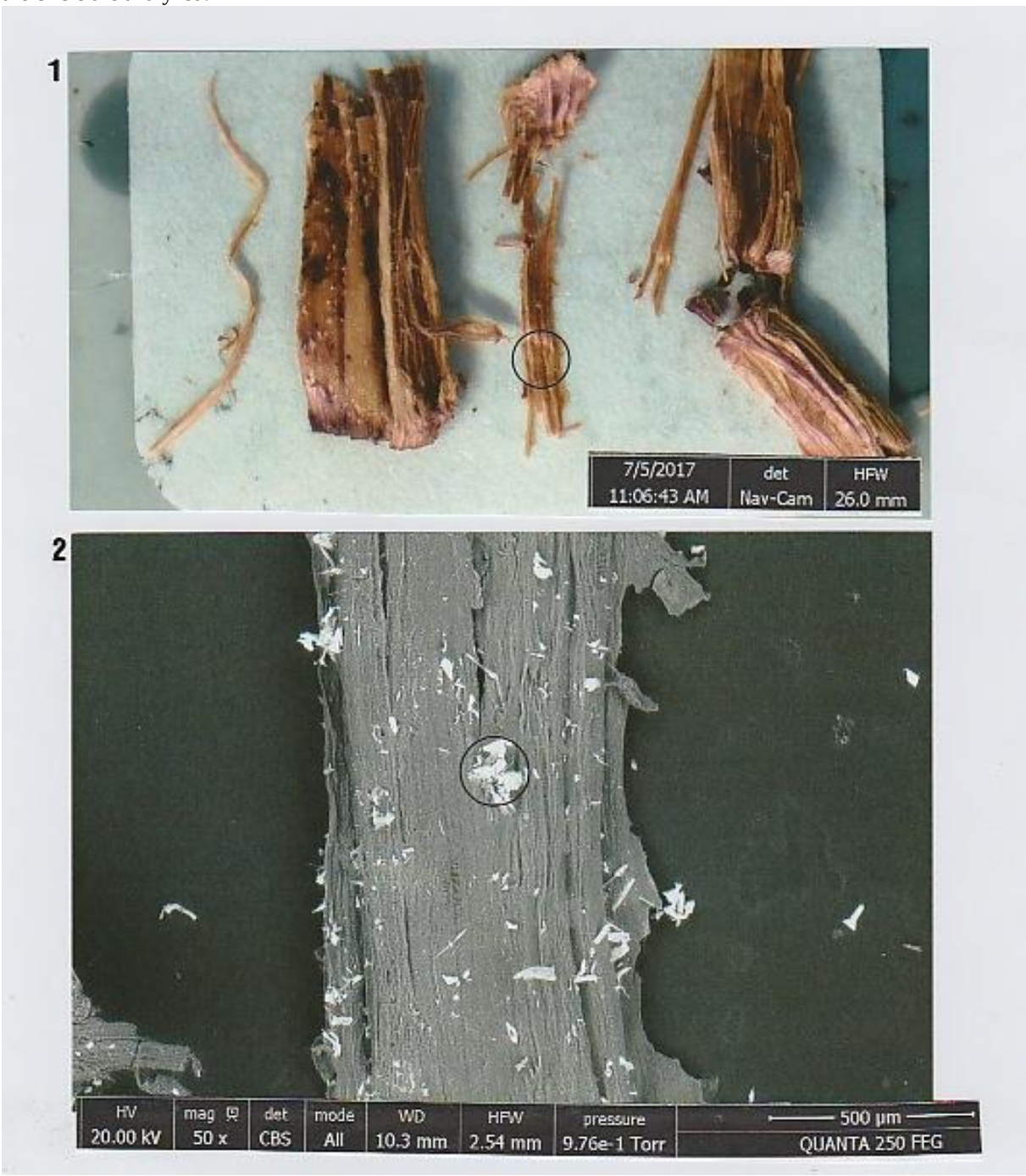

Figure 15. *Above* : SEM photograph (in CBS, 400x) of particles located inside the circle. 1 : central part ; 2 : long micro-phytolith number 2 ; 3 : long micro-phytolith number 3 (little points indicate three other long micro-phytoliths). *Below* : spectrum of the central part.

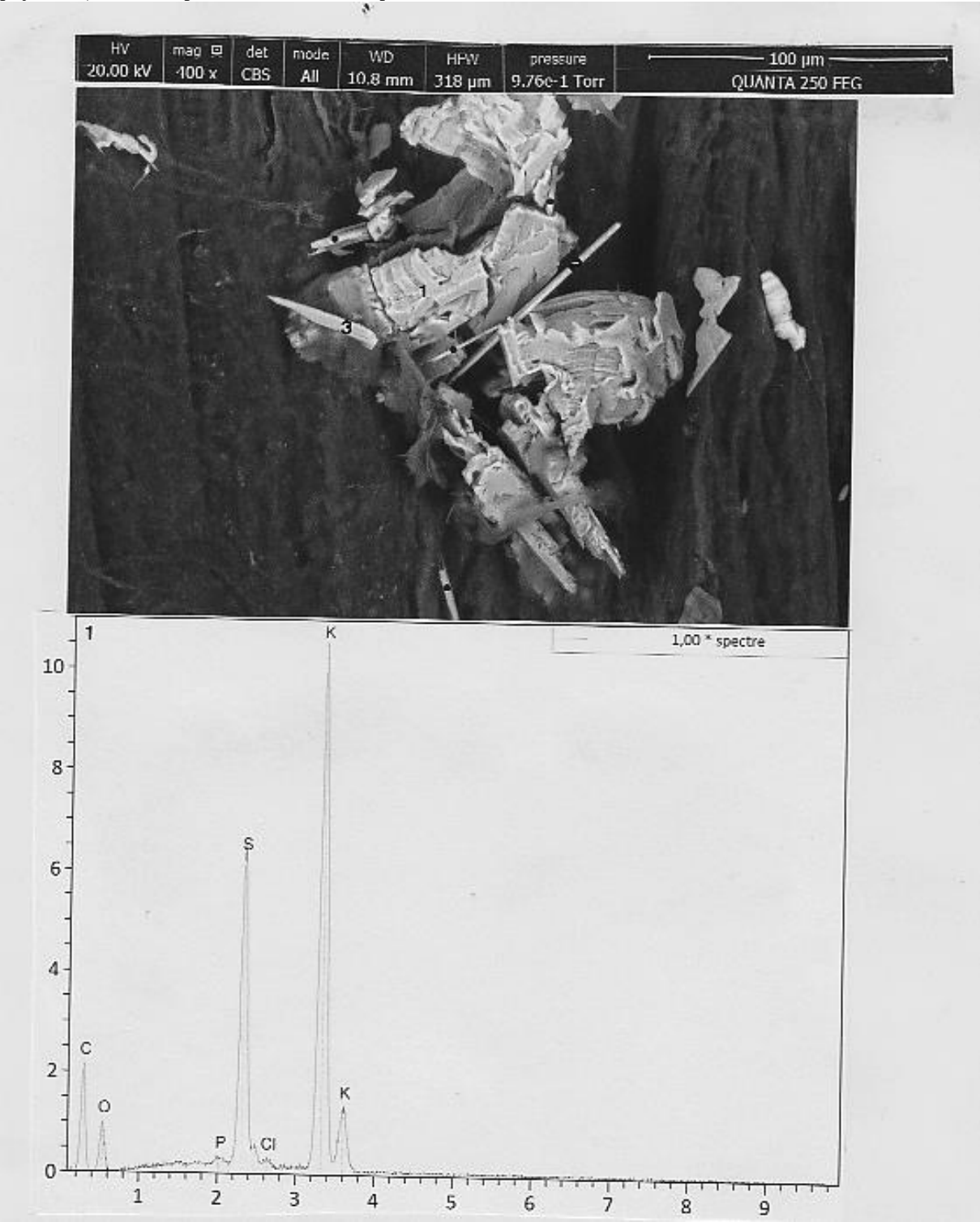

Figure 16. SEM photograph and spectrum of the long micro-phytolith number 2. The SEM photograph (in CBS, 3000x) shows the extremity of this phytolith, where the blue pastille 2 location is analysed ; the red pastille is some location on the background where the substrate is analysed. The corresponding spectras compare elementary analyses realized on the phytolith (in blue) and the substrate (in red).

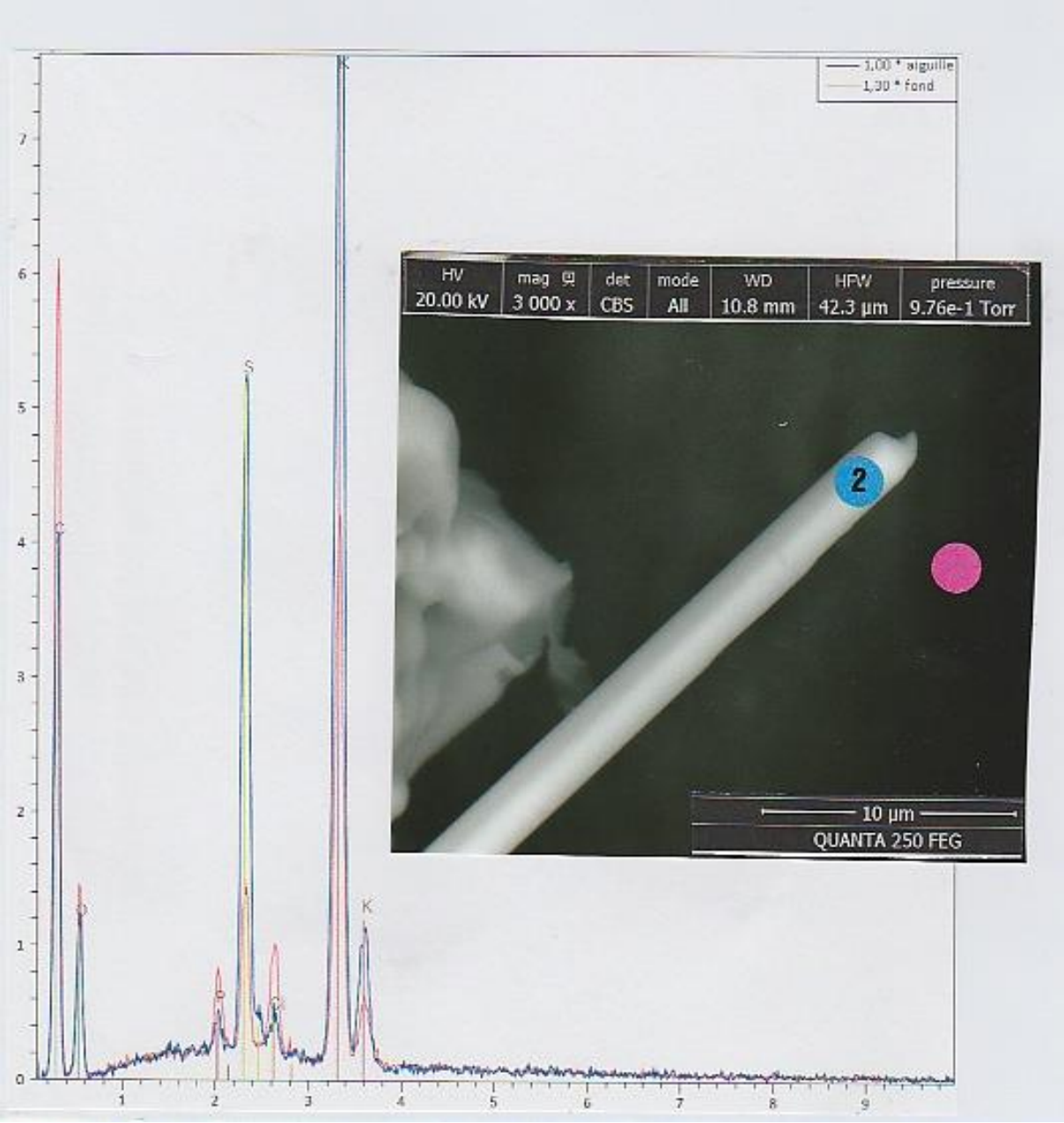

Figure 17. SEM photograph and spectrum of the long micro-phytolith number 3. *Above* : SEM photograph (in CBS, 3000x) shows the extremity of this phytolith. *Below* : spectrum at the black dot.

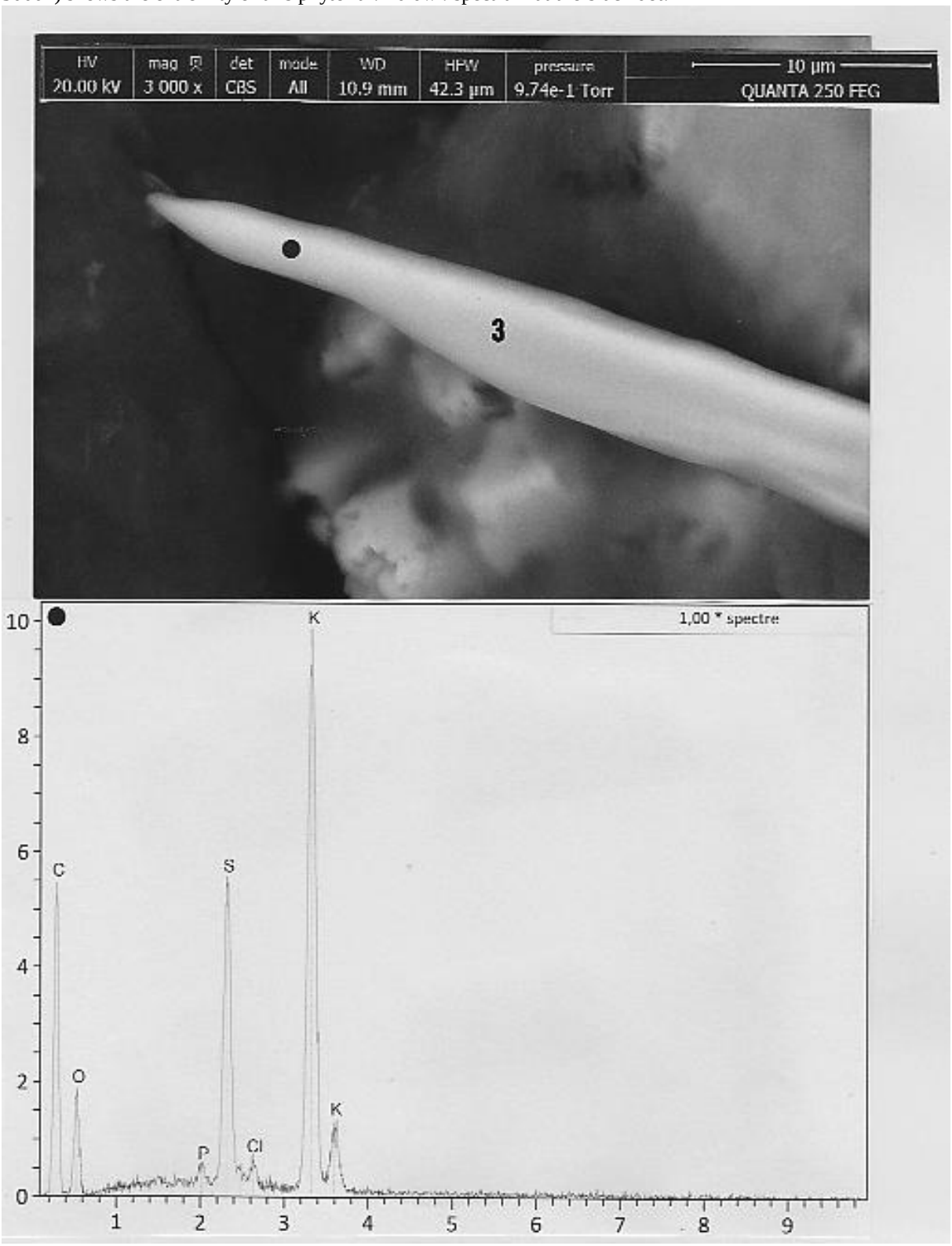

Figure 19. A today sorrel leaf. *Above* : SEM photograph (in CBS, 1000x) of some part of the upper sorrel leaf surface, showing numerous macles under the leaf epiderm.
Below : (upper part) an optical view (5x) of a sample of leaf ; (lower part) the spectrum corresponding to one crystal of the macle.

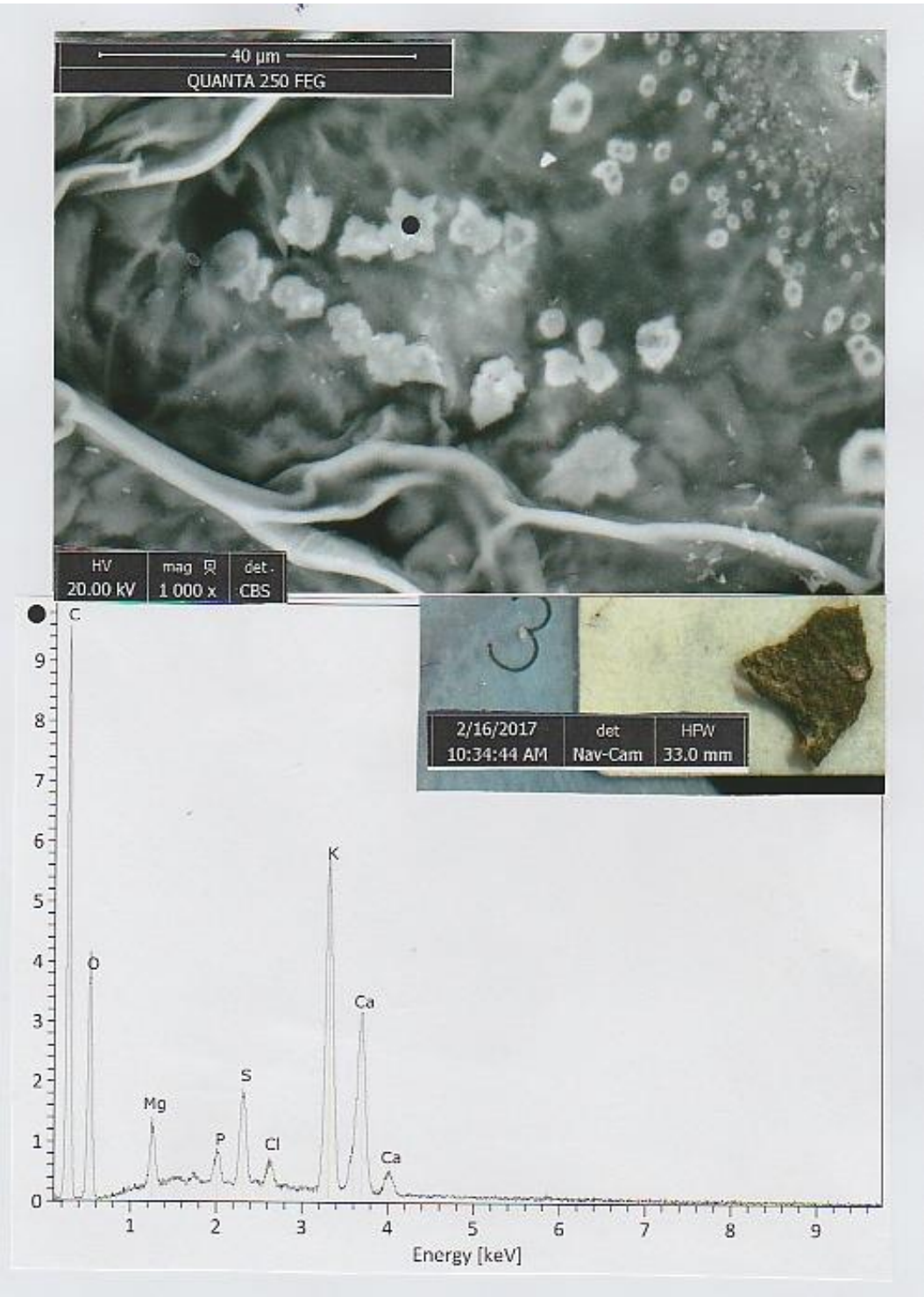

Figure 23. Photographs of today crusts of bread.**1** : the crusts, in optical microscopy (5x) ; the circled crust is that chosen for SEM observations. **2** : SEM photograph (in LFD, 400x) of the crust ; the pointed ellipsoid particle of 27.3 µm long is a yeast (*Saccharomyces cerevisiae*).

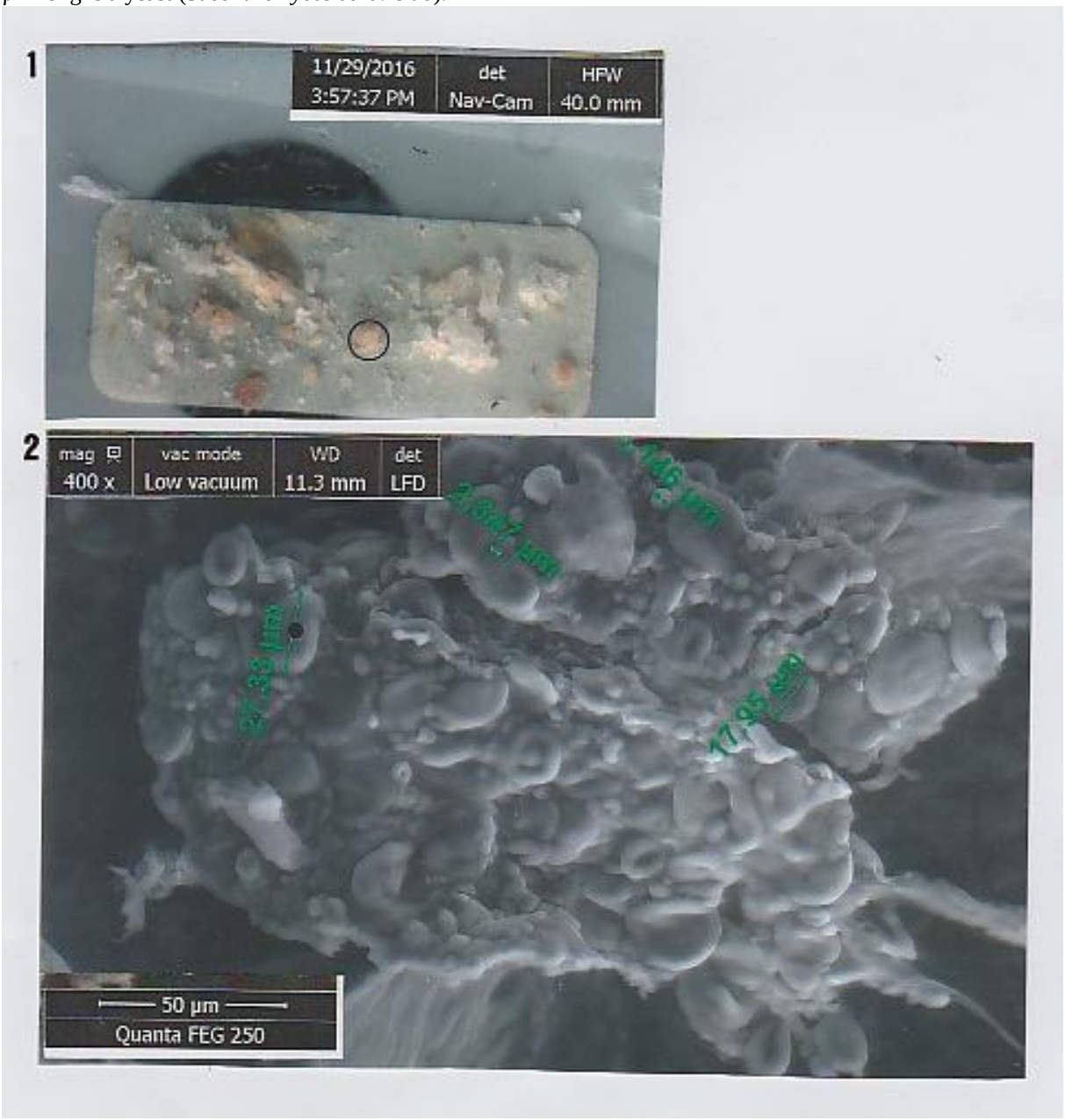

Figure 24. A today wheat flour. **1**. Photograph of the wheat flour, in optical microscopy (3x). **2** : SEM photograph (in LFD, 400x) of the flour. **3** : global spectrum of the flour.

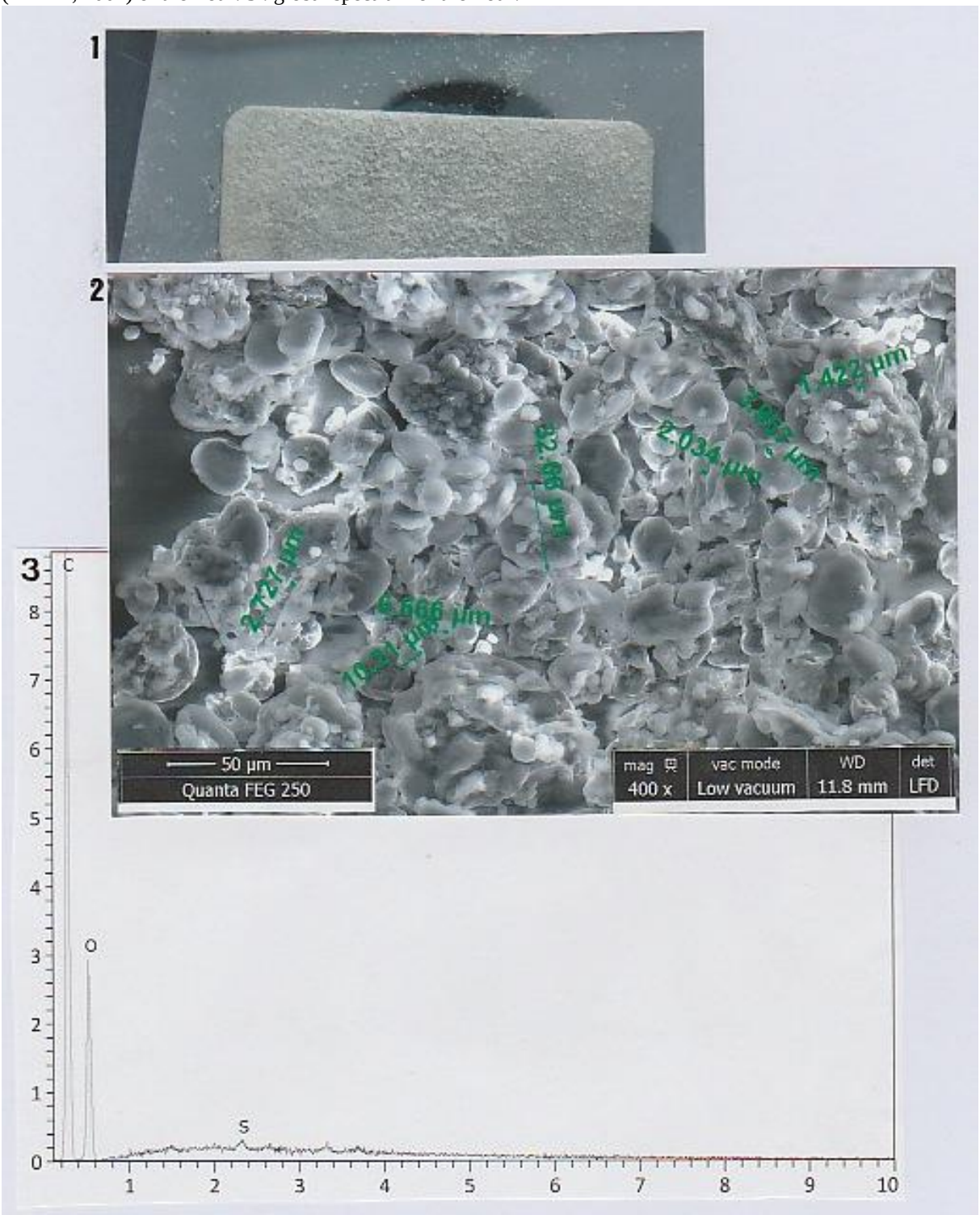

Figure 25. A today rye flour. **1** : photograph of the rye flour in optical microscopy (the circled particle is that chosen for SEM observations). **2** : SEM photograph (in LFD, 400x) of the particle (four starches are indicated by crosses). **3** : global spectrum of the flour(compared to that of the previous one, the global spectrum of rye flour is relatively more rich in potassium, calcium and phosphorus).

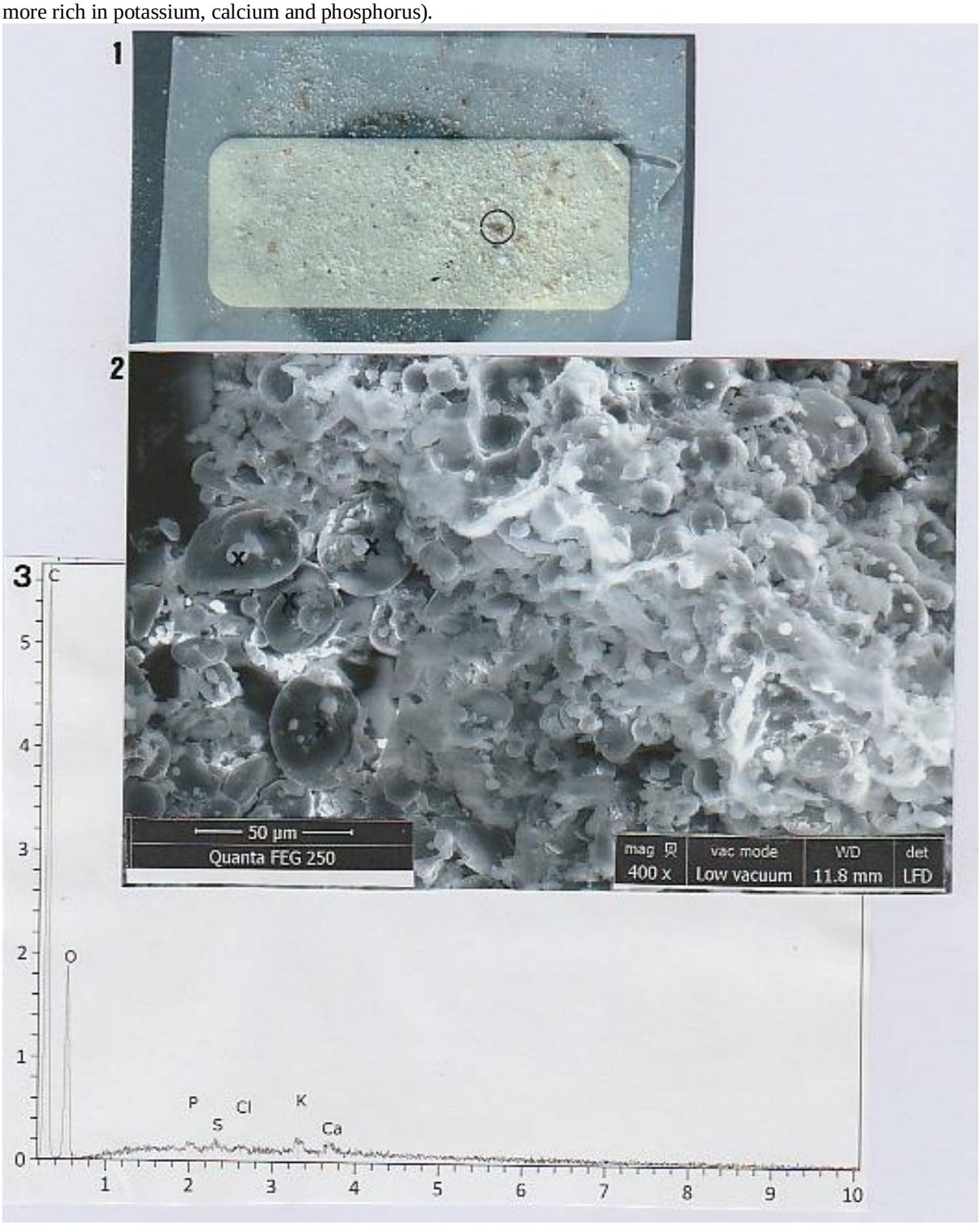

Figure 27. A today dry green garden pea. **1** : section of a dry garden pea, in optical microscopy (3x) ; the circled part is studied by SEM. **2** : SEM photograph (in LFD, 50x) of this circled part (the rectangular area is enlarged in the below SEM photograph). **3** : SEM photograph (in LFD, 250x) of this rectangular area, showing details on starches.

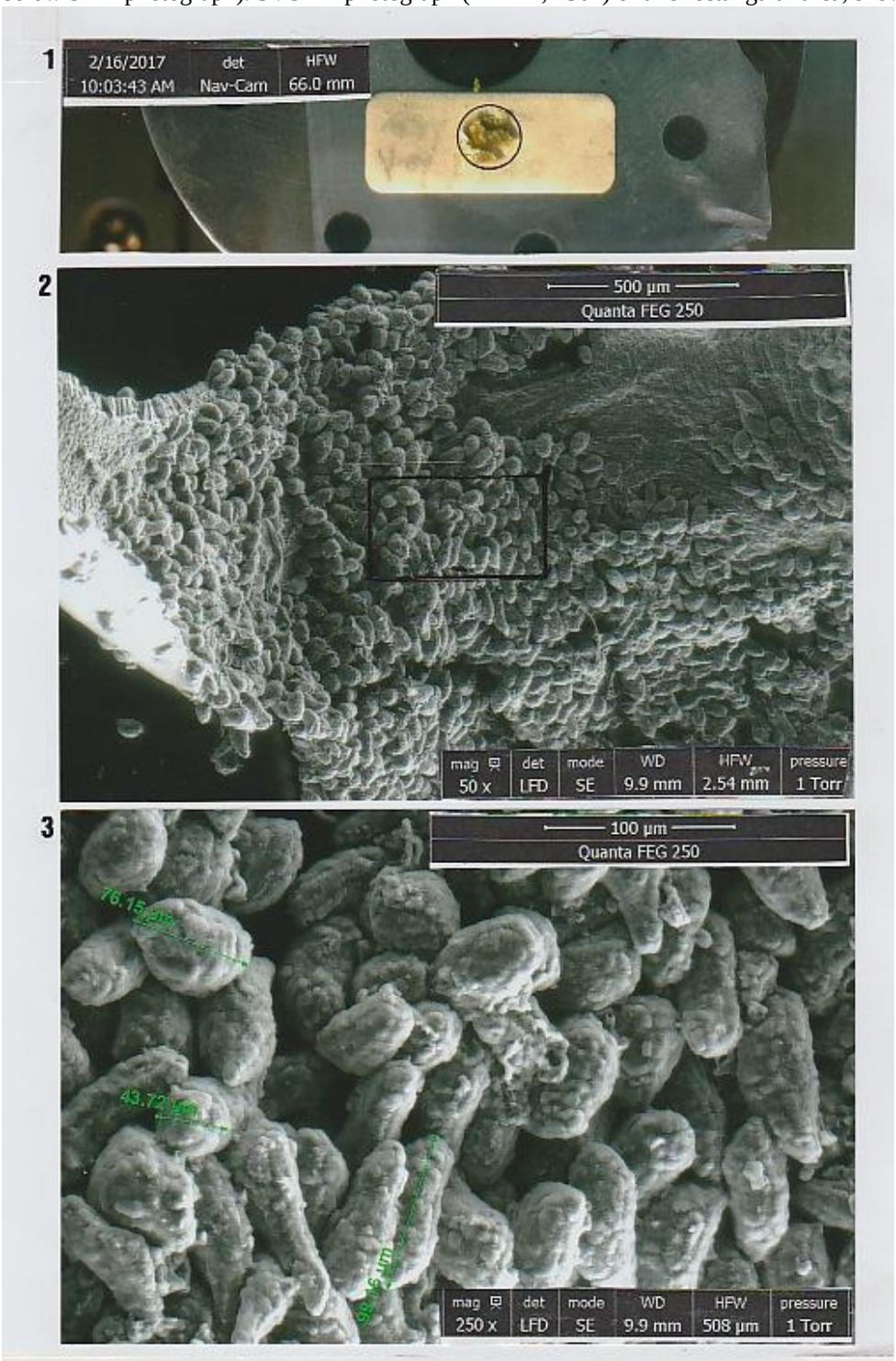

Figure 30. Two today chicken bones. **1**: view of two (1 and 2) chicken bones , in optical microscopy (5x) ; circle indicates the region of bone 2, enlarged in the below SEM photograph. **2** : SEM photograph (in LFD, 25x) of the circled above region ; the circle in its photograph indicates a region of bone 2 with flat appearance.

Figure 31. *Above* : the same photograph (but in CBS) of the previous one ; 1 and 2 indicate the points where EDX analyses are realized . *Below* : spectras at points 1 and 2.

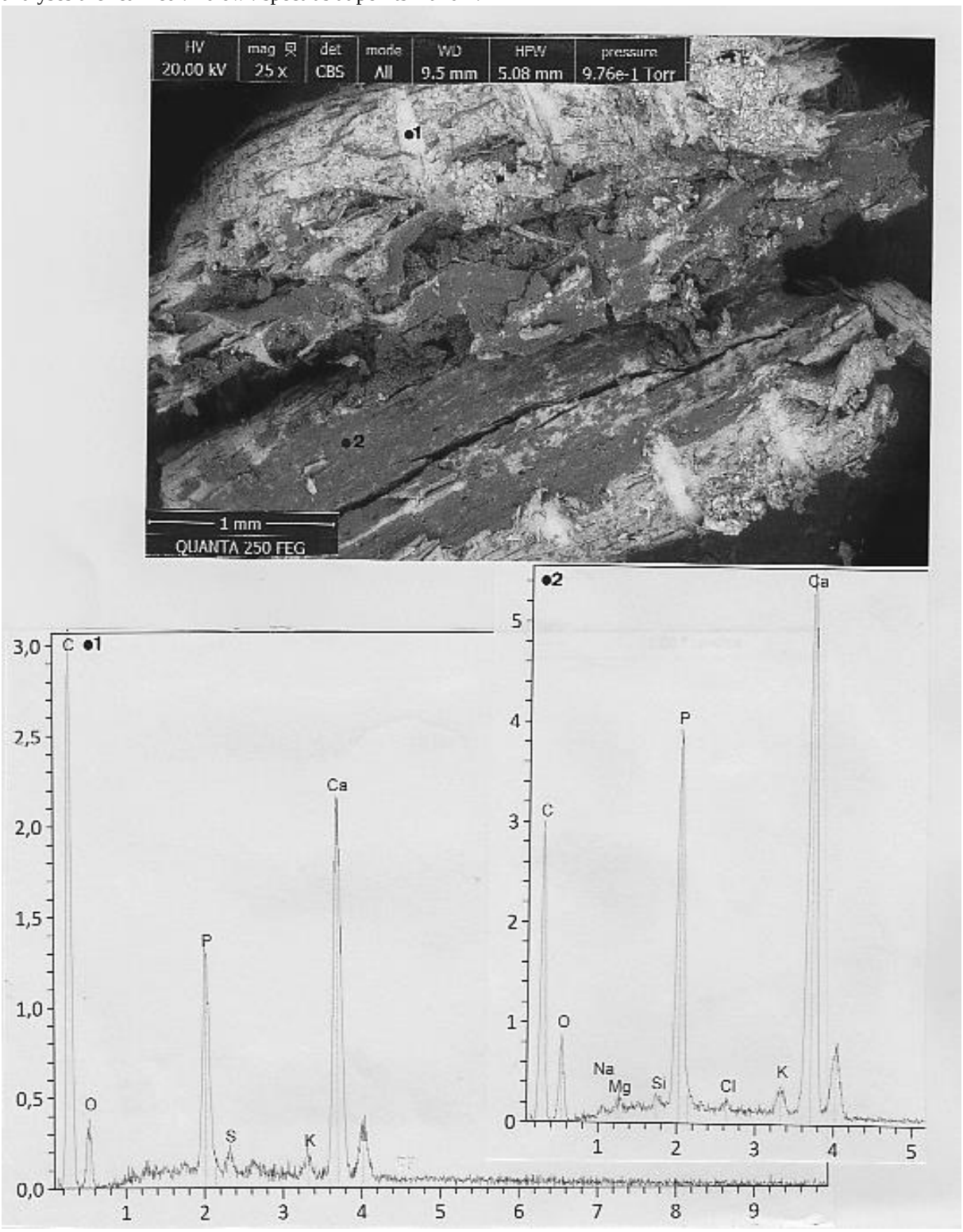

Figure 34. A today cooked extremity of a fish-bone (of trout). *Above* : SEM photograph (in CBS, 50x) showing the fish-bone extremity (1 and 2 indicate the locations where EDX analyses are realized). *Below* : spectras 1 and 2. The intermediary photography is a view (in optical microscopy) of this fish-bone , showing locations of points 1 and 2.

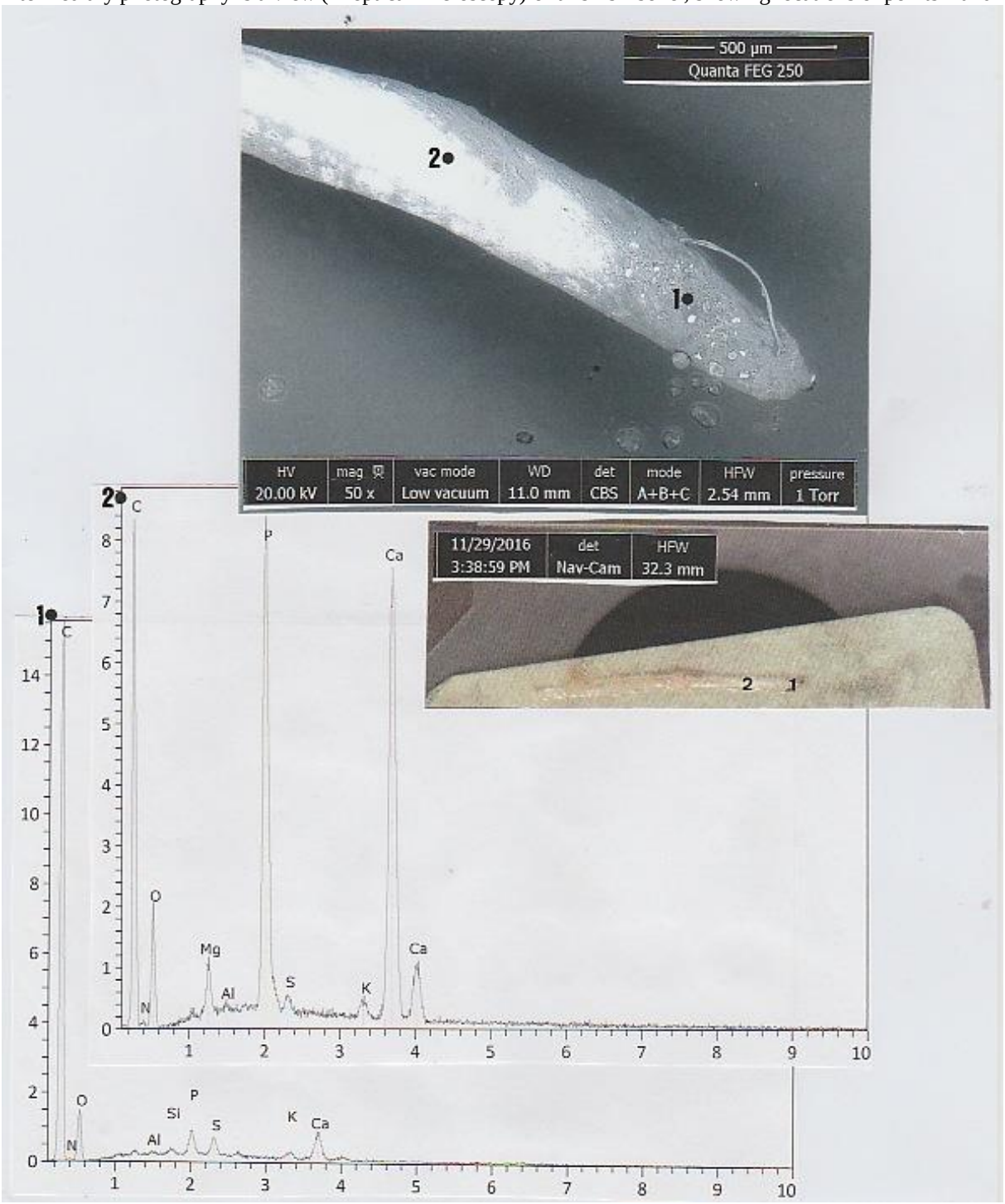

Figure 36. A today cooked fish-scale (of trout). *Above* : SEM photograph (in LFD, 50x) showing some part of the fish-scale ; the black dot indicates the location where EDX analysis is realized. *Below* : spectrum at the black dot. The intermediate photograph shows (in optical microscopy) several cooked fish-scales of trout (it is the circled scales that is studied here).

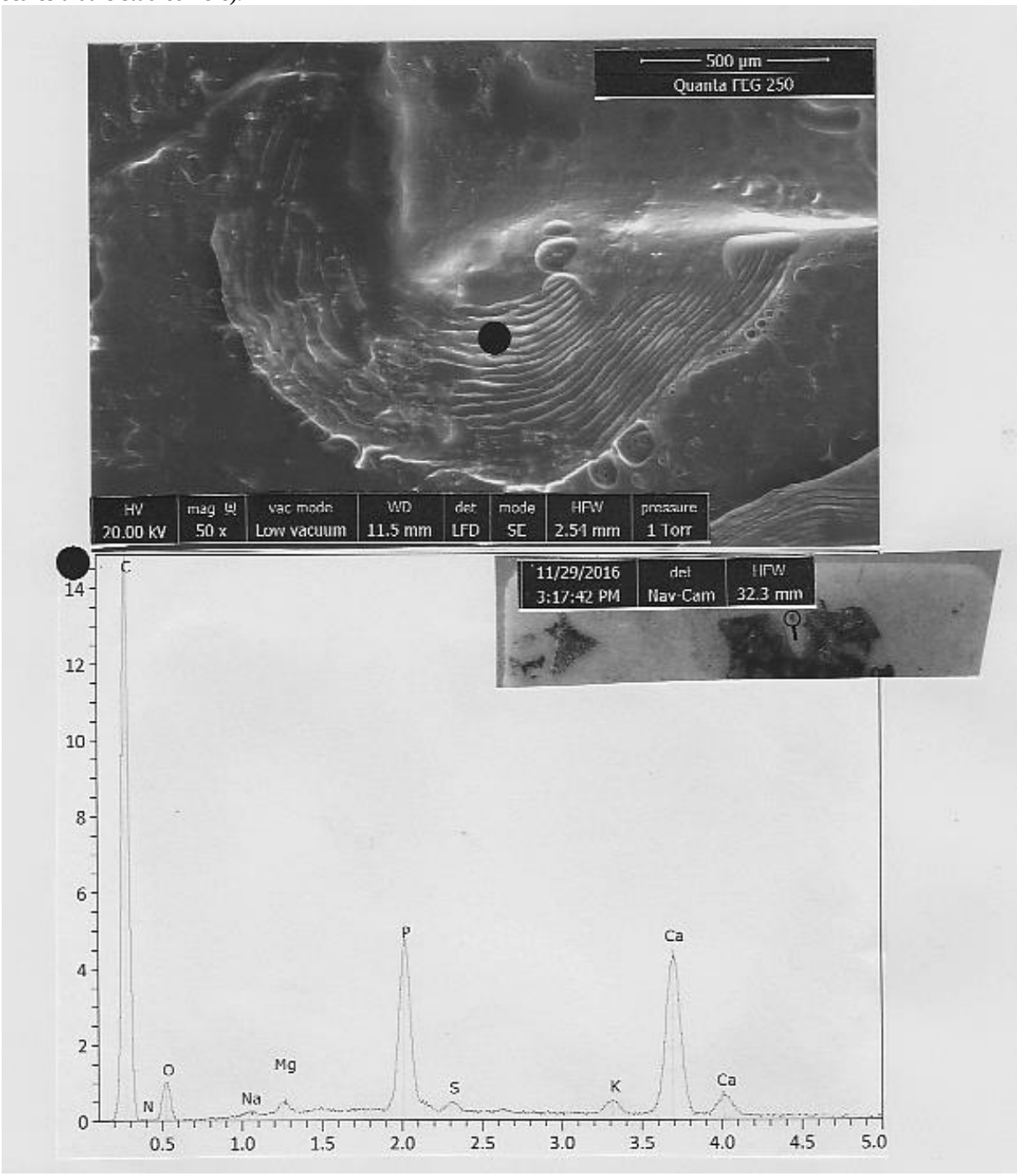

Figure 40. Chestnut-tree pollen grains found in a today chestnut-tree honey.**1**: optical view (65x) of chestnut-tree pollens of reference. **2:** photographs (in optical microscopy, 50x) of four (2.1-2.4) views of chestnut honey spread over a glass slide (arrow points indicate the pollen grains).

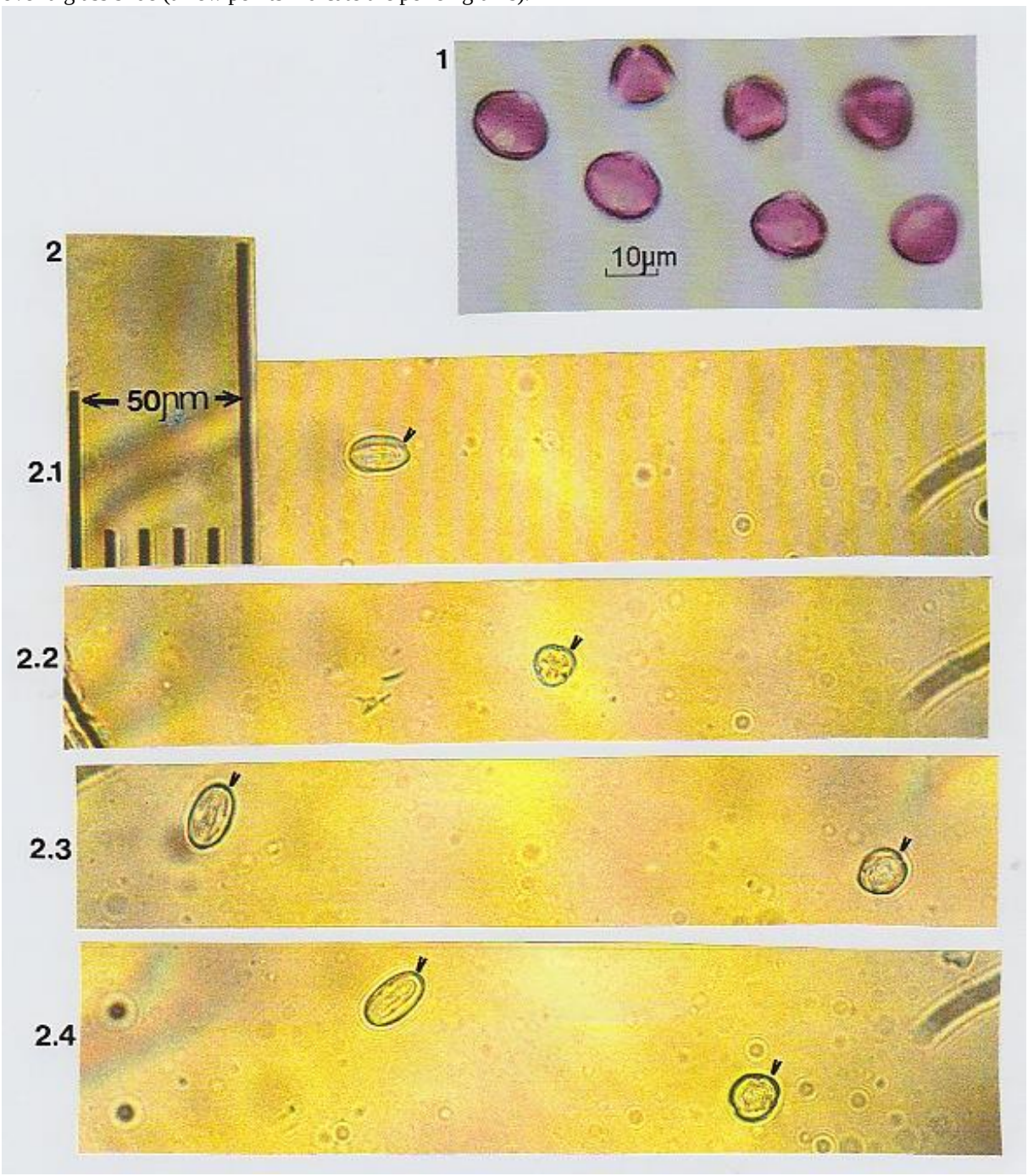

Figure 49. Study of a kaolinite mineral of reference. **1**: the kaolinite powder view, in optical microscopy(3x). **2**: SEM photograph (in CBS, 150x) of some kaolinite fragments of this powder (encircled, five kaolinite crystals). The spectrum below corresponds to the EDX analysis of the longest kaolinite fragment.

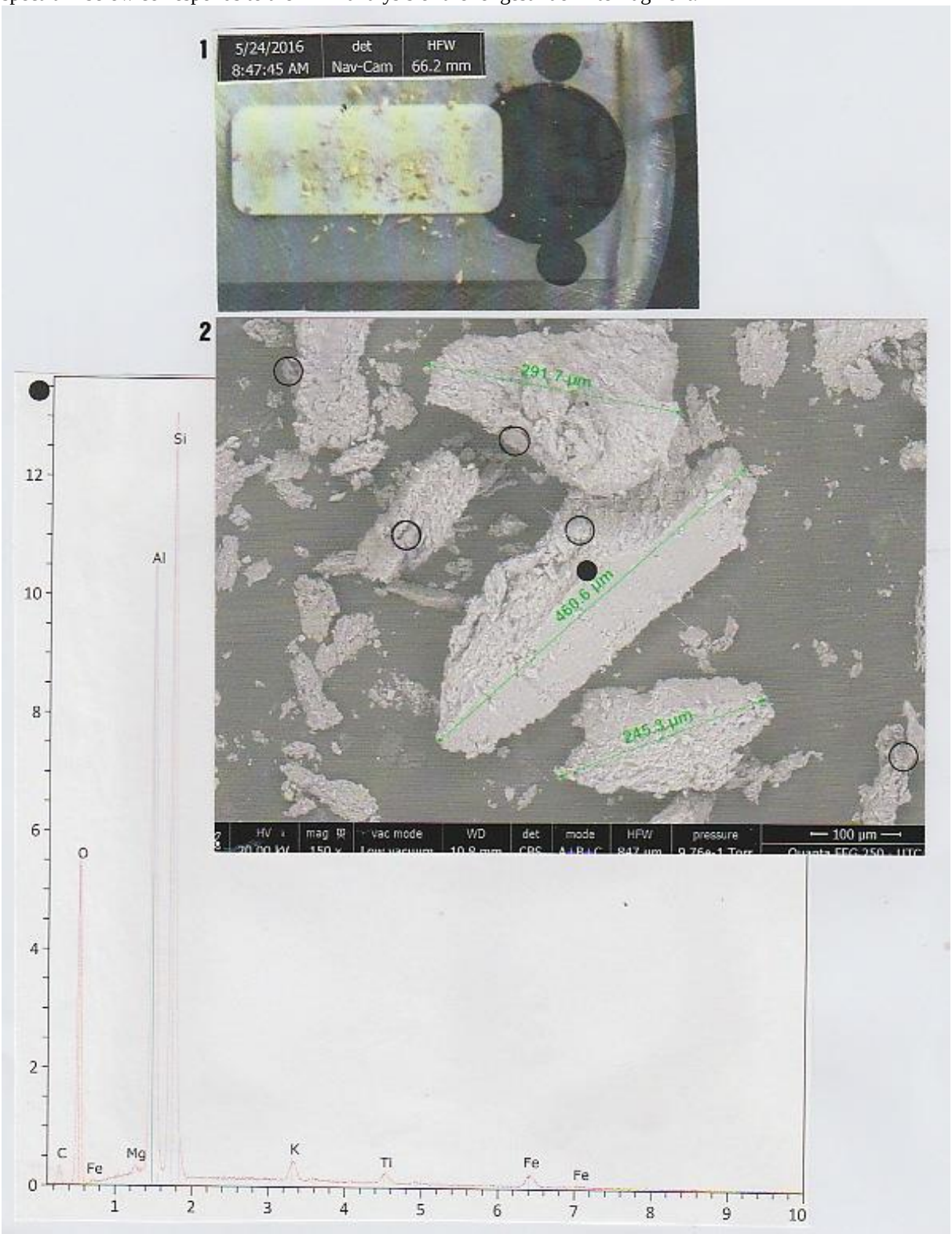

Figure 50. Study of a coral fragment of reference. **1** : the coral fragment, in optical microscopy (3x). **2** : SEM photograph (in LFD, 400x) of the coral surface of this coral fragment. **3** : the corresponding global spectrum.

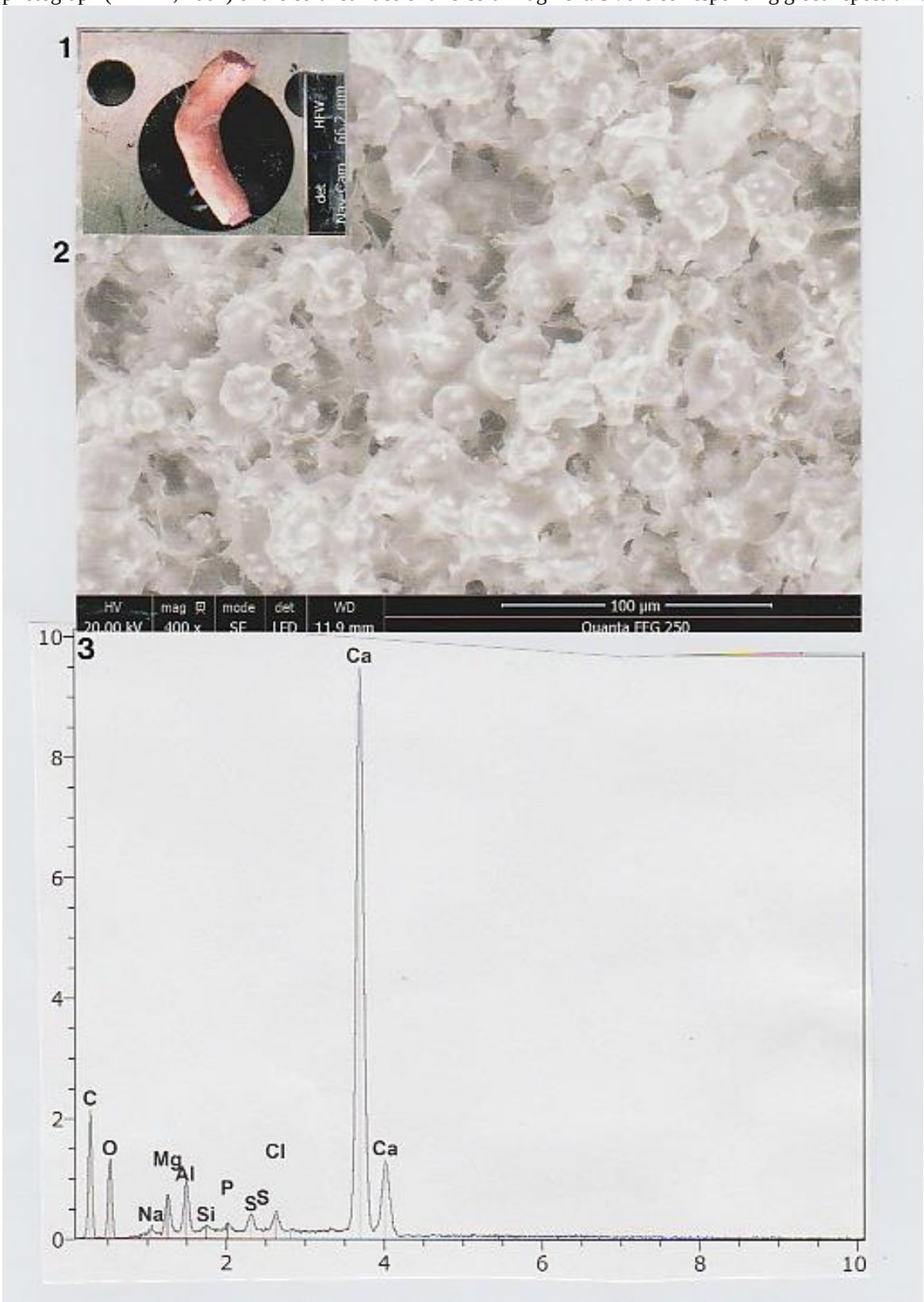

Figure 52. A today sample of sponge. **1** : the sponge sample, in optical microscopy (3x). **2** : SEM photograph (in LFD, 250x) of spicules (S) ; M are filaments of the organic matrix.

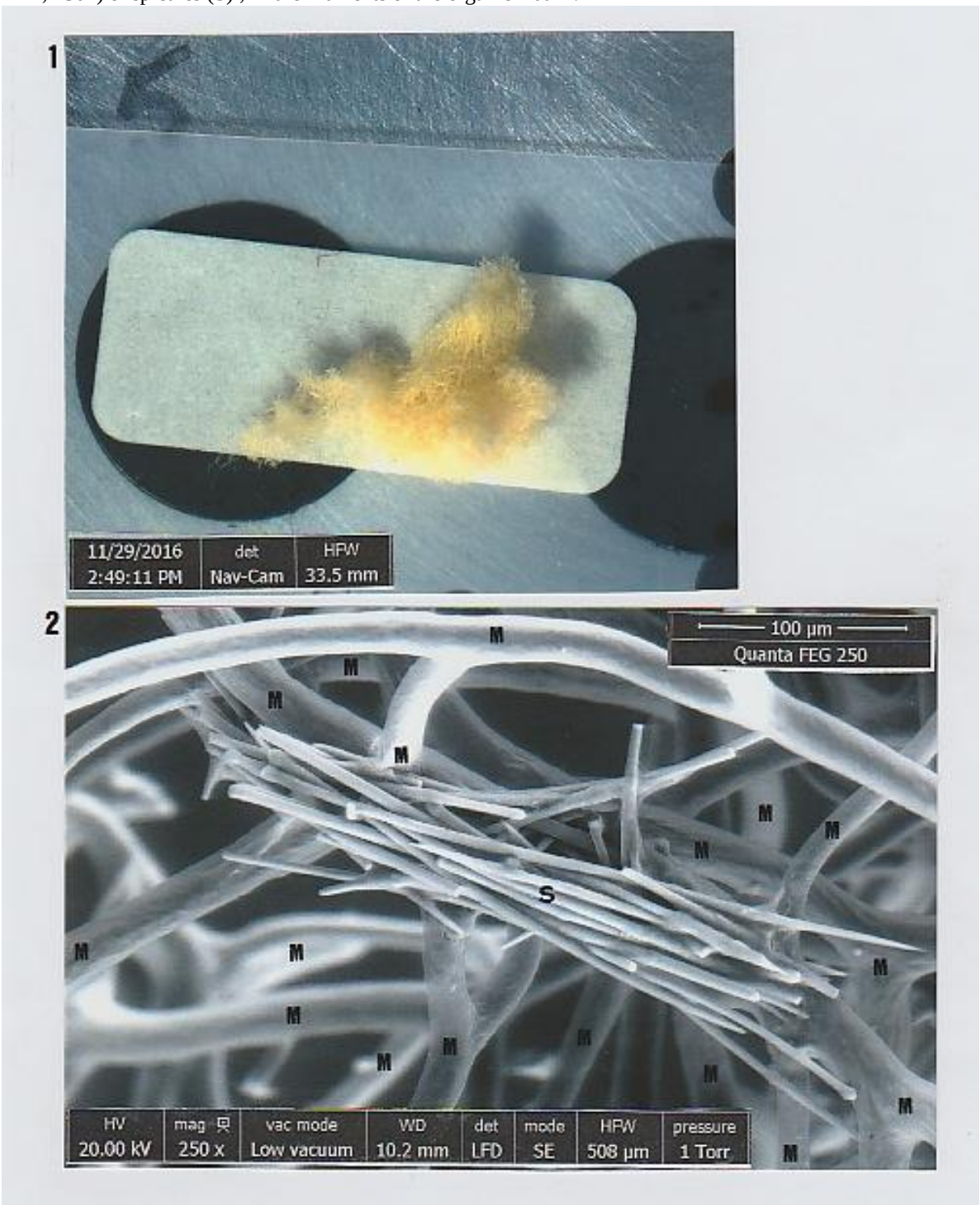

Figure 53. *Above* : the same SEM photograph as that shown in the previous one, but in CBS. *Below* : spectrum of the spicules.

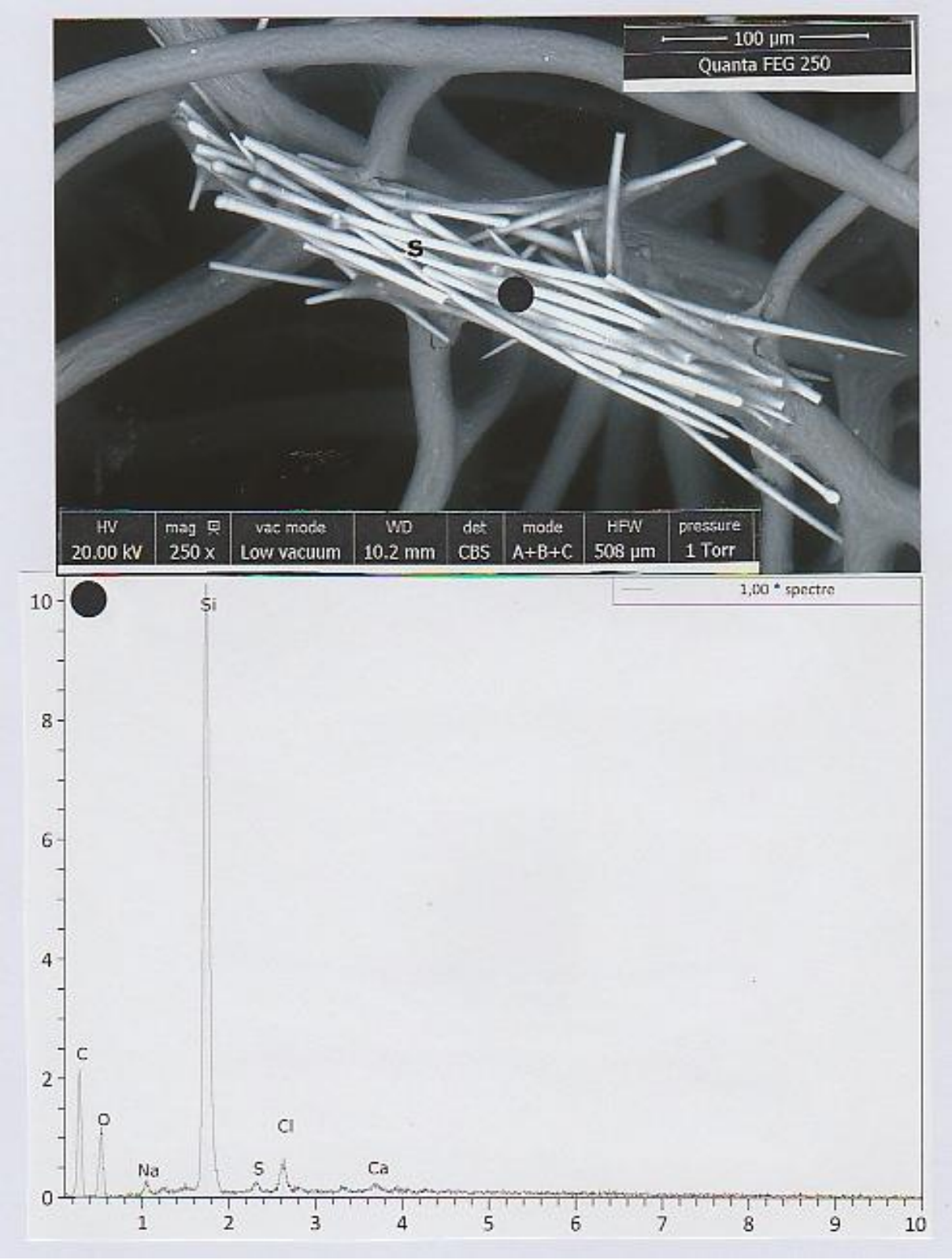

Figure 55. Study of a commercial pumice stone. **1** : pumice stone fragments, in optical microscopy (3x) ; the arrow point indicates the fragment under study (N : black micro-fragments ; Q : a quartz). **2** : SEM photograph (in LFD, 36x) of this fragment (N : black micro-fragment ; **A** : pores in the fragment ; **S** : filamentous parts of the fragment).

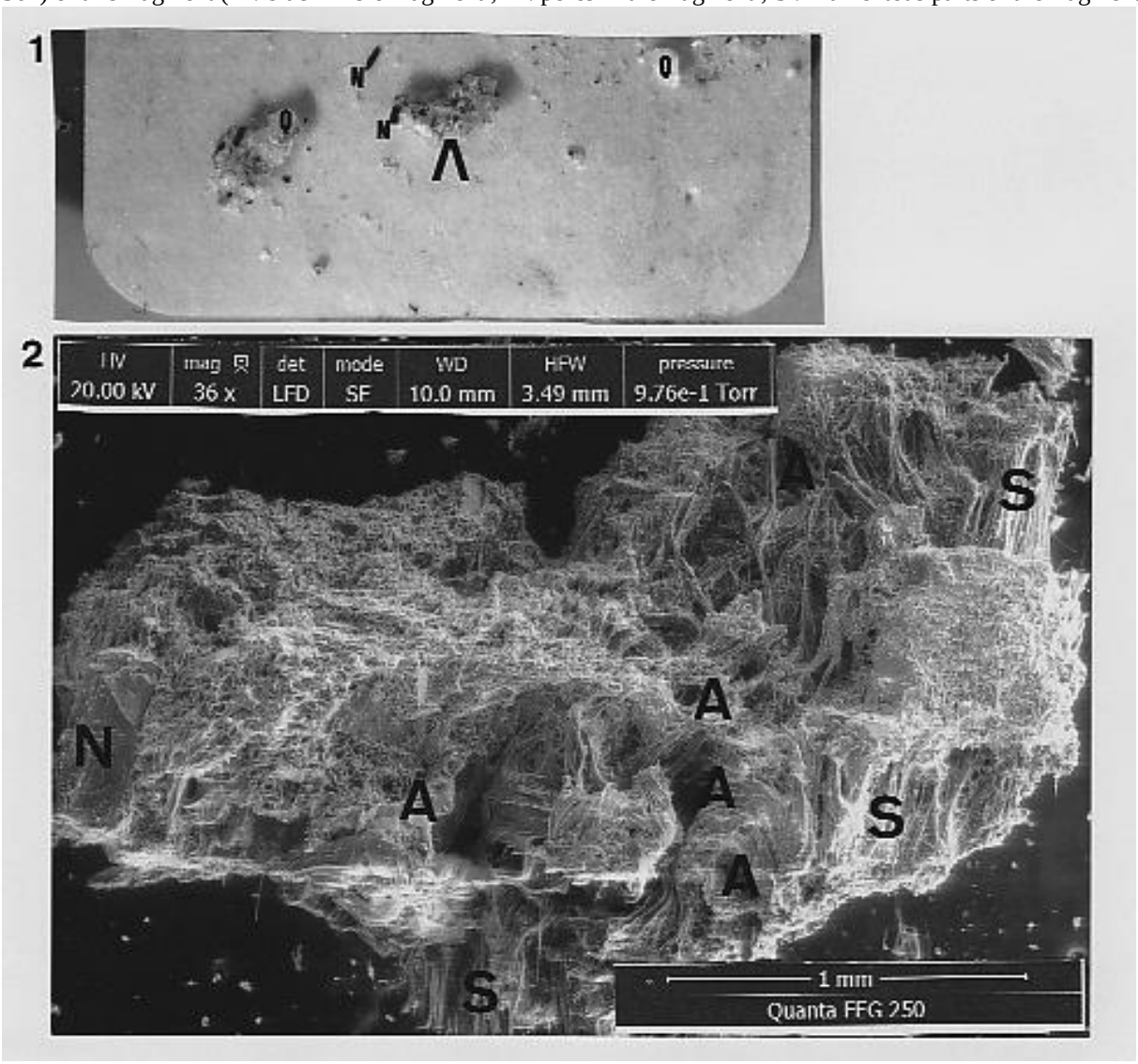

Figure 56 . *Above* : the same photograph as the previous one, but in CBS ; **1** , **2** and **3** indicate the three regions of the fragment studied. *Below* : spectrum of **1**.

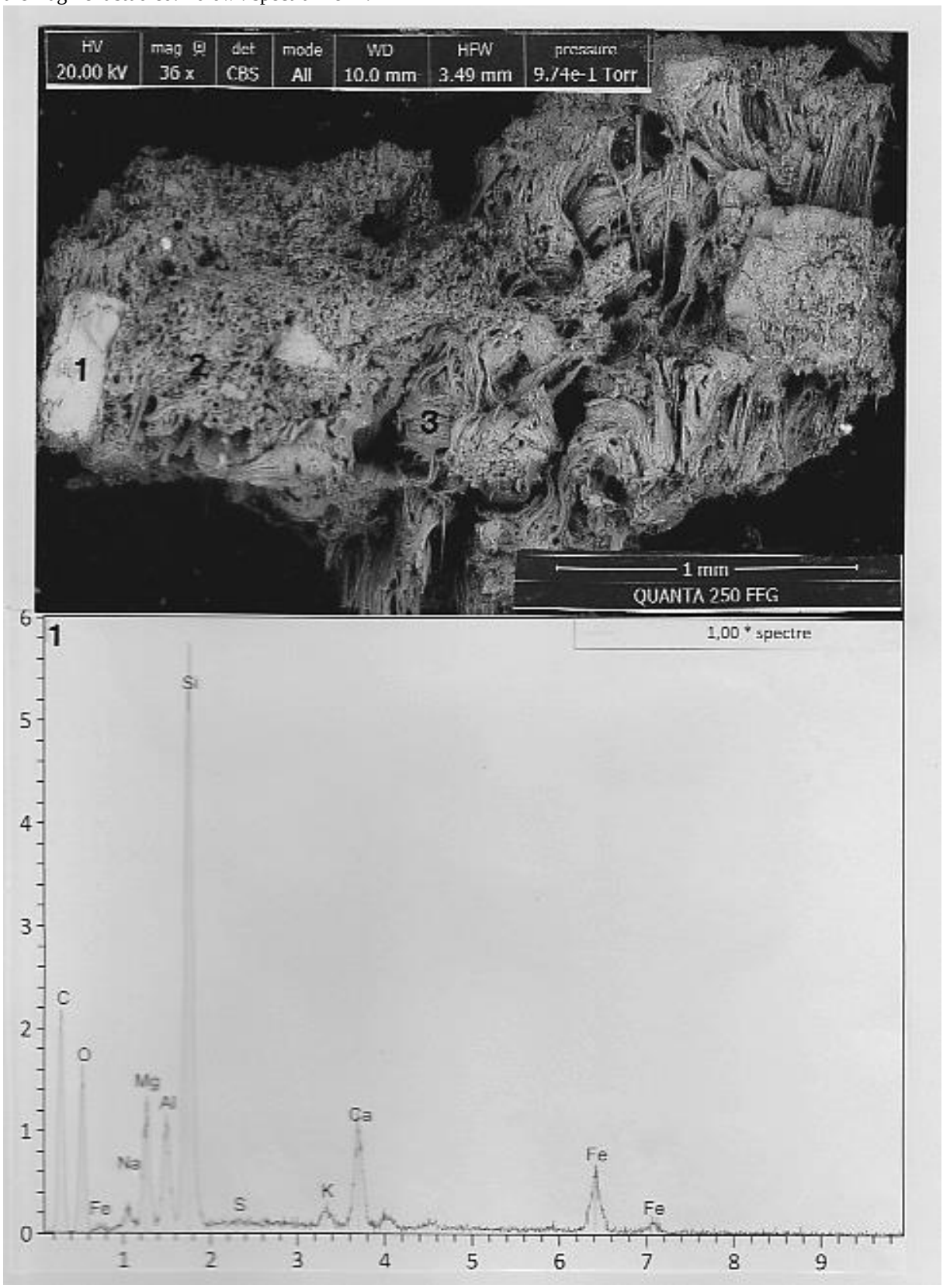

Figure 57. Spectras of **2** (above) and **3** (below).

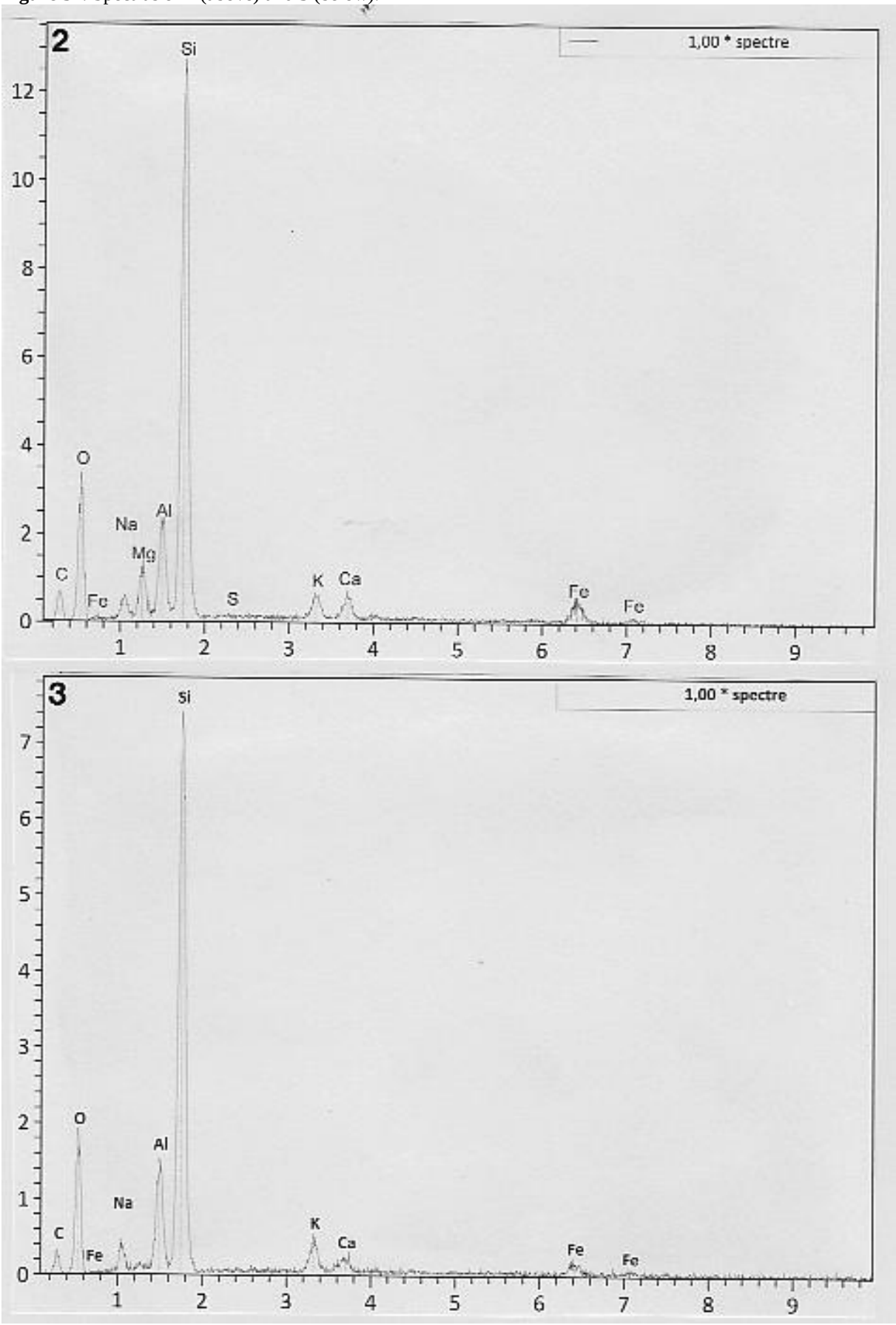

Figure 60. Exploration of a today cooked chicken bone (an osseous part of one leg). *Above* : SEM photograph (in CBS, 25x) of a region of this bone, encircled in the above optical microscopy (3x) view. The numerous cavities observed in this bone fragment correspond to the pneumatisation of this sort of osseous ; the more cooked parts are bright to electrons. The black dot indicates the location where EDX analysis is realized. *Below* : spectrum at the black dot.

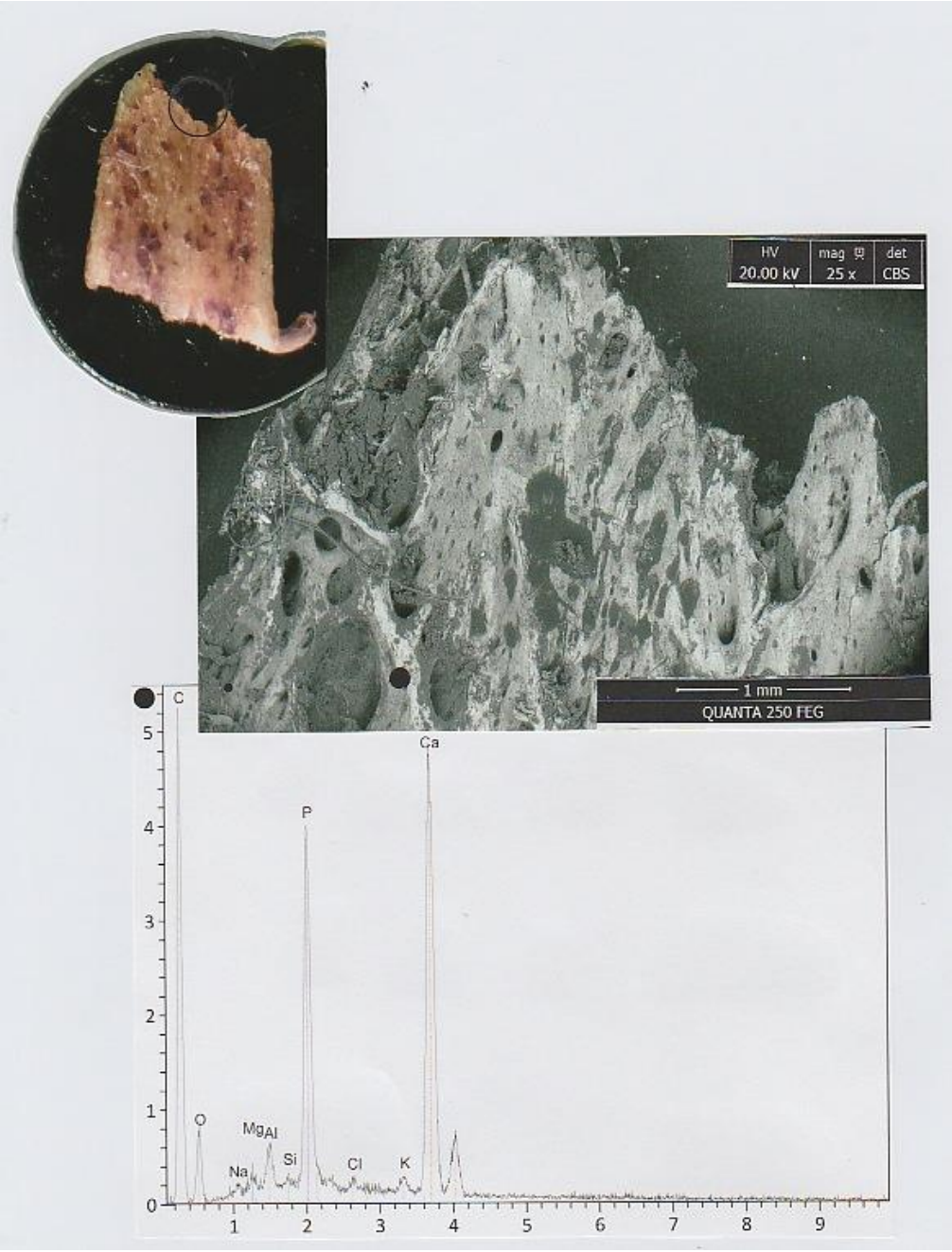

Figure 61. Analysis of a today boiled bone-fish of herring. **1** : a boiled bone-fish photograph, in optical microscopy (3x) ; the circle indicates the region explored. **2** : SEM photograph (in CBS, 50x) of this region ; black micro-points (representating burnt calcium phosphate particles) are aligned along the fish-bone longitudinal axis. **3** : spectrum (in blue) at the black dot indicated.

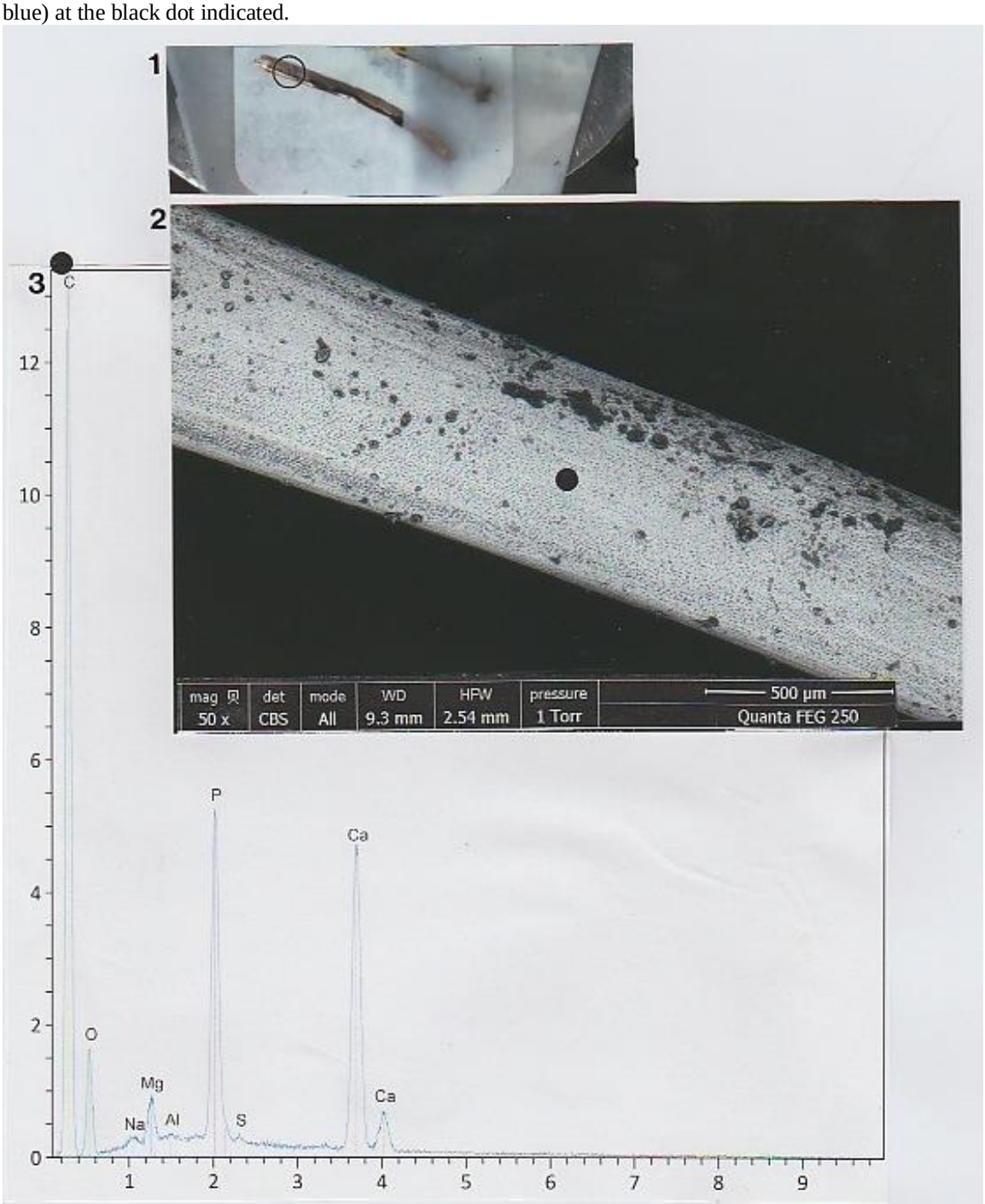

Figure 62. Analysis of a today cooked bone-fish of herring. **1** : a cooked bone-fish photograph, in optical microscopy (3x) ; the circle indicates the region explored. **2** : SEM photograph (in CBS, 50x) of this region ; the black micro-points cover the essential part of the bone-fish surface. **3** : Spectrum (in green) at the black dot indicated.

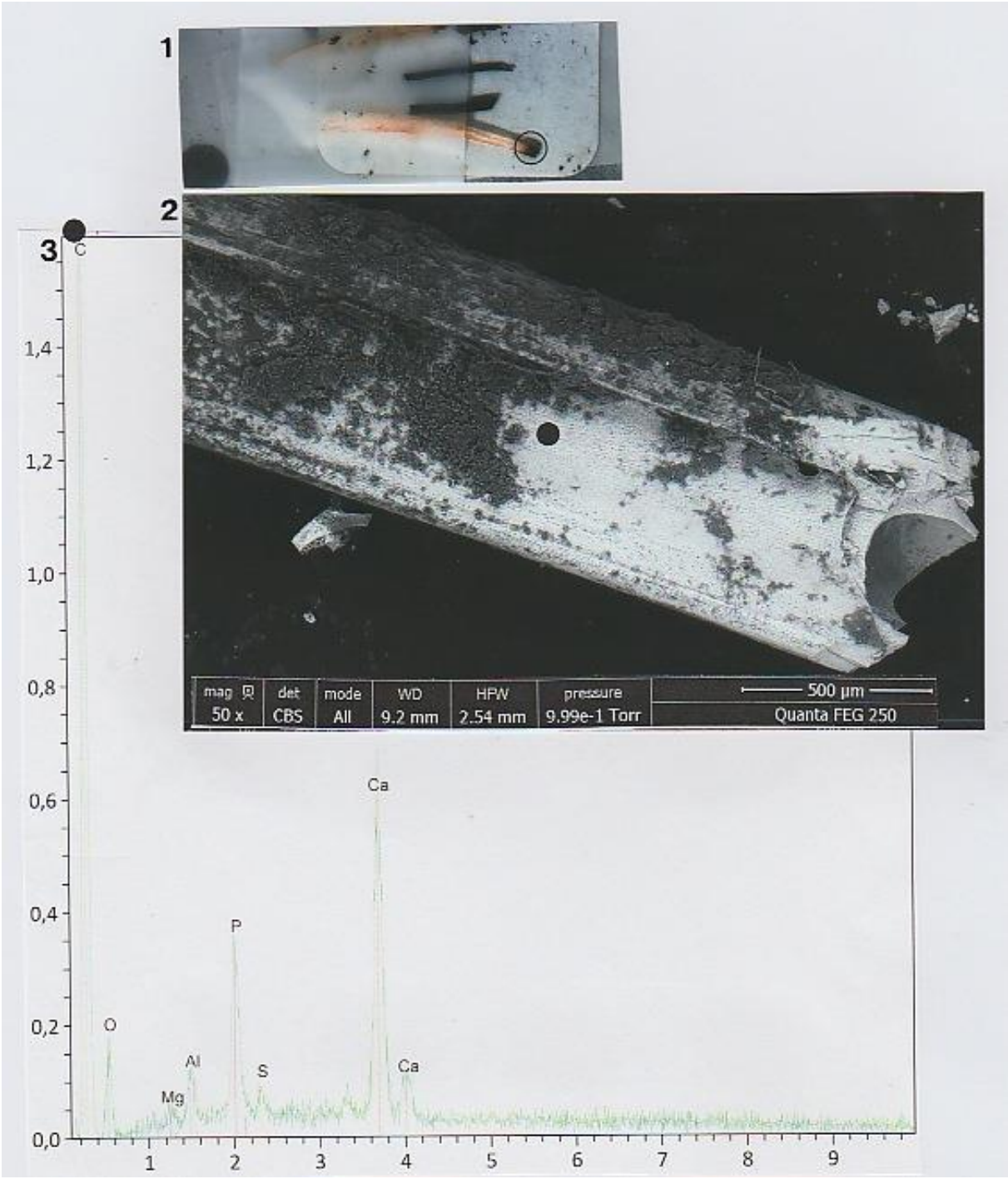

Figure 63. Starches from a today sample of portrige oats. **1** : three portrige oats, in optical microscopy (3x) ; the arrow point indicates that of which the inferior basis is studied. **2** : SEM photograph (in LFD, 19x) showing this basis ; the circle shows the studied region of this basis. **3** : SEM photograph (in LFD, 400x) showing some starches located at the interior of that circle. **4** : the global spectrum of this area (showing peaks C and O, and P, S and Ca).

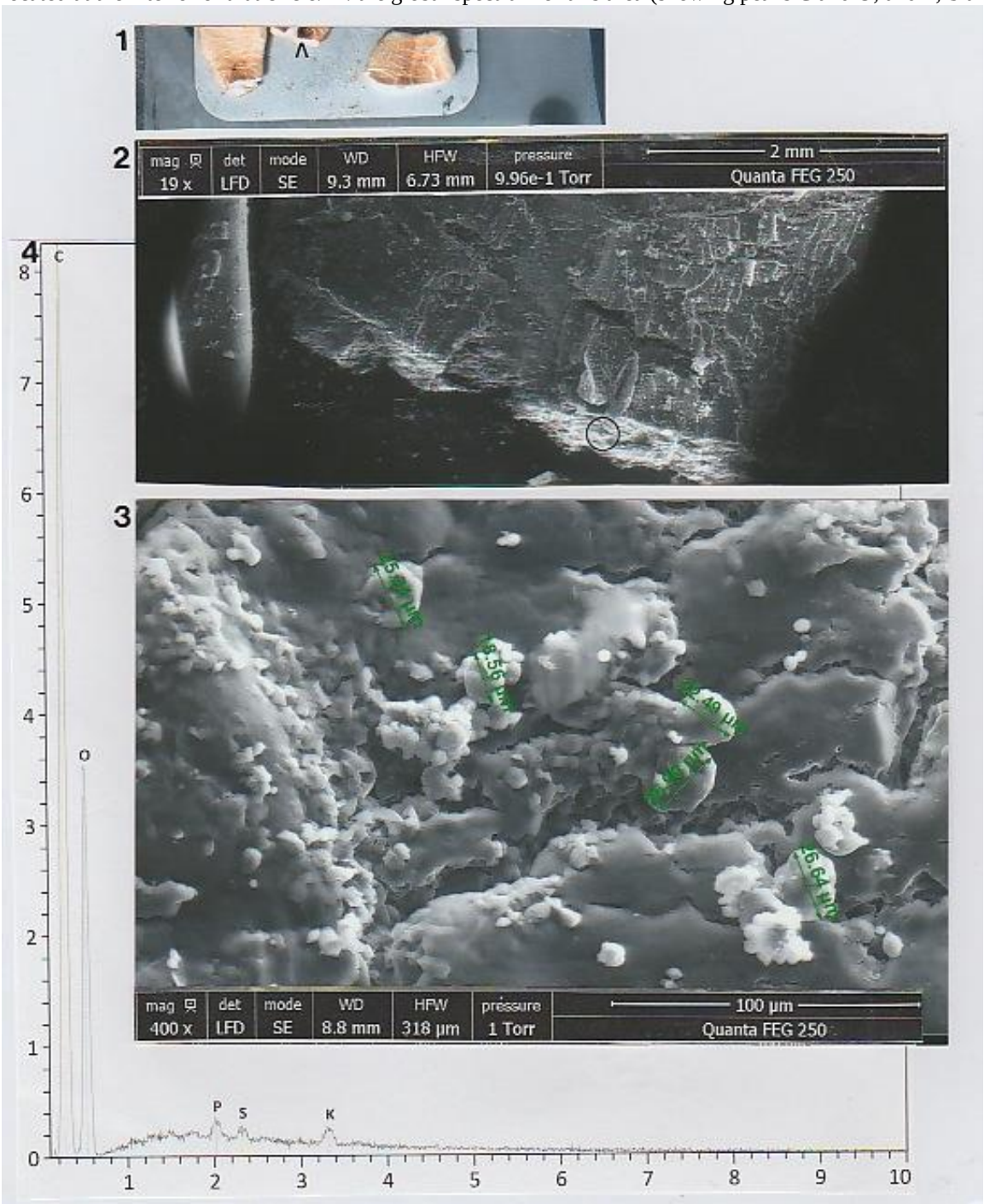

Figure 64. Starches from today samples of flour powder of maize and of flakes potato. **1** : SEM photograph (in LFD, 400x) of maize starch grains. **2** : SEM photograph (in LFD, 200x) of potato starch grains.